Investigations into the structure, function and pharmacology of TREK K2P potassium channels

Conor McClenaghan
DPhil Candidate
OXION: Ion Channels and Disease Initiative
Medical Sciences Doctoral Training Centre
Department of Physics
St Anne's College

Supervisors: Stephen J. Tucker and Frances M. Ashcroft

Submitted in partial fulfilment of the requirements for the degree of Doctor of Philosophy (DPhil in Ion Channels and Disease)

Declaration

The work described in this thesis was carried out in the laboratory of Prof Stephen J Tucker, of the Clarendon Laboratory, Department of Physics, University of Oxford, between September 2011 and September 2015. All work within this thesis is entirely my own unless stated in the text. This work has not been previously submitted for any other degree at the University of Oxford, of any other university.

Conor McClenaghan

(September 2015)

Acknowledgements

Foremost I would like to thank Stephen Tucker for his support throughout my DPhil, for his expert supervision and scientific input, and for mentoring beyond the immediate scientific questions. I was very fortunate to have a supervisor who is so generous with his time and so helpful with advice!

Thank you also to Frances Ashcroft, who has always been a great source of advice and guidance. It was a great experience to work in the Ashcroft lab during my first year, and thank you to Heidi, Peter, Melissa, Caro, Mathilde and everyone else who helped me during that project.

To all the wonderful people who have made working in the Tucker group fantastic (and often fantastically bizarre), thank you! In particular, Gio, Firdaus, Praf, Chet, Emma, Michael, Lejla, Laurianne, Matthias, your help and friendship made coming into the lab an absolute pleasure, even if it didn't sound like that when I was swearing at the oocytes… I've learnt an awful lot from everyone.

My projects heavily relied on the work of our collaborators within the OXION initiative and beyond. In particular I would like to thank Holger Kramer and Rod Chalk for so generously helping with the photo-labelling project. I am very grateful for the help and work of the many members of the Liz Carpenter and Thomas Baukrowitz groups who have contributed so much to productive collaborations.

To all the various inhabitants of Percy Street (permanent and temporary, human and murine), I will not attempt to disambiguate the myriad. But thank you for providing the perfect distractions from work, it's been fun!

Kelsey, you make everything brilliant (even late night patch-clamping). Thank you for your support, for the lab skypes, and for always making me laugh.

To my inspirational brainbox sisters, Maeve and Ciara: you're amazing. But hopefully soon you'll stop picking on me for only having one degree.

Mum and Dad, I owe you everything. I hope you know how much I appreciate your love and support throughout everything. I love you all!

Contents

Abstract

TREK channels are polymodal potassium channels which act as integrators of diverse chemical and physical stimuli to dynamically control the cellular membrane potential. How the channels sense different stimuli, and how this is transduced to channel gating is not fully understood. Here I report the results of electrophysiological investigations into the structure-function relationship and pharmacology of TREK channels. Firstly, the mechanism of action of plant derived alkylamides at TREK-1 was found to be complex and assay-context dependent. Subsequent studies of TREK-2, guided by recent X-ray crystal structures, provide novel insights into the mechanisms of gating in mechano-, temperature-, arachidonic acid- and pH-modulation. Studying the effect of these different gating stimuli, and the effects of different gating mutations on the potency of state-dependent inhibitors reveals the existence of multiple, distinct open conformations. The results of these studies are consolidated into a structural model for polymodal gating in TREK channels.

Keywords: *ion channels, mechano-sensitivity, K2P, TREK-1, TREK-2, TRAAK, polymodal gating, patch clamp electrophysiology, pharmacology, norfluoxetine*.

Chapter 1: Introduction

1. Bioelectricity

The regulated movement of charged ions is vital for life, and this bioelectricity underlies a vast and diverse range of physiological functions. From rapid events, such as action potential propagation, to slow processes like the regulation of gene expression, cellular function in all kingdoms of life relies upon finely controlled ionic conductances (Hille, 2001).

Since Hodgkin and Huxley's seminal studies of the action potential in the squid giant axon the mechanisms by which electrical conductances are mediated have been the subject of extensive work. The initial descriptions of sodium, potassium and leak conductances are now known to be carried by ion channels: gated protein pores which span the cell membrane allowing for the passive permeation of ions down their electrochemical gradient (Hodgkin & Huxley 1952; Hamill et al. 1981).

Bioelectricity can be described in simple terms as an electrical circuit composed of an capacitor (the cell membrane), across which a voltage (the membrane potential) is generated and regulated by the activity of dynamically controlled resistors in parallel (ion channels and pumps) (Hille, 2001).

1.1 The cell membrane

A critical step in the evolution of life was the partitioning of biochemical components within a lipid bilayer. Phospholipids form self-assembling bilayers due to their amphipathic nature, and in water have an intrinsic propensity to form vesicles. In the primordial environment this lipid-surrounded vesicle, the proto-

cell, would have served to concentrate internal components, facilitating life-sustaining reactions, and also provide a barrier to the external environment.

The membrane bilayer is comprised of two opposing phospholipid leaflets which assemble with hydrophobic lipid tails at its core and hydrophilic phosphate-head groups facing outwards towards the solvent. It acts as an insulator due to its dielectric property, separating the conductive intra- and extracellular environments which are rich in charged electrolytes, and as a capacitor, accumulating equal and opposite charges on either side in response to transmembrane voltage. Accordingly membrane capacitance is an important factor in the response time to changes in membrane potential (Hille, 2001).

1.2 The membrane potential

The membrane potential (the voltage across the cell membrane; V_m) arises as a result of the complex actions of many proteins. Firstly, electrogenic pumps couple ATP-hydrolysis to the active transport of ions against their concentration gradient. Prime amongst these pumps is the sodium/potassium ATPase, which co-transports three sodium ions out of the cell whilst carrying in two potassium ions (Morth et al. 2007). The consequences of this are twofold: an imbalance in the concentrations of specific ions inside and outside the cell, and the polarisation of the membrane potential. Together, the chemical concentration gradient and the transmembrane potential define the electrochemical gradient, which in turn determines the energy and directionality of ion movement across the membrane through ion channels.

Ion diffusion according to the electrochemical gradient tends towards equilibrium, and the point at which the net movement of ions is zero is named the reversal potential (E_{ion}). This is elegantly described by the Nernst equation (below), which

can be used to calculate the reversal potential for an ion based upon its intra- and extracellular concentration:

$$E_{\text{ion}} = \frac{RT}{zF} \ln \frac{[ion]_o}{[ion]_i}$$

Where R is universal gas constant, T is temperature (in Kelvin), z is the ion valence, F is the Faraday constant, and $[\text{ion}]_o$ and $[\text{ion}]_i$ are the concentration of ions outside and inside the cell respectively.

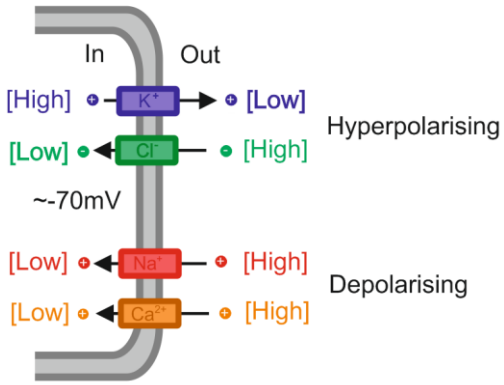

Figure 1: *The passive diffusion of ions through ion channels is determined by the ionic concentrations inside and outside the cell, and by the membrane potential.*

In normal physiology the reversal potential for potassium ions, with their low extracellular and high intracellular concentrations, is negative resulting in an outward driving force at potentials more positive than ~-80mV (Hille, 2001). Therefore, when diffusion is facilitated by the expression of active potassium-selective ion channels potassium leaves the cell. This potassium efflux further polarises the membrane potential, shifting V_m towards E_{K+} (Acosta et al. 2014; Zhang et al. 2008). Conversely, activation of sodium- or calcium-selective channels, for example, would depolarise the membrane potential, again shifting V_m towards the respective reversal potential for the ions. Clearly therefore the relative expression and activity of various ion channels controls the membrane potential. Again, this property can be described with reasonable accuracy by the Goldman-

Hodgkin-Katz (GHK) equation, which allows for the calculation of V_m based upon the concentrations of potassium, sodium and chloride:

$$V_m = \frac{RT}{F} \ln \frac{(P_{Na}[Na]_{o+} P_K[K]_{o+} P_{Cl}[Cl]_i)}{(P_{Na}[Na]_{i+} P_K[K]_{i+} P_{Cl}[Cl]_o)}$$

Where P_{Na}, P_K and P_{Cl} is the relative permeability for each respective ion.

1.3 Ion channel conductances

As we can see, the membrane potential is directly determined by the activity of ion channels. In general ion diffusion through a simple membrane pore obeys Ohm's law:

$$I = V/R$$

Where current (I) scales according to voltage (V) and inversely to resistance (R). As conductance (g) is the reciprocal of resistance we can rearrange the above formula to give:

$$I = V \times g.$$

Here V represents the driving force (df) i.e. the membrane potential minus the reversal potential, so:

$$I = (V_m - Eion) \times g = df \times g$$

In reality conductances in ion channels do not always scale with an Ohmic or GHK relationship with voltage and the biophysical properties of the channel or the relative concentration of intra- or extracellular blockers can confer rectification.

The conductance of a single ion channel is a property of the ion channel conduction pathway, but the extent of activation (open probability, P_o) and channel number (N) can be regulated. The macroscopic conductance (G) for any particular ion channel therefore can thus be described as below:

$$G = N \times P_o \times g$$

1.4 The action potential

In a cell at rest (i.e. one which is not firing an action potential) a standing outward potassium conductance is maintained via "leak channels". The constitutive activity of such channels determines the extent of membrane potential polarisation, which in neurones for example is typically around -70mV (Hille, 2001). Electrically excitable cells are those which are able to generate action potentials where excitability is conferred, firstly, by the additional expression of various channels permeable to sodium and calcium which exhibit low basal activity but which can be activated by external chemical or physical stimuli. These channels may serve to sense, for example, extracellular neurotransmitter molecules in the synaptic cleft, or pressure in free nerve endings of sensory neurones, and their activation facilitates sodium/calcium ion influx down their electrochemical gradient (Delmas et al. 2011; Snyder 2009). Thereafter the action potential is generated by the sequential activation, inactivation and deactivation of voltage-dependent conductances carried by voltage-gated sodium, calcium and potassium channels with varying biophysical properties, as in Figure 2.

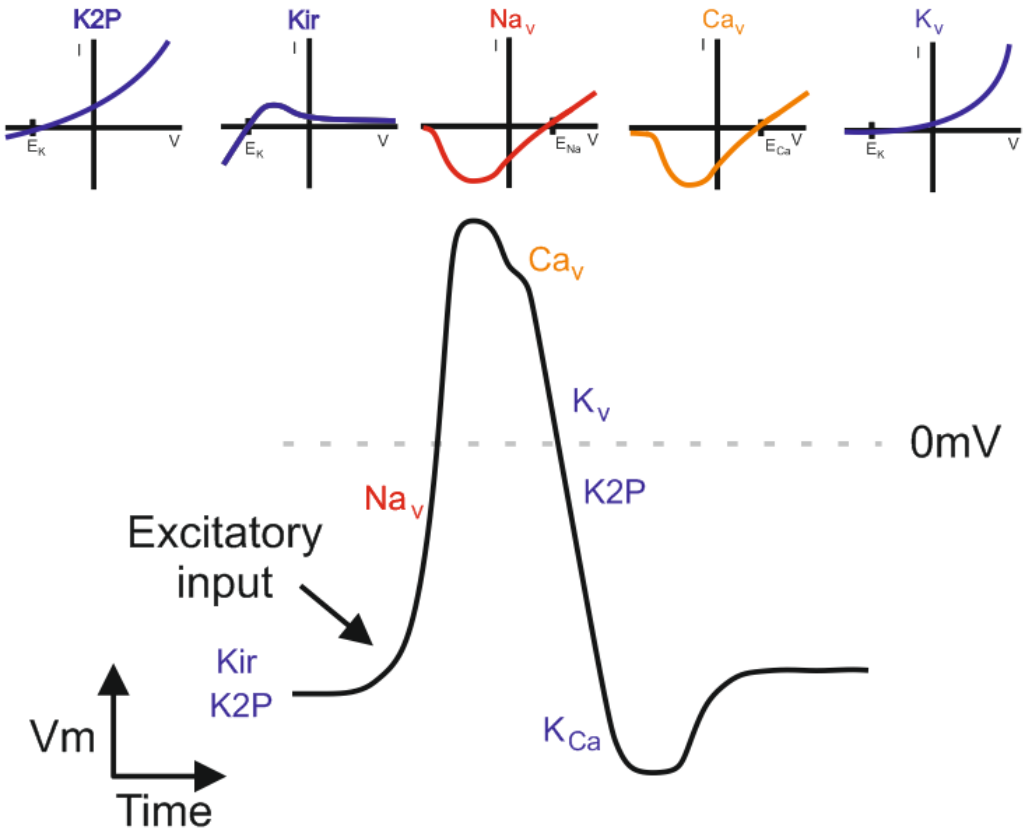

Figure 2: ***The ionic conductances underlying action potential propagation****. Top panels: idealised IV profiles from K2P, Kir, Na_V, Ca_V and K_V channels. Bottom panel: the time course of action potential propagation is the result of the complex behaviour of these channels.*

In non-excitable cells changes in membrane potential also has significant functional implications and underlies diverse processes such as hormone secretion, proliferation, apoptosis, and gene expression (Ashcroft 2000).

1.5 The potassium channel family

Potassium (K^+) channels appear to be ubiquitous in nature and every eukaryotic, eubacterial and archaeal organism for which a full genome has been sequenced contains at least one potassium channel gene, whilst viral potassium channel genes have also recently been discovered (Miller 2000; Thiel et al. 2013). The potassium channel family is the largest collection of ion channels in the human genome and

can be subdivided into three major classes: inward rectifiers (Kir), voltage-gated (K_v), and two-pore domain (K2P) channels (Miller 2000)

Each class is distinguished by unique structural and biophysical characteristics, yet some fundamental properties such as the mechanism by which ion-selectivity is achieved, are conserved across the families. Such shared features suggest that it is highly likely that the many diverse potassium-selective channels can be traced back to a common ancestor, though the identity of the distant relative remains unknown (Thiel et al. 2013; González et al. 2015; Anderson & Greenberg 2001).

The inward-rectifying (Kir) channels show distinctive conductances which deviate from Ohm's law and carry inward currents of significantly greater magnitude than their outward currents. This rectification is the result of intracellular blockade by divalent cations or polyamines. Despite this rectification the outward current is in fact most physiologically relevant and constitutively active Kir channels serve to drive V_m towards E_{K+} at rest (Hibino et al. 2010).

These channels are tetrameric polypeptides formed from subunits comprised of intracellular N- and C-termini and two transmembrane domains flanking a re-entrant pore-loop (P-loop) (Doyle et al. 1998). The subunits assemble to enclose an water-filled central cavity bordered at the extracellular side by the selectivity filter and at the intracellular side by an "inverted tee-pee" structure, the bundle crossing gate, which acts as a steric, hydrophobic barrier to ion permeation in the closed state and opens through an iris-like expansion of the inner pore helices (Kuo et al. 2003; Bavro et al. 2012).

The selectivity filter is highly conserved amongst all K^+ channels which share a common T-X-G-Y/F-G motif, where X is a hydrophobic amino acid, most commonly valine or isoleucine. Crystal structures of numerous potassium channels all show that the filter is formed by backbone carbonyl oxygen atoms which arrange as four planar matrices encaging four ion binding sites (Doyle et al. 1998; Long et al. 2007;

Dong et al. 2015). This precise geometry forms the basis of the exquisite selectivity for potassium ions by allowing for the stabilisation of fully dehydrated potassium ions as they pass through the filter (Doyle et al. 1998; Köpfer et al. 2014). Gating at the selectivity filter has also been described for all three classes of potassium channels and may be mediated by subtle rearrangements in the backbone which result in collapse and disruption of one or more ion binding sites (Bernèche & Roux 2005; Cuello et al. 2010; Ostmeyer et al. 2013). In addition, electron density in X-ray crystal structures predicts the presence of an additional ion binding site in the pore vestibule and at the extracellular interface of the SF (the S0 site).

K_v channels share the basic pore architecture with inward rectifiers but include an additional modular voltage-sensitive domain (VSD) (Long et al. 2007). The VSD is formed of four transmembrane helices (S1-S4); here S4 includes multiple basic residues and moves outward in response to membrane depolarisation. This conformational change is likely coupled to the inner pore S6 helices via the S4-S5 linker and results in opening the bundle crossing gate in voltage-activation (Vardanyan & Pongs 2012). Voltage-activation of potassium channels is the key event for membrane potential repolarisation during action potential propagation. The calcium-activated potassium channels (BKCa, IKCa and SKCa1-3) share topological organisation with Kv channels (with the partial exception of the 7 TM α-subunit of BKCa) and activate upon elevated intracellular calcium levels. Activation of these channels underlies the action potential afterhyperpolarisation which contributes to the refractory period in excitable cells.

The two-pore potassium (K2P) channels were the final potassium channel family to be cloned and exhibit unique structural and functional properties, as discussed below.

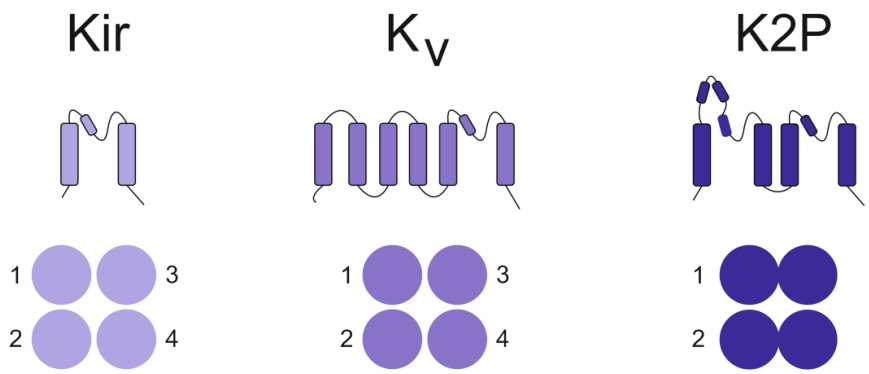

Figure 3: Potassium channel topology: *Top: The basic topology of single Kir, K_V and K2P monomers. Bottom: The quaternary structure of functional tetrameric Kir and K_V channels, and dimeric K2P channels.*

2. Two-pore domain potassium channels

The name "K2P channels" now most commonly refers to dimeric channels comprised of subunits with TM1-P-TM2-TM3-P-TM4 topology (where TMx refers to a transmembrane domain and P refers to a pore loop). The K2P name was initially used to describe the yeast TOK-1 K2P channel, an 8 TM channel comprising TM1-TM7-P-TM8 topology (Ketchum et al. 1995), but hereafter I will use K2P to refer to the large family of 4 TM potassium channels exclusively.

2.1 K2P Evolution

With their dimeric tandem-domain architecture K2P channels are clearly distinct from the other major potassium channel families. These striking differences raise questions about the evolutionary origins of K2P channels, and the point of divergence for the major potassium channel families.

Interestingly genes coding for channels resembling mammalian K2Ps, with the canonical 4 TM/2P monomer structure, have been found in the plants, metazoa and protists (González et al. 2015). In contrast BLAST searches for K2P homologues in prokaryotes have yielded no results to date, which has prompted the assertion that the last common ancestor was in fact a eukaryotic organism (González et al. 2015).

It appears that fungi do not contain K2P channels with this common topology, but rather include the aforementioned 8-TM domain channels such as TOK-1 of *S. cerevisiae* (Ketchum et al. 1995). Both the TOK-1 homologues and the 4 TM K2Ps are thought to be the product of gene duplication events (multiple events in the case of TOK-1) (Prole & Taylor 2013; Ketchum et al. 1995).

2.2 The cloning of the K2Ps

The first identification of a mammalian gene encoding for a 4 TM K2P channel came with the report by Lesage and colleagues of the cloning of a weak-inwardly rectifying potassium channel which the authors named TWIK-1 (for **T**andem of P domains in a **W**eak **I**nward rectifying $\mathbf{K}^+$ channel; *KCNK1*) (Lesage et al. 1996). The primary sequence of *KCNK1* exhibited a novel organisation with two P-loops within a single 4 TM domain subunit resembling the simultaneously-cloned drosophila K2P channel ORK1 (*KCNK0)* (Goldstein et al. 1996). Functional characterisation of TWIK-1 in *Xenopus* oocytes demonstrated very small potassium currents susceptible to block by Ba^{2+}, quinidine and quinine (Lesage et al. 1996).

The discovery of TWIK-1 and the identification of orthologues in *C. elegans* prompted extensive further investigation for homologous proteins. The result of this is our current knowledge of the complete 15 member human K2P family, which can be sub-categorised into 6 clades based upon sequence similarities and functional characteristics, see Table 1 below (Renigunta et al. 2015).

Clade	Channel	Gene	Reference
TWIKs	TWIK-1 (K2P1.1)	*KCNK1*	(Florian Lesage et al. 1996)
	TWIK-2 (K2P6.1)	*KCNK6*	(Chavez et al. 1999; Patel et al. 2000)
	TWIK-2	*KCNK7*	(Salinas et al. 1999)
TREKs	TREK-1 (K2P2.1)	*KCNK2*	(Fink et al. 1996)
	TRAAK (K2P4.1)	*KCNK4*	(Michel Fink et al. 1998)
	TREK-2 (K2P10.1)	*KCNK10*	(Bang et al. 2000)
TASKs	TASK-1 (K2P3.1)	*KCNK3*	(Duprat et al. 1997)
	TASK-3 (K2P9.1)	*KCNK9*	(Kim et al. 2000; Rajan et al. 2000)
	TASK-5 (K2P15.1)	*KCNK15*	(Ashmole et al. 2001; Kim & Gnatenco 2001)
TALKs	TASK-2 (K2P5.1)	*KCNK5*	(Reyes et al. 1998)
	TALK-1 (K2P16.1)	*KCNK16*	(Girard et al. 2001)
	TALK-2 (K2P17.1)	*KCNK17*	(Girard et al. 2001)
THIKs	THIK-1 (K2P13.1)	*KCNK13*	(Rajan et al. 2001)
	THIK-2 (K2P12.1)	*KCNK12*	(Rajan et al. 2001)
TRESK	TRESK (K2P18.1)	*KCNK18*	(Sano et al. 2003)

Table 1: The six clades of human K2P channels

3. K2P channel structure

Whilst the various human K2P channels are differently regulated by numerous diverse factors the channels are predicted to share basic topology and common structural features. Early hydropathy analysis predicted the presence of 4 transmembrane domains and that the channels included a lengthy extracellular domain, and now, with the recent publication of multiple K2P structures, we have remarkable new insight into how these channels form (Lesage et al. 1996; Miller & Long 2012; Brohawn et al. 2013; Dong et al. 2015).

3.1 The TWIK-1 and TRAAK crystal structures

The first sightings of K2P channels were revealed with the back to back publication of TWIK-1 (PDB code 3UKM) and TRAAK (PDB code 3UM7) X-ray crystal structures which immediately unveiled a number of structural features unique to K2P channels, including two-fold symmetrical dimeric assembly, intramembrane fenestrations and a large extracellular helical cap (Miller & Long 2012; Brohawn et al. 2012).

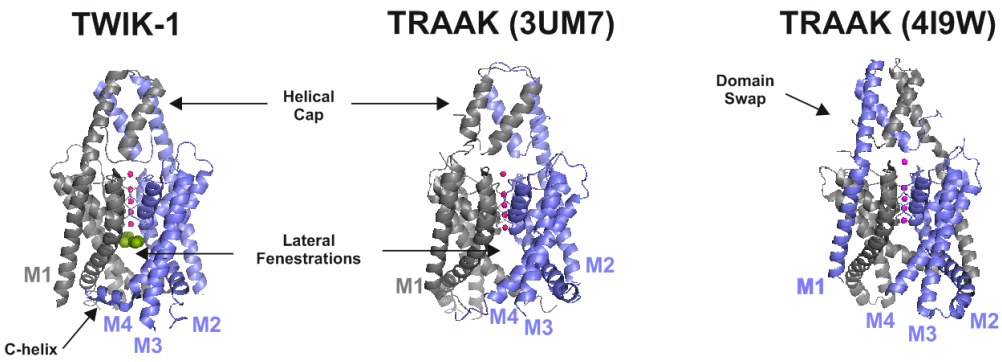

Figure 4: The crystal structures of TWIK-1 (3UKM) and TRAAK (3UM7 and 4I9W). *X-ray crystal structures display the dimeric assembly of TWIK-1 and TRAAK showing the helical cap, lateral fenestrations and potassium ions in the selectivity filter (magenta). A lipid-like tubular density (olive) was resolved within the central conduction pathway in TWIK-1. Increased resolution in the 4I9W TRAAK structure revealed the domain swap of M1 as shown.*

Functional dimers

Both structures were solved of homo-dimeric channels with consequent two-fold symmetry, see Figure 4. The first (M1) and third (M3) transmembrane domains of each monomer formed outer helices with the second (M2) and fourth (M4) transmembrane domains forming the pore lining inner helices. In this respect the channels generally assembled similar to other potassium channels, but an extended helix-turn-helix structure linking the second and third transmembrane helices appears unique to the K2Ps.

The inner helices of both channels contain strictly conserved glycine residues, analogous to the hinge glycines in K_V and Kir channels, and were splayed apart resulting in an opening at the cytoplasmic face of the membrane of >10 Å, characteristic of an open potassium channel (Ye et al. 2010; Long et al. 2007; Jiang et al. 2002). Unlike other potassium channels however, in TWIK-1 and TRAAK M2 exhibited a ~20° kink facilitated by a conserved proline which caused the helix to traverse the membrane at an oblique angle (Miller & Long 2012; Brohawn et al. 2012).

Lateral fenestrations

The different angles of the two inner helices (M2 and M4) resulted in large intramembrane lateral fenestrations, portals within the lipid spanning portion of the channel. These structures were previously unseen in other potassium channels, but are reminiscent of lateral fenestrations recently published in bacterial sodium channels (Bagnéris et al. 2014; Payandeh et al. 2011).

In the TWIK-1 structure tubular electron density, which could be fit by ~11 carbon alkyl chains, penetrated the fenestrations and occupied the inner pore, similar to density observed in the NavAb structure (Payandeh et al. 2011). It is unclear whether this density represents integral lipids bound to the channel which may be involved in channel function or whether it merely reflects detergent molecules used in the crystallisation process (Miller & Long 2012). Regardless, it was suggested that the lateral fenestrations could provide convenient access routes for hydrophobic modulators of K2P channels, such as local anaesthetics and arachidonic acid (Miller & Long 2012; Brohawn et al. 2012).

The extracellular helical cap

Upon cloning the TWIK-1 gene, Lesage and colleagues identified the presence of what was then termed an extended loop region of ~ 55 amino acids linking TM1 with the first pore domain (Lesage et al. 1996). The TWIK-1 and TRAAK structures showed that in fact this sequence forms a helix-turn-helix extracellular cap protruding ~35 Å above the membrane, which provides an explanation for why K2P channels were resistant to inhibition by extracellular toxins and tetraethylammonium (TEA), see Figure 4 (Miller & Long 2012; Brohawn et al.

2012). The cap clearly prevents potassium ions from leaving or entering the selectivity filter unhindered and would block free diffusion. Instead access for ions is facilitated via two "funnel shaped" channels on opposite side of the cap formed by the cap helices and extracellular loops.

Presciently, it had previously predicted that the M1-P1 linker must orientate in close apposition over the selectively filter to form separate Zn^{2+} and ruthenium red binding sites in TASK-3 (Clarke et al. 2008; Czirják & Enyedi 2003; Musset et al. 2006). This finding suggests that the helical cap structure is likely conserved amongst other mammalian K2Ps.

Conservation of the canonical potassium selectivity filter

Both channels displayed a selectivity filter very similar in structure to that seen in other K^+ channels (Miller & Long 2012; Brohawn et al. 2012; Doyle et al. 1998). As expected for a permeant channel density for 4 ions was resolved within the selectivity filter, with an additional density in the S0 site above the filter.

Notably, TWIK-1 has been reported to undergo dynamic changes in selectivity (Chen et al. 2014a; Ma et al. 2011), which is dependent on a unique threonine (T118) in the first pore loop (Chen et al. 2014b). As the crystallised selectivity filter appears as expected for a potassium selective channel the basis for dynamic selectivity changes remains mysterious.

The M4 region

The TWIK-1 and TRAAK structures differed in the arrangement of the distal M4 region. Whilst in TWIK-1 a helix break in M4 resulted in a distinct amphipathic

helix parallel to the membrane (the C-helix) in TRAAK (3UM7) M4 traversed the membrane more perpendicularly, see Figure 4.

Domain swap architecture and M4 helical rearrangement in TRAAK

In a second study the TRAAK channel was crystallised using antigen binding fragments (FAB) to increase the resolution to 2.75 Å (4I9W) revealing "domain-swapped chain connectivity", see Figure 4 (Brohawn et al. 2013). Here the refined resolution of the electron density around the top of the helical cap showed unequivocally that the first transmembrane domain and first cap helix was in fact switched 180°, see Figure 4 (Brohawn et al. 2012; Brohawn et al. 2013). The functional purpose of this domain swap remains to be established, but perhaps this confers increased structural integrity to the channel to stabilise potential expansive gating movements in mechano-activation.

Additionally, the FAB-TRAAK structure exhibited an intriguing rearrangement of M4 in one chain, which may comprise part of the conformational changes involved in channel gating, as discussed below (Brohawn et al. 2013).

3.2 The TREK-2 crystal structure

During the course of this project crystal structures for the TREK-2 channel were resolved in two distinct conformations, see Figure 5 (Dong et al. 2015). Together with additional co-crystal structures of the protein bound by norfluoxetine and fluoxetine derivatives, and with the functional studies described here, these structures provide significant new insights into TREK channel function, as will be discussed extensively in this thesis.

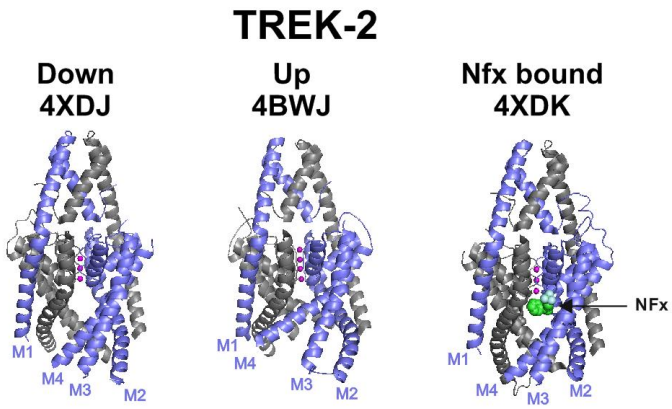

Figure 5: The crystal structures of TREK-2 in distinct conformations, and bound by norfluoxetine (NFx). *The TREK-2 channel was crystallised in two distinct conformations, an upward movement of M4 differentiates the "up" structure (4BWJ) from the "down" structure (4XDJ), whilst ion occupancy of the selectivity filter varied from 3 in the down structure to 4 in the up structure. Note, lipid-like electron density within the conduction pathway was observed in the down structure but is not shown here. NFx (shown in green) was bound within the fenestrations in the 4XDK structure which resembled the apo-down conformation with 3 ions in the selectivity filter.*

The TREK-2 structures shared significant structural features with the closely-related TRAAK structure published by Brohawn and colleagues, including lateral fenestrations which could be open or closed depending on the position of TM4. Intriguingly, the different TREK-2 channels showed differences in ion occupancy within the selectivity filter, which may indicate differences in the conductivity of the two channels (Dong et al. 2015).

3.3 Common and divergent features of K2P channels

Thus TWIK-1, TRAAK and TREK-2 share numerous critical features which may point to common structural characteristics amongst K2P channels. However the diversity in function and regulation amongst the various K2P channels is suggestive of significant variations across the family, some of these potential differences are discussed below.

Homo-mers and hetero-mers

All K2P structures published to date are formed of homo-dimers yet it has been proposed that TASK-1 and TASK-3, and perhaps more surprisingly TWIK-1 and TREK-1 are capable of forming heterodimers (Czirják & Enyedi 2002; Kang, Han, et al. 2004; Mi Hwang et al. 2014).

How hetero-mulitmerisation occurs remains to be established. Most pertinently, whether the domain-swapped architecture observed for TRAAK, and latterly for TREK-2 is maintained in hetero-mers is an interesting open question. One would anticipate that the interfacial interactions between TM1 and TM2 would differ significantly between a domain swapped and non-domain swapped hetero-meric channel.

The helical cap

All mammalian K2P channels likely contain the large helical cap, and following the description of the AqK2P from the marine sponge *Amphimedon queenslandica* this feature can perhaps be generalised across metazoa (Wells et al. 2012). However polymodal plant K2P-like channels (AtK2P) cloned from *Arabidopsis thaliana* do not appear to include a helical cap, with TM1-PH1 linkers only being ~5 – 20 amino acids long (González et al. 2015). Meanwhile the K2P-like NgKC channel (identified in the protist *Naegleria gruberi*) also has a reduced TM1-PH1 linker of approximately 41 AAs which has been described as a "quasi-helical cap domain".

This brings into question the necessity of the cap for the function of mammalian K2Ps. Remarkably TREK-1 channels retain function and can be mechanically activated following deletion of the entire TM1-PH1 linker (Maksaev et al. 2011). How such truncated channels assemble in the absence of the extracellular cap is a

mystery. The truncated channels clearly cannot include the domain-swapped architecture predicted for TREK-1 which suggests that channels can fold stably in multiple different global conformations.

Elsewhere the disulphide bridge between adjacent subunits at the tip of the helical cap in TWIK-1, TRAAK and TREK-2 is not common throughout the family as the critical cysteine is not conserved in TASK-1, TASK-3, THIK-1 and THIK-2.

N- and C-termini

All K2P structures solved so far have been from severely truncated channel constructs and all exclude the intracellular N- and C-termini (Miller & Long 2012; Brohawn et al. 2013; Lolicato et al. 2014; Dong et al. 2015). This is unfortunate, particularly in the consideration of TREK channel function as both termini have been implicated in biophysical function and regulation.

N-terminal truncations of TREK-1 have been reported to shift ion selectivity, whilst truncations of TREK-2 were reported to alter the probability for occupancy of sub-conductance states (Thomas et al. 2008; Simkin et al. 2008). Meanwhile the C-terminus of TREK-1 and TREK-2 is a critical regulatory module which confers sensitivity to phosphorylation, intracellular acidification, and numerous other factors (Kim et al. 2001; Kim, Gnateco et al. 2001; Murbartián et al. 2005; Patel et al. 1998).

Therefore the crystal structures provide vital insights into the core domain of the channels but at this stage the structure and function of important regulatory domains remain a mystery.

Towards an understanding of K2P structure-function

K2Ps are regulated by a vast range of factors including protons, temperature, mechanical force, lipids and fatty acids, and pharmacological modulators. How structure relates to function in K2Ps is the main focus of the studies described here, with particular focus on the TREK subfamily.

4. The TREK Subfamily

4.1 TREK channels in the beginning

Perhaps the first identification of TREK channels came with the description of the S-type current in sensory neurones of the sea snail *Aplysia,* a background potassium current that was inhibited by both serotonin and intracellular cAMP injection (Siegelbaum et al. 1982). Later, single channel recordings of mammalian cardiac myocytes identified a potassium channel which displayed macroscopic outward rectification and was activated by arachidonic acid and intracellular acidification (Kim & Clapham 1989). These pioneering experiments demonstrated functional properties which were subsequently shared by the newly cloned TREK channels.

4.2 TREK Channel Cloning

The cloning of TREK-1, TRAAK and TREK-2 was first reported in a series of papers from the Michel Lazdunski and Donghee Kim groups (Fink et al. 1996; Fink et al. 1998; Bang et al. 2000; Lesage et al. 2000). These reports detailed the identification of three outwardly rectifying K^+ channels from rodent brain cDNA libraries: TREK-1, TREK-2 and TRAAK. The degree of sequence homology and shared functional

properties between the three novel channels led to their subsequent sub-categorisation of into the same "TREK subfamily". TREK-1 and TREK-2 share 78% homology (63% identity) whilst TREK-1 and TRAAK share 69% homology (45% identity) (Fink et al. 1996; Fink et al. 1998; Bang et al. 2000; Lesage et al. 2000).

4.3 Molecular heterogeneity

Splice variants

A number of splice variants and alternative-translation-initiation (ATI) isoforms in TREK channels increase the molecular heterogeneity *in vivo*.

Splice variants in the three TREK channel genes (*KCNK2, KCNK4* and *KCNK10*) produces N-terminal variants in all three proteins (Fink et al. 1996; Fink et al. 1998; Bang et al. 2000; Lesage et al. 2000). Splice variant proteins have been variously reported to: reduce TREK-1 whole cell currents in a dominant negative fashion (Veale et al. 2014; Rinné et al. 2014), alter expression levels of TREK-2 (Gu et al. 2002) or have no clear effect on TRAAK function (Fink et al. 1998).

ATI-isoforms

The identification of ATI sites was first demonstrated for TREK-1 where a leaky natural Kozak sequence results in inconsistent translation initiation and a mixed population of full length and TREK-1ΔN1-56 channels (Thomas et al. 2008). TREK-1ΔN1-56 channels reportedly display small whole cell currents in *Xenopus* oocytes, larger single channel conductances (short form conductance 83 ± 5pS, long form conductance 60 ± 4pS at -60mV) and decreased selectivity (Thomas et al. 2008).

Additionally decreased fluoxetine and carvedilol sensitivity has been reported for the short ATI-isoform, but this may be confounded by the small whole cell currents observed for the short isoform in oocytes (Eckert et al. 2011; Kisselbach et al. 2014).

Three ATI-isoforms of TREK-2 have also been reported (Simkin et al. 2008). Again these isoforms had varying single channel conductances (shortest form ~52pS, long and intermediate forms conductance ~188-224pS). For TREK-2 no effect on selectivity was observed, but decreased relative activity of the long isoform and differences in occupancy of subconductance states have been reported (Kang et al. 2007; Simkin et al. 2008).

In contrast, no effects on the rate of Ba^{2+} inhibition was observed for the TREK-2 ATI isoforms (Zhuo et al. 2015). It was therefore suggested that the N-terminal truncations do not alter the conformation of the filter and so N-terminal truncations must mediate their effects on conductance via altering the resistance of the channel outside of the selectivity filter (Zhuo et al. 2015).

4.4 TREK channel expression

TREK-1, TRAAK and TREK-2 were initially cloned from rodent brain where all three channels show significant expression and extended investigation has documented widespread expression elsewhere (Fink et al. 1998; Fink et al. 1998; Bang et al. 2000; Lesage et al. 1996; Medhurst et al. 2001).

Central nervous system

Strong TREK-1 mRNA expression has been reported as in the olfactory bulb, hippocampus, cerebellum, striatum, thalamus, amygdala and spinal cord whilst

TRAAK mRNA expression is reportedly most intense in the olfactory system, cerebral cortex, hippocampus, amygdala, temporal cortex and cerebellum (Medhurst et al. 2001; Fink et al. 1998; Fink et al. 1996) TREK-2, meanwhile, is mainly expressed in the caudate nucleus, cerebellum, occipital lobe, putamen and thalamus (Medhurst et al. 2001; Lesage, Terrenoire, et al. 2000; Bang et al. 2000).

Glial-cell expression has also been documented with TREK-1 and TREK-2 observed at the transcript and functional level in cortical astrocytes (Minieri et al. 2013; Gnatenco et al. 2002; Zhou et al. 2009; Woo et al. 2012).

Peripheral nervous system

TREK channels are also strongly expressed in sensory and autonomic neurones of the peripheral nervous system. The small and medium diameter neurones of the dorsal root ganglion (DRG), and rat sensory trigeminal neurones express TREK-1, TREK-2 and TRAAK (Maingret et al. 2000; Alloui et al. 2006; Acosta et al. 2014; Kang et al. 2005; Braun et al. 2015; Yamamoto et al. 2009). Analysis of the relative frequency of recording single channel currents indicated that TREK-2 (along with TRESK) was the major background potassium channel in DRG cells (Kang et al. 2005; Kang & Kim 2006). Elsewhere TREK-1, but not TREK-2 or TRAAK, is highly expressed in the sensory Nodose ganglia, whilst TREK-2, but not TREK-1 or TRAAK, is highly expressed in the motor neurones of the mouse superior cervical ganglion (Cadaveira-Mosquera et al. 2012). This latter finding extends TREK channel expression to the autonomic nervous system (Cadaveira-Mosquera et al. 2011; Cadaveira-Mosquera et al. 2012).

TREK channels may act as sensors at nerve terminals and there is evidence for axonal trafficking in the rat sciatic nerve (Bearzatto et al. 2000)

Smooth muscle

Functional TREK-1 protein and mRNA expression has been reported in the basilar artery, mesenteric resistance arteries, pulmonary arteries and skin micro-vessels (Blondeau et al. 2007; Garry et al. 2007; Gardener et al. 2004). Meanwhile TREK-2 mRNA was also found in pulmonary arteries (Garry et al. 2007).

TRAAK expression was detected alongside TREK-1 in human myometrium smooth muscle cells whilst TREK-1 is also expressed in human detrusor smooth muscle cells of the bladder (Buxton et al. 2010; Lei et al. 2014; Tertyshnikova et al. 2005).

In the heart TREK-1-like currents have been recorded from atrial and ventricular myocytes (Terrenoire et al. 2001). TREK-1 mRNA levels were measurably higher in endocardial myocytes compared to epicardial myocytes when assessed by RT-PCR (Tan et al. 2004). Notably TREK-1 expression in porcine atria appears to be downregulated by atrial fibrillation (Schmidt et al. 2014). In contrast, generally, mRNA levels for TREK-2 and TRAAK in the heart appear to be significantly lower (Liu & Saint 2004).

Other tissues

TREK-1 is also present at the transcript level in the lung, kidney, heart, skeletal muscle and ovary, and functional channels have been identified in periodontal ligament fibroblasts, alveolar epithelial cells, vascular endothelial cells, prostate cancer cells, adrenocortical cells and a human keratinocyte cell line (HaCaT) (Fink et al. 1996; Ohara et al. 2006; Schwingshackl et al. 2012; Voloshyna et al. 2008; Enyeart et al. 2002; Kang, Kim, et al. 2007).

TREK-2 is also expressed in the placenta, lung, liver, skeletal muscle, pancreas, kidney, colon, small intestine and testis and functional studies have identified

TREK-2–like channels in insulin-secreting MIN6 cells, HaCaT keratinocytes and B lymphocytes (Bang et al. 2000; Lesage, Terrenoire, et al. 2000; Kang, Choe, et al. 2004; Zheng et al. 2009a; Kang, Kim, et al. 2007).

TRAAK appears to display a more restricted expression pattern, but is also seen at the transcript level in the placenta (Fink et al. 1998; Medhurst et al. 2001).

4.5 TREK channel regulation

Early studies showed that the TREK channels displayed a polymodal nature and could be regulated by a diverse range of chemical and physical stimuli, see Figure 6. TREK channel activity is variously modulated by mechanical forces, temperature, intra- and extracellular protons, polyunsaturated fatty acids, lipids and lysophospholipids, signalling cascades downstream of G-protein coupled receptors, and a range of pharmacological agents (Noël et al. 2011).

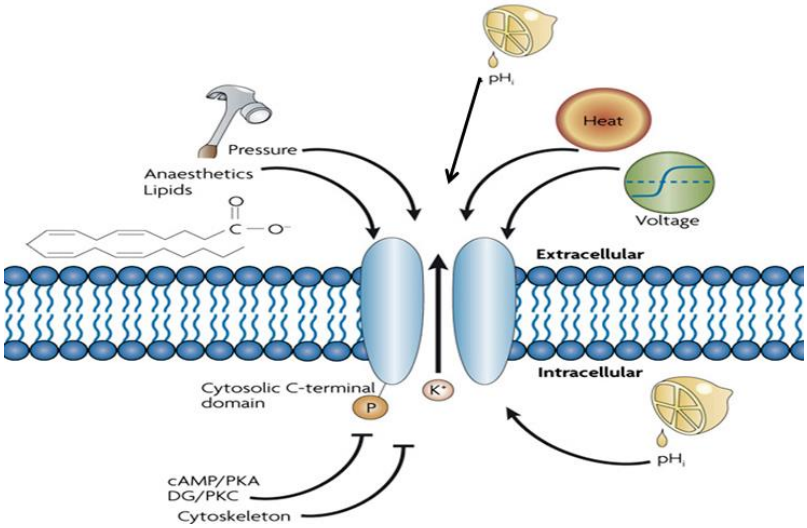

Figure 6: TREK channels as polymodal sensors. *TREK channels are modulated by a range of stimuli; note PKA/PKC pathways do not regulate TRAAK channel function (figure adapted from* Honoré 2007*).*

Mechano-sensation

The TREK family are defined by their activation by mechanical forces (Maingret et al. 1999; Patel et al. 1998; Fink et al. 1998; Bang et al. 2000; Brohawn et al. 2014). Application of negative and positive pressure via the patch pipette activates all three channels, as does cell poking (Brohawn et al. 2014).

Progressive deletion of the C-terminus of TREK-1 and TREK-2 appears to reduce sensitivity to stretch, but truncated proteins do retain some sensitivity (Maingret et al. 1999; Kim, Gnatenco, et al. 2001). Interestingly the C-terminus is not as critical for TRAAK mechano-sensitivity (Kim, Bang, et al. 2001).

That mechano-sensitivity is retained upon reconstitution of channels in simple lipid bilayer proves that all three channels directly sense changes in the bilayer (Brohawn et al. 2014; Michael Clausen - unpublished). These recent findings were pre-empted by studies which demonstrated that mechano-sensitivity was retained, and in fact augmented, in excised membrane patches and cell attached patches in which the cytoskeleton was disrupted pharmacologically (Liu et al. 2008; Lauritzen et al. 2005; Maksaev et al. 2011). These results indicate that the cytoskeleton may dampen the effect of stretch application on TREK channels, perhaps by anchoring the membrane and conferring resistance to pressure, thereby buffering the internal tension.

Recent developments in our understanding of mechano-activation in TREK channels will be discussed at length in Chapter 5 and Chapter 8 in this thesis.

Thermo-sensation

Approximate ~10 fold increases in currents for 10°C changes in temperature have been reported for TREK-1, TREK-2 and TRAAK within the range of 24 and 42°C

(Maingret et al. 2000; Kang et al. 2005; Chapter 5). This increase in macroscopic current is predominantly the result of increased open probability (Kang et al. 2005). The mechanism of temperature activation of TREK channels remains to be established (Schneider et al. 2014). This is discussed in greater detail in Chapters 5 and 8.

pH regulation of TREK channels

The effect of pH will be described extensively in Chapters 6 and 8 but briefly, TREK channels show sensitivity to variations in proton concentration of both the extracellular and intracellular solution. Interestingly, both TREK-1 and TREK-2 show robust activation upon intracellular acidification whilst in contrast TRAAK is activated by alkalinisation (Maingret et al. 1999; Honoré et al. 2002; Kim, Bang, et al. 2001; Kang et al. 2005). The activation of TREK-1/-2 requires critical C-terminal regions and the effect of acidification can be mimicked by mutation of a single conserved glutamate (E321 in TREK-1, long form numbering; E337 in TREK-2 isoform C numbering) (Honoré et al. 2002).

Furthermore pH activation sensitises TREK-1, TREK-2 and TRAAK to mechano-activation, indicating a synergistic relationship (Maingret et al. 1999; Kim, Bang, et al. 2001; Kim, et al. 2001).

In addition extracellular pH modulates all three TREK channels. Both TREK-1 and TRAAK are inhibited by extracellular acidification, whilst TREK-2 is activated by acidification (Cohen et al. 2008; Sandoz et al. 2009). Mutagenesis experiments demonstrate that a conserved extracellular histidine is the proton sensor in all three channels (Cohen et al. 2008; Sandoz et al. 2009). Meanwhile, the difference in directionality of the extracellular pH effect has been attributed to differences in another extracellular loop, the P2-TM4 linker (Sandoz et al. 2009).

Fatty acids

Another characteristic regulatory mechanism for TREK channels is activation by poly-unsaturated fatty acids (PUFAs). An early study of TREK-1 showed robust and reversible activation of the channel by a number of *cis*-unsaturated fatty acids at micro-molar concentrations, including arachidonic acid (AA), oleate and docoahexaneoate (Patel et al. 1998). This study suggested that fatty acid alkyl chain length was not critical for activation but that alcohol or methyl ester derivatives of AA were inactive, as were the saturated fatty acids palmitate and arachidate.

Similar results were attained for TRAAK (Fink et al. 1998). Notably, here, arachidonic acid activation was observed in the presence of 5,8,11,14-eicosatetraynoic acid (ETYA) and other inhibitors of arachidonic acid metabolism, indicating that AA acts directly.

TREK-2 modulation follows an identical pattern; polyunsaturated fatty acids robustly activated recombinant channels whilst saturated derivatives showed little effect (Bang et al. 2000). Additionally, Bang and colleagues demonstrated that elaidic acid, the *trans*-isomer of *cis*-oleic acid failed to activate TREK-2, indicating some stereo-specificity.

All three TREK channels could be activated by PUFA application to either side of the membrane (Bang et al. 2000; Fink et al. 1998; Patel et al. 1998). However when a membrane impermeant analogue of arachidonic acid (arachidonyl-CoA) was applied to the outside of TREK-2 no activation was observed, in contrast to clear activation when applied intracellularly (Kim, Gnatenco, et al. 2001).

Further discussion of the mechanism of arachidonic acid can be found in Chapters 5 and 8.

Anionic phospholipids and lysophospholipids

Complex effects of the anionic phospholipid PIP_2 (phosphatidylinositol-4,5-bisphosphate) on TREK channels have been reported. PIP_2 was initially reported to evoke strong activation of TREK-1, which was able to lock channels in a pH_i-activated state and mask voltage sensitivity via a C-terminal interaction (Chemin et al. 2005; Lopes et al. 2005). Synergistic relationships between PIP_2 and pH_i- and mechano-activation were reported (Lopes et al. 2005; Chemin et al. 2005).

However a later study by Chemin reported dual effects wherein PIP_2 inhibited TREK-1 currents in some patches. The reason for this complex behaviour is not clear, though a distinct C-terminal region was implicated in the inhibitory effect (Chemin et al. 2007). PIP_2 has been reported to inhibit TREK-2 in B lymphocytes, whilst membrane delimited production of PIP_2 reportedly inhibits recombinant TREK-1 and TREK-2 (Zheng et al. 2009b).

Lysophosphatidylcholine (LPC) and platelet aggregating factor (PAF) activate TREK-1 and TRAAK with micromolar potency (Maingret et al. 2000). Here the effect of LPC was lost when applied to excised patches, indicating that an indirect effect was most likely (Maingret et al. 2000).

G-protein coupled receptor modulation and phosphorylation

Numerous reports have detailed the sensitivity of TREK-1 and TREK-2 to phosphorylation by protein kinase A (PKA), protein kinase C (PKC) and protein kinase G (PKG). The inhibitory effect of phosphorylation of the TREK-1/-2 C-terminus by PKA and PKC has been suggested to underlie TREK-1 inhibition following activation of G_s- and G_q- coupled receptors (Patel et al. 1998; Lesage, Terrenoire, et al. 2000; Chemin et al. 2003; Murbartián et al. 2005; Devilliers et al.

2013). Whilst inhibition after G_q-coupled receptor activation has also been suggested to be in part due to direct inhibition by diacylglycerol (Chemin et al. 2003; Chemin et al. 2005), though this is controversial (Lopes et al. 2005; Kang et al. 2006). PKG modulation has been reported to increase TREK-1 currents via phosphorylation at the C-terminus (Koh et al. 2001), though this was not reproduced elsewhere (Lloyd et al. 2009).

Voltage

TREK channels display marked outward rectification in their macroscopic current voltage relationship despite linear or inwardly rectifying single channel conductances (for TREK-1, and TRAAK/TREK-2 respectively) due to increases in open probability at depolarised potentials (Maingret et al. 2002; Kim, Gnatenco, et al. 2001; Kim, Bang, et al. 2001; Bang et al. 2000).

Clearly K2P channels do not include the voltage-sensing domain observed in K_v channels and so voltage-activation of TREK channels must occur via a different mechanism (Toombes & Swartz 2014; Brohawn et al. 2012; Miller & Long 2012; Dong et al. 2015).

Initially it was suggested that voltage-sensitivity was dependent on C-terminal phosphorylation (Bockenhauer et al. 2001), but this was subsequently contested (Maingret et al. 2002; Kang, Choe, et al. 2007). Recent extensive work in the Thomas Baukrowitz lab has instead led to a model wherein voltage-sensitivity arises due to the activatory effect of permeants ion entering a non-conductive selectivity filter from the intracellular side (unpublished).

Other modulation

ATP (adenosine triphosphate) activation of TREK-like channels from bovine adrenal zone fasciculata (AZF) cells, and in rat ventricular myocytes has been reported, though the mechanism is unknown (Enyeart et al. 2002; Tan et al. 2002). Elsewhere inhibition of TREK-2 by the oxidising agent 5,5'-dithio-bis(2-nitrobenzoic acid) (DTNB; Ellman's reagent) has been demonstrated (Park et al. 2008). However, in direct contrast another oxidising agent, hydrogen peroxide (H_2O_2), has been reported to increase TREK-2 currents (Kim et al. 2007). These results may imply that TREK channels may been regulated physiologically by reactive oxygen species, and TREK-1 expression in CHO cells has been reported to confer protection for ROS-induced apoptosis (Sun et al. 2008).

4.6 TREK channel pharmacology

Inhibitors

The lack of potent and selective modulators of TREK channels has led to the channels being described as "pharmacological orphans" and currents are unusually insensitive to the classical potassium channel inhibitors tetraethylammonium (TEA) and 4-aminoo-pyridine (4-AP) (Bagriantsev et al. 2013). However a number of clinically used drugs and other small molecules do in fact modulate TREK channels, and it has been proposed that these effects may underlie some of the beneficial or adverse effects of the drugs (Duprat et al. 2000; Heurteaux et al. 2006; Heurteaux et al. 2004; Meadows et al. 2001).

A range of TREK channel inhibitors have been reported, including antidepressants, antipsychotics, local anaesthetics and beta/alpha adrenoreceptor blockers

(Heurteaux et al. 2006; Kennard et al. 2005; Thümmler et al. 2007; Nayak et al. 2009; Punke et al. 2003; Kisselbach et al. 2014). Though some reports of specificity for TREK-1 and TREK-2 over TRAAK have been reported, this is often only shown for single concentrations and so slight differences in potency cannot be ruled out (Thümmler et al. 2007). Indeed whilst reports have suggested, for example, fluoxetine/norfluoxetine do not inhibit TRAAK channels preliminary results in my experiments indicate they in fact do (unpublished results). Potency differences may be explained by the effect of different open probabilities for TREK-1/TREK-2/TRAAK channels on state-dependent drug binding.

The binding sites and mechanism of action of these clinically used drugs is not well understood. Kennard and colleagues reported a state-dependent mechanism for fluoxetine at TREK-1 on the basis of the drug showing decreased efficacy in activatory-mutant channels (Kennard et al. 2005). This result provided a basis for my investigations of norfluoxetine/fluoxetine inhibition of TREK-2 described in this thesis. State-dependence can now be extended as a general principle for other diverse TREK channel inhibitors carvedilol and fluphenazine on the basis of my results (see Chapter 5).

Interestingly, despite diverse chemical structures many of the reported TREK channel blockers (including norfluoxetine/fluoxetine, carvedilol and fluphenazine) are cationic amphipaths. It remains to be established if this property is critical for their action, but this may provide a unifying chemical fingerprint for a class of TREK channel inhibitors. A description for the mechanism of state-dependent inhibition by these drugs is provided in Chapters 5 and 8.

Elsewhere, extracellular inhibition by ruthenium red and curcumin have been described (Braun et al. 2015; Enyeart et al. 2008).

Furthermore it is not clear whether all compounds exert direct inhibition, and this needs to be systematically demonstrated. One indirect mechanism of action has

been proposed for the anti-cancer agent oxiplatin, which may adversely provoke cold allodynia via down regulation TREK/TRAAK channel expression (Descoeur et al. 2011). Elsewhere, spadin, a sortilin-derived peptide (see section below on regulatory proteins) has been proposed as a TREK-1 inhibitor which may mediate its effects by both direct block and increased channel internalisation (Mazella et al. 2010).

A non-specific bilayer-couple hypothesis for TREK channel activation by amphipathic compounds wherein the partitioning of molecules into the bilayer changes membrane curvature has been proposed (Honoré 2007). This may account for the action of certain charged "cup-former" modulators, such as chlorpromazine and tetracaine (Patel et al. 1998).

I provide a list of numerous reported TREK channel inhibitors, please see Table 1.

Class	Inhibitor	Channel	Notes	Reference
Antidepressants	Fluoxetine	TREK-1, TREK-2	IC_{50} 7-19 µM at (*XO, HEK293)*	(Heurteaux et al. 2006; Kennard et al. 2005)
	Norfluoxetine	TREK-1, TREK-2, TRAAK	IC_{50} 9 µM TREK-1, 5 µM TREK-2 (*XO)*	(Kennard et al. 2005; Yin Yao Dong et al. 2015)
	Paroxetine	TREK-1	IC_{50} 6 µM (*HEK293)*	(Heurteaux et al. 2006)
	Sertraline	TREK-1	IC_{50} 3 µM (*HEK293)*	(Heurteaux et al. 2006)
	Fluvoxamine	TREK-1	IC_{50} 9 µM (*HEK293)*	(Heurteaux et al. 2006)
	Citalopram	TREK-1	IC_{50} 190 µM (*XO)*	(Eckert et al. 2011)
	Mirtazapine	TREK-1	IC_{50} 130 µM (*XO)*	(Eckert et al. 2011)
	Doxepin	TREK-1	IC_{50} 244 µM (*XO)*	(Eckert et al. 2011)
	Escitalopram	TREK-1	IC_{50} 81 µM (*HEK293)*	(Lin et al. 2015)
Antipsychotics	Chlorpromazine	TREK-1,	IC_{50} 3 µM TREK-1 (COS7*)*	(Patel et al. 1998;

		TREK-2		Thümmler et al. 2007)
	Fluphenazine	TREK-1, TREK-2	IC_{50} 5 µM TREK-1 (COS7)	(Thümmler et al. 2007)
	Haloperidol	TREK-1, TREK-2	IC_{50} 6 µM TREK-1 (COS7)	(Thümmler et al. 2007)
	Flupenthixol	TREK-1, TREK-2	IC_{50} 2 µM TREK-1 (COS7)	(Thümmler et al. 2007)
	Loxapine	TREK-1, TREK-2	IC_{50} 20 µM TREK-1 (COS7)	(Thümmler et al. 2007)
	Pimoxide	TREK-1, TREK-2	IC_{50} 2 µM TREK-1 (COS7)	(Thümmler et al. 2007)
	Penfluridol	Native bTREK-1	IC_{50} 0.2 µM (*AZF*) IC_{50} 0.3 µM bTREK-1 *(HEK293)*	(Gomora & Enyeart 1999; Enyeart et al. 2002)
	Fluspirilene	Native bTREK-1	IC_{50} 0.2 µM (*AZF*)	(Gomora & Enyeart 1999)
β-blocker	Carvedilol	TREK-1, TREK-2	IC_{50} 2 µM TREK-1 *(HEK293)* IC_{50} 20 µM TREK-1 *(XO)* IC_{50} 24 µM TREK-2 *(XO)*	(Kisselbach et al. 2014)
Local anaesthetics	Bupivacaine	TREK-1	IC_{50} 370 µM (COS7)	(Punke et al. 2003)
	Lidocaine	TREK-1	IC_{50} 180 µM *(HEK293)* Y352, P355 critical	(Nayak et al. 2009)
Neuroprotective	Sipatrigine	TREK-1, TRAAK	IC_{50} 4 µM *(HEK293),* slightly reduced sensitivity in TRAAK	(Meadows et al. 2001)
Ca^{2+} channel blockers	Niguldipine	bTREK-1	IC_{50} 0.8 µM (*AZF*)	(Liu et al. 2007)
	Nifedipine	bTREK-1	IC_{50} 8 µM (*AZF*)	(Liu et al. 2007)

	Amlodipine	bTREK-1	IC_{50} 0.4 µM (*AZF*)	(Liu et al. 2007)
	Flunarizine	bTREK-1	IC_{50} 2 µM (*AZF*)	(Liu et al. 2007)
	Mibefradil	bTREK-1	IC_{50} 0.5 µM (*AZF*)	(Gomora et al. 1999)
	Diltiazem	TREK-1, TREK-2	IC_{50} 180 µM TREK-1 (*COS7*) IC_{50} 330 µM TREK-2 (*COS7*)	(Takahira et al. 2005)
Cannabinoid	Anandamide	TREK-1	IC_{50} 5 µM (*AZF*)	(Liu et al. 2007)
Inorganic dyes	Ruthenium red	TREK-2, TRAAK	IC_{50} 0.2 µM TREK-2 (*XO*) D135 critical Efficacy lower in TRAAK	(Braun et al. 2015)
Amphipaths	Tetracaine	TREK-1	79 % at 100 µM (*COS7*)	(Patel et al. 1998)
Amino acid	L-methionine	TREK-1	Low milli-molar (*COS7*)	(Baker et al. 2008)
Natural phenol	Curcumin	bTREK-1	IC_{50} 0.9 µM (*AZF*) only active from outside	(J. A. Enyeart et al. 2008)
Methylxanthines	Caffeine	TREK-1	IC_{50} 377 µM (*CHO*) inhibition reduced in S348A mutant	(Harinath & Sikdar 2005)
	Theophylline	TREK-1	IC_{50} 486 µM (*CHO*) inhibition reduced in S348A mutant	(Harinath & Sikdar 2005)
Chalcone	Sulphonamide chalcone	TREK-2	IC_{50} 62 µM (*HEK293*)	(Kim et al. 2010)
Peptide	Spadin	TREK-1	IC_{50} 71 nM (*HEK293*) no effect on TREK-2 or TRAAK	(Mazella et al. 2010; Moha Ou Maati et al. 2012)
Pyrimidine	ML45	TREK-1	60% at 100 µM (*XO*)	(Bagriantsev et al. 2013)
Ion	Lead	TREK-2	IC_{50} 16 µM (*XO*)	(Kim et al. 2005)

Abbreviations: bTREK-1 - native bovine TREK-1;, XO – Xenopus oocytes; HEK293 – human endothelial kidney

cells; CHO – Chinese hamster ovary cells; AZF – adrenal zona fasciculata cells;

Table 1: *List of published TREK channel inhibitors.*

Activators

An emerging number of TREK channel activators have also been reported. These diverse modulators include volatile and gaseous anaesthetics, neuroprotective agents and nonsteroidal anti-inflammatory drugs (NSAIDS).

The volatile anaesthetics (VAs) chloroform, diethyl ester, halothane and isoflurane were first shown to activate TREK-1 and TREK-2 at low milimolar concentrations, with no effect on TRAAK (Patel et al. 1998; Lesage, Terrenoire, et al. 2000). Deletion of the distal C-terminus of TREK-1 abolished the activatory effect without significantly affecting basal gating properties, indicating a role for VA interaction (Patel et al. 1999). Notably, the TASK-1 C-terminus was not critical for activation by halothane, which may indicate that the binding site in TASK channels is different. TREK-1 knockout mice show decreased sensitivity to anaesthesia, implicating the channels in the therapeutic mechanism (Heurteaux et al. 2004).

The gaseous anaesthetics xenon, nitrous oxide (N_20) and cyclopropane also activate TREK-1 (Gruss et al. 2004). In this case activation was not abolished by C-terminal truncation, though it was reduced. This might indicate that the mechanisms of action of gaseous and volatile anaesthetics at TREK channels are different.

The fenamate class of NSAID drugs also activate TREK channels. In this case flufenamic acid, niflumic acid, mefenamic acid and (5,6,7,8-Tetrahydro-naphthalen-1-yl)-[2-(1H-tetrazol-5-yl)-phenyl]-amine (BL-1249) activate TREK-1, TREK-2 and TRAAK (Veale et al. 2014; Takahira et al. 2005). Here the mechanism of action is unknown, but is likely a direct modulation of channel activity as it

retained in excised patches (unpublished results). Fenamates activate the short form ATI TREK-1 isoform as well as the full length channel, and activation is not mediated via cyclooxygenase inhibition as TREK-activity is not shared by other the NSAIDs ibuprofen and indomethacin (Veale et al. 2014).

Elsewhere a yeast-screen assay identified a novel activator of TREK-1, TREK-2 and TRAAK, ML67-33 (Bagriantsev et al. 2013). The drug is capable of activating channels in excised patches indicating a direct mechanism of action, but kinetics of activation were slower in inside-out patches compared to outside-out patches which may suggest the drug acts from the extracellular side (Bagriantsev et al. 2013).

Additionally, 2-Aminoethoxydiphenyl borate (2APB) shows moderate potentiation of TREK-1, TREK-2 and TRAAK but has increased potency at TREK-2 (Beltrán et al. 2013; Zhuo et al. 2015). A direct effect is likely as activation is observed in excised patches, and likely involves the C-terminus (Beltrán et al. 2013; Zhuo et al. 2015).

Further, a number of neuroprotective agents show activatory effects on TREK channels including riluzole (Duprat et al. 2000; Cadaveira-Mosquera et al. 2011; Enyeart et al. 2002), the phytochemicals baicalein and wogonin (Kim et al. 2011), and 4-(2-butyl-6,7-dichlor-2-cyclopentylindan-1-on-5-yl) oxobutyric acid (DCPIB)(Minieri et al. 2013).

Again, I provide a list of numerous reported TREK channel activators, please see Table 2.

Class	Activator	Channel	Notes	Reference
Volatile anaesthetics	Chloroform, halothane, isoflurane	TREK-1, TREK-2	Low milimolar concentrations. ~2 fold activation *(COS7)*. ΔC 48 abolishes effect in TREK-1.	(Patel et al. 1999; Lesage, Terrenoire, et al. 2000)
Gaseous anaesthetics	Xenon, nitrous oxide, cyclopropane	TREK-1	80% of each gas provoked mild activation (~30%) *(HEK293)*	(Gruss et al. 2004)
Fenamates	Flufenamic acid, niflumic acid, mefanamic acid, BL-1249	TREK-1, TREK-2, TRAAK	BL-1249 30-100 more potent than other fenamtes *(COS7)*. Also activates TREK currents in rat bladder strips.	(Takahira et al. 2005; Veale et al. 2014; Tertyshnikova et al. 2005)
Carbazole	ML67-33	TREK-1, TREK-2, TRAAK	EC_{50} 36 μM TREK-1. Increases currents 11-15x fold *(HEK293)*. Likely works from outside.	(Bagriantsev et al. 2013)
IP3-receptor inhibitor	2-APB	TREK-1, TREK-2, TRAAK	Most potent and efficacious at TREK-2. C-terminal interaction site *(XO)*.	(Beltrán et al. 2013; R.-G. Zhuo et al. 2015)
Neuroprotective agents	Riluzole	TREK-1, TREK-2, TRAAK	Transient at TREK-1, stable activation of TRAAK.	(Duprat et al. 2000; Enyeart et al. 2002)
	DCPIB	TREK-1, TREK-2	10 μM: 5 fold activation at TREK-1, 10 fold activation at TREK-2 *(COS7)*.	(Minieri et al. 2013)
	Baicalein, wogonin	TREK-2	100 μM activate in cell attached and excised patches	(Kim et al. 2011)
Chalcone	Sulphonate	TREK-2	EC_{50} 167 μM	(Kim et al.

	chalcone 11		*(HEK293)*	2010)
Ion	Zinc	TREK-2	EC_{50} 82 µM, 3 fold activation *(XO).* Extracellular cap and P1 loop critical, including H156.	(Kim et al. 2005)
Gases	Carbon monoxide and nitric oxide	TREK-1	CO donor CORM-2 (at 30 µM) and NO donor SIN-1 (at 10 µM) provoked ~2 fold activation. Effect inhibited by PKG inhibitors.	(Dallas et al. 2008)
Amphipath	Trinitrophenol	TREK-1	0.4 mM increased currents ~4 fold	(Patel et al. 1998)

Abbreviations: XO – Xenopus oocytes; HEK293 – human endothelial kidney cells; CHO – Chinese hamster ovary cells; 2-APB - 2-Aminoethoxydiphenyl borate; DCPIB - 4-(2-butyl-6,7-dichlor-2-cyclopentylindan-1-on-5-yl) oxobutyric acid.

Table 2: *List of published TREK channel activators.*

4.7 Regulatory proteins

TREK channels are likely to form part of multi-molecular complexes at the membrane. Recently studies have begun to untangle these interactions showing that TREK channels associate with, and are modulated by, diverse regulatory proteins and cytoskeletal elements.

These interaction partners include A-kinase anchoring protein (AKAP150) which associates with TREK-1 and TREK-2 and up-regulates channel activity, the microtubule associated protein Mtap2 and β-COP which both increase surface expression of TREK-1 and TREK-2 without affecting biophysical properties of the

channels, and the neurotensin receptor 3 (NTSR3 or sortilin) which complexes and may be involved in the down-regulation of TREK-1 by spadin (Sandoz et al. 2006; Sandoz et al. 2008; Kim et al. 2010; Mazella et al. 2010; Moha Ou Maati et al. 2012). Additionally a recent study demonstrated that localisation of TREK-1 and TREK-2 with phospholipase D modulates channel activity indirectly by controlling local phosphatidic acid (PA) concentrations (Comoglio et al. 2014). These interactions appear specific to TREK-1 and TREK-2 with no associated interactions reported for TRAAK channels.

The activity of TREK channels is also likely modulated by the cytoskeleton. This in illustrated in part by reports of increased channel activity upon patch excision, and by the sensitisation to mechano-activation following pharmacological disruption of the cytoskeleton (Lauritzen et al. 2005). Interestingly, a reciprocal modulation of the cytoskeleton by TREK channels was also reported, with overexpression of all three channels resulting in the formation of actin-enriched filopodia-like structures in mammalian cells (Lauritzen et al. 2005).

Elsewhere polycystin PC1 and PC2 proteins have been implicated in the sensitisation of TREK channels to mechanical activation in murine proximal convoluted tubule epithelial cells via interactions with the cytoskeleton (Peyronnet et al. 2012). Lastly, the actin-associated β_{IV}-spectrin protein has recently been reported to interact with TREK-1 in murine cardiac myocytes and may act to determine cellular localisation of the channel (Hund et al. 2014).

5. TREK channel function

The expression pattern and unique polymodal nature of TREK channels means the channels can act as integrators of diverse physical and chemical stimuli, coupling environmental sensing to electrical activity. At a cellular level TREK channel

activity will regulate both the resting membrane potential (RMP) and repolarisation of action potentials (AP).

In normal physiological conditions a potassium conductance carried by activated TREK channels would hyperpolarise cells towards the potassium reversal potential, and so the level of expression and activation of TREK channels will contribute to RMP. Indeed TREK conductances have been demonstrated to exert hyperpolarising effects on RMP in a number of tissues, including sensory neurones and atrial myocytes (Acosta et al. 2014; Zhang et al. 2008).

The voltage sensitivity of TREK channels also means that channel activation is greater at depolarised potentials. This in turn means that increased TREK-mediated conductances would be expected to contribute to repolarisation of the action potential. Interestingly AP-like behaviour has been recapitulated in HEK293 cells expressing TREK-1 alone following current injections calculated to mimic voltage-gated sodium channel depolarisation (MacKenzie et al. 2014). In addition, decreased TREK-1 expression in cardiac myocytes of a mutant β_{IV}-spectrin mouse resulted in prolonged AP repolarisation, demonstrating a physiological role for TREK-1 in repolarisation (Hund et al. 2014).

At a systems level TREK channels have been implicated in a wide range of functions, including somato-sensation, neuroprotection, depression, anaesthesia and regulation of smooth muscle tone amongst others.

5.1 TREK channels in somato-sensation

The expression of TREK-1, TREK-2 and TRAAK in sensory afferents of the DRG, trigeminal and Nodose ganglia, coupled with their regulation by mechanical and thermal stimuli, indicates a functional role in the sensing of noxious and innocuous touch and temperature. Consistent with this, ablation of the TREK-1, TREK-2 or

TRAAK genes in isolation or combination results in mechanical allodynia phenotypes (Alloui et al. 2006; Noël et al. 2009; Pereira et al. 2014). Knockout of TREK-1 and TREK-2 both decreases prostaglandin E2 (PGE2) sensitisation to osmotic insult, an effect not seen for TRAAK, as expected considering the lack of cAMP regulation of the latter (Alloui et al. 2006; Pereira et al. 2014; M Fink et al. 1998).

Additionally, alterations in temperature sensing have also been reported in all three knockout mice which exhibit thermal hyperalgesia at low intensity stimuli. This difference in response between knockout and wild type disappears at higher intensities (>50°C) for TREK-1 and TREK-2 knockouts yet is maintained in TRAAK knockouts (Alloui et al. 2006; Noël et al. 2009; Pereira et al. 2014). Meanwhile double knockout of TREK-1 and TRAAK confers increased sensitivity to noxious cold (12°C), whilst knockout of TREK-2 increased saphenous nerve firing between 21-30°C which suggests that TREK-2 may sense innocuous cold whilst TREK-1 and TRAAK sense noxious cold.

It is noteworthy that the half-maximal activation point for the channels is around 37°C, meaning the channels display maximum sensitivity to temperature changes in the physiological range (Schneider et al. 2014). TREK channels are co-expressed with the thermo-sensitive TRPV1 and TRPM8 channels in trigeminal primary afferents and thus are likely involved in temperature sensation.

In the CNS, labelling of TRAAK has been reported in neurones of the preoptic area of the hypothalamus (POA) in rats, a region of the brain which is thought to be involved in thermal-homeostasis (Wechselberger et al. 2006).

Together these results demonstrate that the TREK channels are critical for mechano- and thermo-sensation.

A recent study has demonstrated that TREK-1 is a major mediator of morphine-induced analgesia. TREK-1 knockout mice displayed reduced analgesia in a range of

models, including temperature insult, post-operative pain and neuropathic pain models (Devilliers et al. 2013). Remarkably however, ablation of TREK-1 had no significant effect on the serious adverse effects of morphine (constipation, respiratory depression and withdrawal), suggesting that selective central modulation of TREK-1 could have substantial therapeutic potential in the treatment of pain (Devilliers et al. 2013).

5.2 Neuroprotection

The modulation of TREK channels by environmental changes associated with central nervous system insult such as intracellular acidification and generation of arachidonic acid has prompted speculation that the channels may be involved in neuroprotection (Lauritzen et al. 2000; Buckler & Honoré 2005). Theoretically activation of TREK channels would hyperpolarise cells and could thereby decrease excitotoxicity. In support of this theory the neuroprotective effects of TREK channel modulators such as α-linoleic acid (LNA), arachidonic acid (AA), riluzole and sipatrigine have been well documented (Lauritzen et al. 2000; Duprat et al. 2000; Meadows et al. 2001).

Interestingly a number of studies point towards such a protective role: Firstly, knockout of TREK-1 resulted in decreased survival rate and increased seizure frequency induced either by kainic acid or pentylenetetrazol (PTZ), or following reperfusion after carotid artery occlusion-induced global ischaemia, and spinal cord ischaemia (Heurteaux et al. 2004). The neuroprotective effect of LNA and AA was also lost in TREK-1 knockout, but this was not seen for TRAAK KO (Heurteaux et al. 2004). Knockout mouse studies also suggest that TREK-1 is neuroprotective after focal ischaemia induced by atmospheric decompression (Vallee et al. 2012).

Knockout mice showed increased susceptibility to decompression sickness, death, and neurological impairment.

In contrast, TRAAK knockout itself conferred a neuroprotective phenotype to mice following focal cerebral ischaemia. This was explained by a unique metabolic profile in knockout mice including increased brain levels of the osmolytes taurine and *myo*-inositol which may protect from the toxic effects of cellular oedema (Laigle et al. 2012). This result implies that abolishing TRAAK function is neuroprotective, which contrasts to the supposition for TREK-1, but may be supported by the protective effect of the TREK/TRAAK channel inhibitor sipatrigine.

5.3 Other CNS functions

Intriguingly, TREK-1 knockout confers a depression-resistant phenotype (Heurteaux et al. 2006). Knockout mice performed differently to their wild type congeners in a battery of behavioural tests of depression, with results showing striking similarity to wild type mice treated with the antidepressant fluoxetine. In addition, decreased corticosterone levels in response to stress, increased serotonergic excitability in the dorsal raphe nucleus, increased basal dentate gyrus neurogenesis and increased fluoxetine-induced neurogenesis were observed in knockout mice, all of which may imply roles in the aetiology or pharmacotherapy of depression (Heurteaux et al. 2006). Elsewhere the anti-depressive effect of a TREK-1 specific inhibitory peptide spadin has also been reported (Mazella et al. 2010; Moha Ou Maati et al. 2012). Interestingly, human genetic polymorphisms in the *KCNK2* gene have been associated with major depressive disorder, comorbidity with psychotic symptoms, and the likelihood of beneficial response to fluoxetine and/or citalopram (Liou et al. 2009; Congiu et al. 2015; Perlis et al. 2008).

TREK-1 knockout in mice also imbues decreased sensitivity to volatile anaesthetics (Heurteaux et al. 2006). These drugs activate TREK-1 and TREK-2 channels which would be expected to decrease neuronal excitability and may be integral to their therapeutic action.

Effects on spatial learning of specific knockdown of TREK-2 in the entorhinal cortex have also been reported, and neurotensin-induced spatial learning facilitation is abolished in TREK-2 knockout mice (Deng et al. 2009; Xiao et al. 2014). Additionally the expression of TREK-2 in cerebellar granule cells may suggest a role in motor co-ordination (Simkin et al. 2008). However TREK-1, TREK-2 and TRAAK knockouts have been subjected to a broad range of tests for learning and memory, and motor coordination and no significant phenotype was observed (Mirkovic et al. 2012).

Roles for TREK-1 in astrocyte function and glutamate release and in regulating immune cell transmigration across blood brain barrier have recently been suggested (Bittner et al. 2013; Woo et al. 2012).

5.4 TREK channels outside the nervous system

TREK-1 is expressed in rat atrial and ventricular tissues where it may be involved in the ionotropic effects of β-adrenergic input or mechano-electrical feedback for repolarisation (Terrenoire et al. 2001; Tan et al. 2004). In addition, roles for TREK-1 in the endothelium-derived vasodilatory response in mesenteric arteries and for fatty-acid induced vasodilation of the basilar artery have been suggested (Garry et al. 2007; Blondeau et al. 2007), but these effects were not recapitulated in a later study (Namiranian et al. 2010).

Elsewhere, regulation of TREK channels by the NO/cGMP/PKG pathway has been implicated in the control of myenteric contractility (Sanders & Koh 2006), and

TREK-1 alone, or TREK-1 in combination with TRAAK have been implicated in the control of smooth muscle tone in human bladder and myometrial smooth muscle cells, respectively (Lei et al. 2014; Baker et al. 2008; Baker et al. 2010; Tertyshnikova et al. 2005; Buxton et al. 2010).

TREK-2 has been reported to be involved in the protection from apoptosis in the kidney (Peyronnet et al. 2012), whilst pro-proliferative TREK channel activity has been suggested for prostate cancer cells, where the level of TREK-1 expression correlates to disease progression (Voloshyna et al. 2008). In contrast decreased TREK-1 expression in lung alveolar epithelial has been associated with increased proliferation (Schwingshackl et al. 2012).

Additionally, TREK-1 currents in adrenal zone fasciculata (AZF) cells may indicate a role for the channel in endocrine cells. Here ATP-regulation of TREK-1 may couple channel activity to metabolic stimuli and cortisol secretion from AZF cells is stimulated by curcumin (Enyeart et al. 2002; Enyeart et al. 2008).

Functional TREK-2 expression in insulin secreting MIN6 cells has also been reported where regulation of RMP by TREK-2 may control secretion in this pancreatic β-cell line (Kang, Choe, et al. 2004).

A TREK-2-like current has also been reported in B lymphocytes and a B cell derived cell line (WEHI-231) (Zheng et al. 2009a). Again it was proposed that TREK-2 may regulate RMP and thereby influence calcium influx, proliferation and apoptosis (Zheng et al. 2009a).

Lastly, TREK-1–like currents have been reported in periodontal ligament fibroblasts where the channel may contribute to masticatory stress-induced hyperpolarisation (Ohara et al. 2006).

6. Gating models for TREK channels

The precise mechanism of TREK channel gating is currently unknown, however a number of theories have recently been proposed based on extensive functional and structural investigations.

TREK channels gated at the selectivity filter

One theory includes the principle of a constitutively open inner cytoplasmic gate. This has been proposed based upon blocker access studies which suggest that access to the intracellular quaternary ammonium binding site in TREK-1 is unhindered in closed channels (Rapedius et al. 2012; Piechotta et al. 2011). This presents a clear deviation from the classical bundle-crossing gate mechanism of K_V and Kir channels, and implies that the primary gating element exists elsewhere.

Gating at the selectivity filter in TREK (and other K2Ps) has been suggested for modulation by numerous stimuli (Cohen et al. 2008; Bagriantsev et al. 2011; Zilberberg et al. 2001). Stabilisation of the open channel by extracellular potassium indicates that filter-gating occurs, and mutations around the pore helices profoundly activate the channels, yet the precise structural mechanism remains to be delineated (Cohen et al. 2008; Bagriantsev et al. 2011). Interestingly it has been proposed that numerous modalities converge upon a singular selectivity filter gate, and that intracellular modulation is transduced via the C-terminus and M4 to couple regulation to filter gating (Bagriantsev et al. 2011; Bagriantsev et al. 2012). Decoupling of the C-terminal domain by introduction of a triple glycine linker at the distal end of M4 (to impart flexibility) results in loss of C-terminal regulation, and increased external pH regulation (Bagriantsev et al. 2012). This latter finding

indicates that C-terminal activation stabilises the filter-gate in an open conformation and blunts modulation via the separate extracellular-pH mechanism (Bagriantsev et al. 2012).

Activation of the channel via intracellular mechanisms is thought to involve the C-terminus coupling with the membrane (Sandoz et al. 2011). This presumably entails an upwards movement of the proximal C-terminus, which contains a multiply-charged amphipathic helix facilitating lipid head group interactions. Coupling of the C-terminus to the filter-gate would necessitate conformational changes within the connecting M4 helix and it has been suggested that this movement can occur independently and additively in each monomer (Bagriantsev et al. 2012). This break down in subunit symmetry in gating would represent another diversion from classical potassium channel activation, which involves concerted movements of subunits.

However, the filter-gate model has been challenged by an alternative model recently proposed for TRAAK where an upward movement of M4, and consequent closure of the fenestration abolishes access for an occlusive lipid which gated the channel, see Figure 8 (Brohawn et al. 2014).

Are TREK channels lipid-gated?

Recent crystal structures show a potential route for hydrophobic drugs through the lateral fenestrations and thus the possibility remains that long-chain QA blockers could access their binding site through the membrane, potentially confounding the interpretations of the aforementioned blocker access studies (Piechotta et al. 2011). However, the presence of a lipid at the QA binding site in a closed channel, as proposed in the Brohawn model, would be expected to decrease the kinetics of QA

block, which was not observed experimentally (Rapedius et al. 2012; Piechotta et al. 2011).

The recent resolution of the gain-of-function G124I and W262S TRAAK mutants showed channels with open fenestrations, see Figure 8 (Lolicato et al. 2014). In these structures no lipid-like density was observed, despite the access route being present, which may be explained by a loss of lipid molecule during the crystallisation process, or alternatively may indicate that the presence of the lipid in the aforementioned TRAAK and TREK-2 structures is an artefact of their crystallisation.

Thus, it appears unlikely that lipid occupancy in the space occupied by the tubular electron density in TREK-2 and TRAAK crystal structures acts as a primary gating element, though further work is required to conclusively prove this.

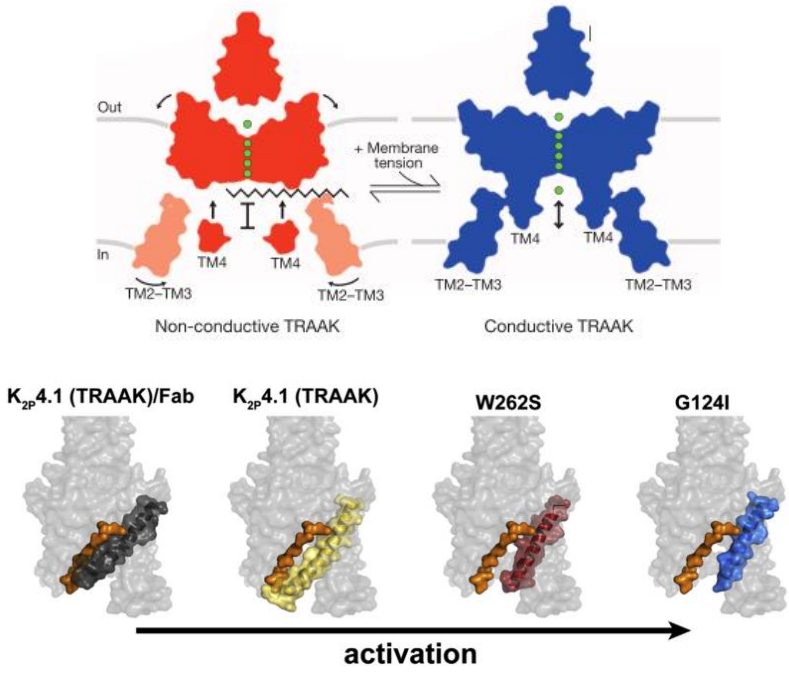

Figure 8: Proposed gating models for TRAAK (taken from Brohawn et al. 2014 and Lolicato et al. 2014). *Top: Brohawn and colleagues' model for TRAAK actiation where **s**tretch activation includes an upward movement of TM4 (M4,) closing the fenestrations and prevents access for the gating lipid (zigzag line). Bottom: Lolicato and colleagues model for TRAAK activation where gain of function mutants show increased M4 straightening.*

Proposed gating mechanisms in other K2P channels

Interestingly, elsewhere an inner gate in K2P channels has been proposed based on investigations of the drosophila ORK1 channel where access of barium for its intracellular binding site was decreased in glycine-to-valine mutant channels (KCNK0). These mutations, chosen to mimic the bundle-crossing gated *Shaker* channel, were proposed to stabilise a closed inner-gate (Ben-Abu et al. 2009). However, with the recent resolution of TREK-2 and TRAAK in multiple conformations it is hard to imagine how these particular mutations would introduce steric or hydrophobic hindrance in TREK channels.

Lastly, a hydrophobic barrier consisting of a ring of leucine sidechains within the inner pore has been mooted as a possible gating element in the related TWIK-1 channel (Aryal et al. 2014). The homologous residues in TREK channels are smaller (glycine and alanine) and so the contribution of this region to gating is predicted to be lower. Still, the possibility of some hydrophobic contribution to permeation energy or channel gating in TREK channels remains.

Therefore significant questions about the mechanisms by which K2P channels gate persist. The objectives of my DPhil project could largely be categorised into 2 themes. Firstly, we wished to better elucidate the relationship between structure and function in TREK channels with particular focus on the structural basis for polymodal regulation. Secondly, I wished to investigate the mechanism of action of pharmacological modulators of the channels, both postulated activators in the case of the alkylamides, and inhibitors such as norfluoxetine, carvedilol and fluphenazine.

Chapter 2: Methods

In this chapter I will detail the methods used in the preparation and implementation of electrophysiological investigations of TREK channel function as expressed in *Xenopus* oocytes. All chemicals were purchased from Sigma unless otherwise stated.

1. *Xenopus* oocyte preparation

Adult female *Xenopus* laevis were sacrificed by immersion in 5% tricaine methanesulfonate (MS-222) for 15 minutes before death was confirmed by decapitation, in accordance with project and personal licenses of the Animals (Scientific Procedures) Act 1986 and after approval by the University of Oxford's Local Ethical Review process. Oocytes were removed from adult female *Xenopus* laevis (Xenopus 1, Dexter, MI, USA) and dissociated by a 2-step incubation protocol wherein cells were first incubated for 30 min in a Ca^{2+} free defolliculation buffer consisting of (in mM): 83 NaCl, 2 KCl, 1 $MgCl_2$ and 10 HEPES (pH 7.6) supplemented with 2mg/ml collagenase (type A; Roche). Cells were then rinsed in enzyme free defolliculation buffer before a 40 min second incubation step in fresh 2 mg/ml collagenase solution. Defolliculated stage V and VI oocytes were selected for injection (additional manual defoliculation was used when necessary). For storage cells were maintained in ND96 solution containing (in mM): 96 NaCl, 2 KCl, 1.8 $CaCl_2$, 1 $MgCl_2$, 10 HEPES, 2.5 sodium pyruvate (pH 7.4) supplemented with 50 μg/ml gentamycin, 50 μg/ml tetracycline, 50 μg/ml ciprofloxacin and 100 μg/ml amikacin.

2. Molecular biology, cRNA preparation and injection

2.1 Point mutations

The long human TREK-1 isoform c (NP_001017425), short hTRAAK isoform (ACH86094), full length hTREK-2 isoform 3 (NP_612191) and hTASK-1 (NP_002237) were used and referred to as wild type. All mutations, truncations and chimeras were made onto these background sequences.

K2P channel constructs subcloned into the oocyte expression pBF vector were used for all molecular biology. The pBF vector incorporates 3' and 5' untranslated regions of the *Xenopus* β–globin gene to boost expression (Krieg & Melton 1984), as well as a 5' GCCGCCACC Kozak sequence preceding the start codon.

Polymerase chain reaction (PCR) mutagenesis

Mutagenesis was performed using mutant codon-containing forward and reverse primers (Sigma Aldrich) and PCR reactions carried out using a modification of the Pfu Ultra DNA Polymerase kit (Agilent Technologies), mutagenesis method as below:

37.5 µl molecular biology grade water

5 µl Pfu ultra reaction buffer

3 µl primer mix (1.5µl of both the forward and reverse primers, at 10 mM)

1 µl dNTPs (10 mM of each nucleotide)

1 µl of template DNA (~100 ng/µl)

1 µl Pfu Ultra enzyme

1.5 µl DMSO

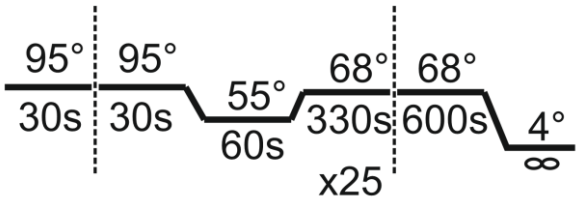

Figure 1: *Reaction protocol for mutagenesis PCR reactions using Pfu Ultra DNA Polymerase kit (temperatures in °C).*

The resultant PCR reaction product was supplemented with 1µl DpnI endonuclease enzyme (10 units/µl; Thermo Scientific) and incubated at 37°C for 1 hour, after which the reaction was cleaned up using the QiaQuick PCR purification kit (Qiagen) and eluted in 30 µl of molecular biology grade water.

Heat shock transformation

80 µl of chemically competent DH5α cells (Invitrogen) was added to the purified PCR product and incubated on ice for 25 min. The cell mixture was then subjected to heat shock by immersion in water at 42°C for 45 sec before being returned to ice for a further 5 min prior to plating. Cells were then plated by pipetting onto agar plates (Luria Broth agar supplemented with 0.05% carbenicillin) and spread uniformly using a single-use plastic spreader. Plates were incubated at 37°C overnight and once colonies were visible plates were kept at 4°C until inoculation. For inoculation a single colony was picked using a standard plastic pipette tip and incubated in 4ml Luria Broth at 37° and 200 rpm for 12-16 hours.

DNA Extraction

DNA was extracted from transformed cells following overnight culture. Briefly, the cell suspension was pelleted by centrifugation (2,000g for 10 min) before alkaline

lysis extraction using the QiaPrep Spin Miniprep kit (Qiagen). Samples were eluted into 50 µl of molecular biology grade water which typically yielded 100-500 ng/µl concentrations. The resultant clean samples were sent for sequencing (Source Bioscience, Oxford) using either the SP6 forward sequencing primer (ATTTAGGTGACACTATAG), the pBFR7 reverse sequencing primer (CTACATTTTGGGGGACAAC), or both.

2.2 Chimeric channel generation

PCR

Chimeric constructs were created using overlap extension PCR using Pfu Ultra DNA Polymerase kits (Agilent Technologies). Reaction protocols were as described above for mutagenesis but overlap extension PCR involved firstly, the generation of two intermediate constructs which were then mixed for a second step to yield the final chimeric sequence, as shown in Figure 2.

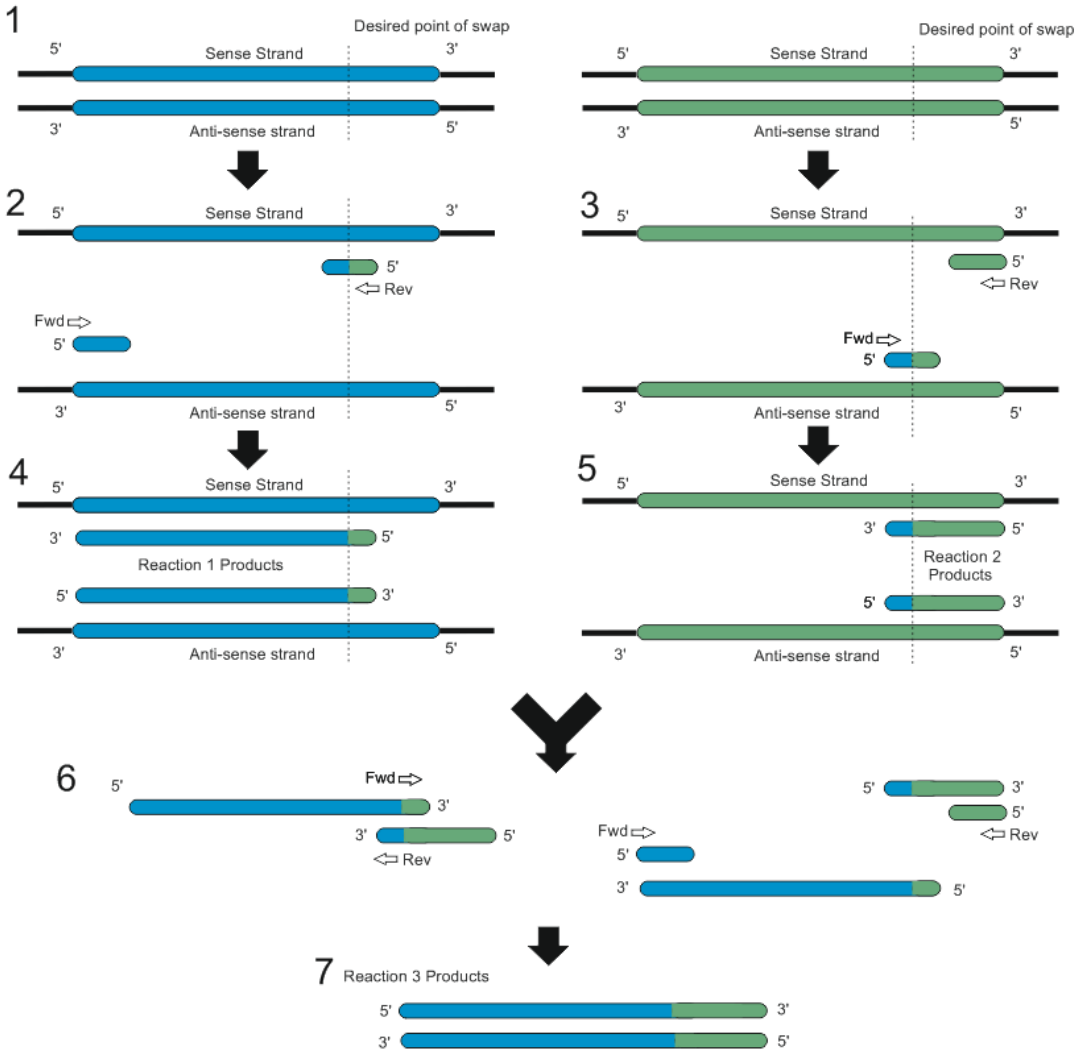

Figure 2: Overlap extension PCR. *1) The two constructs in which the domain swap is desired with the gene of interest in blue or green. 2) Reaction 1 set up to include a forward primer complementary to the antisense strand (including restriction enzyme site at 5' end), and a reverse primer which is complementary to the final gene sequence of the sense strand of the blue construct at the 3' end and complementary to the desired sequence of the green construct at the 5' end. 3) Reaction 2 set up to include a forward primer with the 3' end complementary to the antisense strand of the green construct with the 5' end including the desired sequence of the blue construct, and a reverse primer complementary to the sense strand and including the desired restriction enzyme site at the 5' end. 4 and 5) The respective PCR products from Reactions 1 and 2. 6) The resultant PCR products of reactions 1 and 2 are mixed with the initial forward and reverse primers from Reaction 1 and Reaction 2 respectively. 7) Final product from Reaction 3 with complete chimeric construct (flanked by desired restriction enzyme sites)*

Restriction enzyme digest

The chimeric product of the second overlap extension step was then digested with restriction enzymes using the reaction mixture below:

25 µl PCR product

5 µl 10x Buffer D (Promega)

2.5 µl XbaI (10 units/µl)

2.5 µl BgiII (10 units/µl)

15 µl molecular biology grade water

Restriction enzyme digestion reactions were incubated for one hour at 37°.

Gel purification

Following digestion the resultant products were isolated by electrophoresis using a 1% agarose gel (110 mV for 25 min), the desired band was cut and gel purification was performed using QiaQuick Gel Purification kit (Qiagen).

Ligation

Ligation into XbaI/BgiII digested pBF vector was performed using T4 DNA Ligase (Promega) using the following reaction mixture:

10µl Cut insert DNA (PCR product)

2.5µl Cut vector DNA (to give approximate 4:1 ration of insert to vector)

1.5 µl 10x T4 DNA ligase buffer

1 µl T4 DNA ligase enzyme (3 units/µl)

2.3 Truncated channel generation

Truncated constructs were generated using forward and reverse primers incorporating XbaI and BgiII recognition sequences respectively. PCR reactions using these truncation primers, digestion, purification and ligation were conducted as described above.

2.4 cRNA production and injection

The desired channel construct was initially linearised using MluI:

15µl Channel Construct (in pBF, 100-500 ng/µl)

5µl 10x Buffer D (Promega)

4µl MluI (10 units/µl)

26µl molecular biology grade water

Digestion reactions were incubated for one hour at 37°C, purified using QiaQuick columns and eluted into RNAse free Eppendorf tubes using RNAse free water (Qiagen).

Transcription

Cut DNA was transcribed using the Amplicap™ SP6 Kit (Cambio) and cleaned using the RNAeasy Mini Kit (Qiagen) before running on an electrophoresis gel to assess RNA integrity. Concentration was measured using a Nanodrop 1000 Spectrometer (Thermo Scientific).

Injection

Cells were injected up to 4 days post-isolation and injected with between 1-4 ng of RNA. Experiments were performed 12-24h post injection. For measurements of basal whole cell currents cells were injected with 4 ng of RNA and recorded exactly 24 hour post-injection.

3. Drug Preparation

Samples of spilanthol and IBA were provided by Pfizer. Desiccated purified solid was dissolved in 100% DMSO at a concentration of 100mM and aliquoted into glass vials. Vials were purged with N_2 and stored at -80°C. On the day of experimenting vials were defrosted and DMSO stocks were dissolved in 0.1% DMSO-containing ND96 (1 in 1000 dilution; final DMSO concentration 0.2%).

Norfluoxetine (Toronto Research Chemicals), carvedilol, fluphenazine, BL-1249 and arachidonic acid were dissolved in DMSO and thawed prior to dissolution in aqueous buffers for final concentrations. Serial dilutions were performed for dose response experiments and DMSO levels were supplemented to maintain a constant concentration across the dilution range. Final DMSO concentration did not exceed 0.3%, unless otherwise stated.

Tetrapentylammonium chloride and barium chloride were added to directly to aqueous buffers and diluted accordingly.

4. Two-electrode Voltage Clamp Electrophysiology

The recording setup was arranged as indicated below in Figure 3. Electrodes were pulled from thick-walled borosilicate glass (Harvard Apparatus) and filled with 3 M KCl. Cells were placed in a plastic recording chamber of ~350 µl volume. ND96 bath solution was used for all recordings; pH was adjusted using either NaOH or HCl. Oocytes were perfused with solution via a peristaltic pump perfusion system. Data was acquired with pClamp (Axon Instruments); currents were recorded using a GeneClamp 500 amplifier (Axon Instruments) and digitised using a Digidata 1322A (Axon Instruments). Currents were recorded from voltage protocols as described for each experiment. Unless otherwise stated, currents recorded from voltage steps to 0 mV were reported.

Temperature was controlled via an in-line perfusion heating controller (Multi Channel Systems) and measured using a K101 Digital Thermometer (Voltcraft) placed in the bath solution close to the cell. For solutions used at elevated temperatures the pH was adjusted to the desired value whilst the solution was at the intended elevated temperature to avoid undesired temperature-dependent shifts in pH.

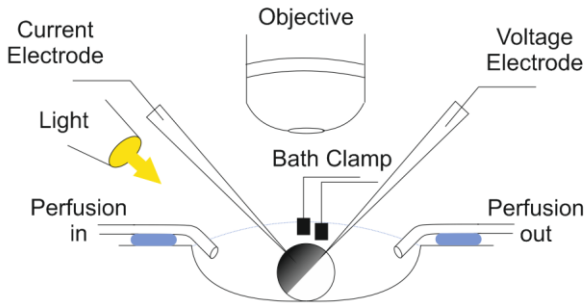

Figure 3: The Two-Electrode Voltage Clamp Set Up. *Oocytes placed in recording chamber and submerged in solution. The oocyte was impaled by two glass microelectrodes (connected to Gene Clamp 500 amplifier and Digidata 1322A digitiser) to record membrane voltage (voltage electrode) and inject current to maintain voltage clamp (current electrode). Transmembrane voltage recorded in reference to the 0mV bath voltage maintained by the bath clamp. Perfusion inflow and outflow was controlled by a peristaltic pump.*

5. Patch Clamp Electrophysiology

Giant-patch electrodes were pulled from thick-walled borosilicate glass (Harvard Apparatus) and polished to give pipette resistances around 0.4-0.8 MΩ when filled with patch solution. Recording were performed within bath solution upon a glass slide mounted atop an inverted Nikon Eclipse TE-2000-U microscope. Pipette solution contained (in mM) 116 NaCl, 4KCl, 1 $MgCl_2$, 1.8 $CaCl_2$, 10 HEPES (pH 7.4); whilst bath solution contained (in mM) 120 KCl, 1 NaCl, 2 EGTA, 10 HEPES (pH 7.3). Patches were perfused via a gravity flow perfusion system and the bath solution application was controlled by an RSC-200 Rapid Solution Changer (Bio-Logic). Data was acquired with pClamp (Axon Instruments), currents were recorded using an Axopatch 200B (Axon Instruments), filtered at 1 or 2 kHz and sampled at 10 kHz (Digidata 1322A, Axon Instruments). Macroscopic currents from inside out patches were recorded from voltage ramps and steps as described for each experiment. Currents from 0 mV steps were reported unless stated otherwise.

As current recordings from TREK channels have a propensity to increase over time (run up) in excised patch clamp experiments only patches where current levels had stabilised within 1min post-excision were used for analysis. For quantification of mechano-activation only patches with stable basal currents >150 pA (at +60mV) were used.

For tests of mechano-sensitivity ~-11mmHg of negative pressure (calibrated using a Druic DPI260 Pressure Indicator) was applied through the patch pipette manually using a 1ml syringe.

Reproducible levels of suction were generated by retracting the piston in the syringe by 0.04ml using the graduations on the syringe, and locked using a plastic three-way valve. Suction was applied by opening the three-way valve so that the syringe pressure was equalised with the pipette holder and electrode. Stable mechano-activation was regularly observed in unreported preliminary experiments for 1-2 minutes which was taken as reassurance that the system was capable of maintaining stable pressure levels.

Rapid pressure application, required for analysis of mechano-activation kinetics, was achieved by quickly opening the three-way valve manually. This manual application allowed for reproducible, rapid activation of TREK-2 which was indistinguishable in latency from subsequent unreported experiments conducted with an HSPC-1 High-Speed Pressure Clamp system (ALA Scientific).

Due to the endogenous expression of a mechano-sensitive non-selective cation channel in the oocytes stretch activation of TREK currents was measured at 0mV (Yang & Sachs 1990). At this membrane potential the endogenous component was minimised.

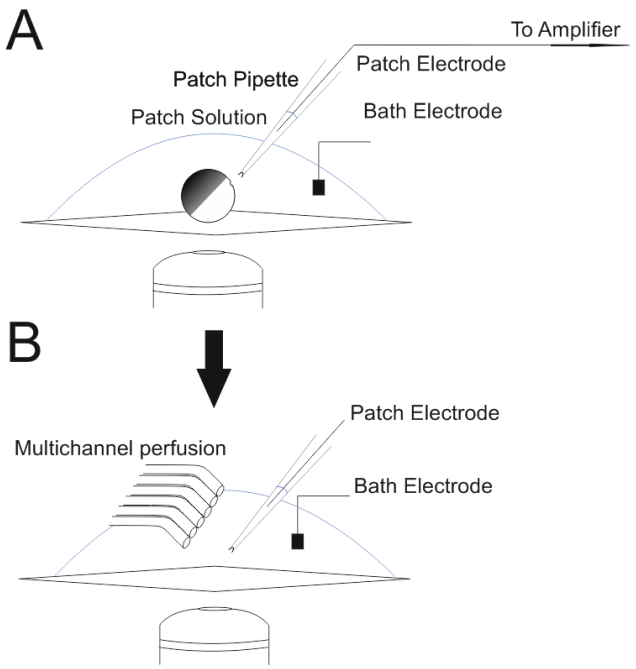

Figure 4: The patch clamp recording setup. *The oocyte was placed upon a glass slide over an inverted microscope. A gigaseal was formed by placing a glass microelectrode (pipette resistance 0.4-0.8MΩ) upon the surface of the oocyte and releasing a small amount of positive pressure. After seal formation the inside-out configuration was reached by rapid excision of the patch from the cell (A). Then the cell was removed from the bath and the patch electrode brought into the vicinity of the multichannel perfusion system (B).*

6. Data Analysis

Data was analysed using Clampfit (Molecular Devices) and Microsoft Excel. Percentage inhibition was calculated from stable basal currents following excision using the equation below:

$$\%\ inhibition = \left(1 - \left(\frac{Iinhibited}{Ibasal}\right)\right).100$$

Where *Iinhibited* refers to the recorded current in each concentration of drug and *Ibasal* refers to the measured current prior to drug administration. Dose response curves were fitted by the Hill equation:

$$\%\ Inhibition = Inhmax\ .\ ([drug]^H/(IC50^H+[drug]^H))$$

Where Inhmax refers to the maximal inhibition, IC50 is the concentration at which 50% of the maximal inhibition was observed and H is the Hill coefficient.

Fold activation was calculated from the following equation:

$$Fold\ activation = \frac{Iactivated}{Ibasal}$$

Where *Iactivated* refers to the current level following application of activating stimuli and *Ibasal* refers to the stable basal current. Data was presented as mean ± S.E.M.

All experiments shown were repeated for n ≥ 3. Unpaired Student t-Tests were performed using Microsoft Excel for analysis of statistical significance of data sets with normal distribution (as assessed using the Kolmogorov-Smirnov test function of MATLAB, significance at 5% level). Where normal distribution could not be assessed (i.e. when sample sizes were small) a Wilcoxon Rank Sum test was performed using MATLAB to test for significant differences in population medians.

Chapter 3: Alkylamide regulation of TREK channels

1. Introduction

At the time of starting these studies in 2011 our understanding of the relationship between K2P structure and function underwent a major change with the publication of X-ray crystal structures of TWIK-1 and TRAAK (Miller & Long 2012; Brohawn et al. 2012). In this way the field had begun to catch up with the advancements made in the study of other potassium channels, such as the voltage-gated and inward rectifier channels (Long et al. 2007; Nishida et al. 2007). However despite these advances there remains a dearth of pharmacological modulators for the K2P family.

2. The search for TREK channel modulators

For millennia, ever since Hippocrates prescribed willow extract to ease the pain of labour in 400BC it has been standard practice in the search for biologically active molecules to turn to plant derived molecules in the hope of finding new lead compounds and precursors. At the outset of this project we were interested in the alkylamides, a group of phytochemicals with newly found effects on K2P channels. This family of molecules are abundant in a number of plants used in both folk medicine and Eastern cuisine for their somatosensory effects (Dubey et al. 2013).

One widely used plant genus is *Spilanthes* (also mentioned as *Acmella*), a member of the asteraceae family. The flowering heads of *S. Acmella* (commonly known as the "toothache plant" in India, or "Jambu" in Brazil) are used in various traditional remedies for a variety of purposes including as an analgesic agent, local anaesthetic and anti-inflammatory agent (Hossain et al. 2012; Peiris et al. 2001; Dubey et al. 2013). Alkylamides comprise the major phytochemical constituents of *Spilanthes*, the most abundant of which is spilanthol ((2E,6Z,8E)-N-isobutylamide-2,6,8-decatrienamide (Leng et al. 2011; Yasuda et al. 1980).

Elsewhere alkylamides are also abundant in plants of the *Xanthoxylum* genus, which includes the Sichuan pepper. Interestingly an alkylamide isolated from these peppercorns, hydroxy-α-sanshool, was identified as an inhibitor of the TASK-1, TASK-3 and TRESK K2P channels (Bautista et al. 2008). It was proposed that hydroxy-α-sanshool inhibition of TASK and TRESK channels in sensory neurons would provoke action potential propagation in the neurons by depolarising the membrane potential and thereby elicit the tingling paraesthesia associated with chewing the peppercorns. Further investigations have also demonstrated effects of sanshool on a number of other ion channel targets, including TRP and voltage gated sodium channels, which may also contribute to their complex somatosensory profile (Koo et al. 2007; Riera et al. 2009; Tsunozaki et al. 2013).

Alkylamides, as the name suggests, are comprised of a long alkyl tail and a polar amide head group, see Figure 1. This amphipathic nature is similar to biological fatty acids and lysophospholipids, many of which are known to modulate TREK channel activity (Patel et al. 1998; M Fink et al. 1998; François Maingret et al. 2000; Comoglio et al. 2014).

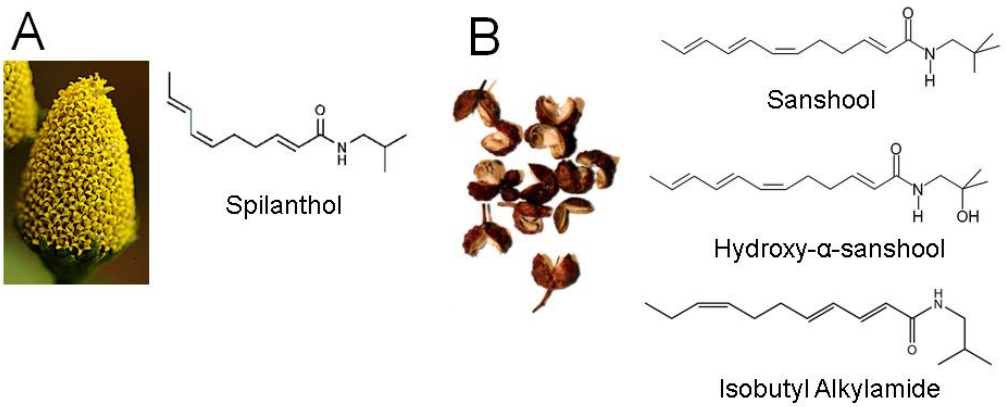

Figure 1: Plant derived alkylamides. *A) The flowering head of Spilanthes Acmella and the chemical structure of spilanthol. B) Szechuan peppercorns and the chemical structure for sanshool (α-sanshool), hydroxy-α-sanshool and isobutyl alkylamide (IBA).*

Whilst Bautista and colleagues reported no significant effect of hydroxy-α-sanshool on TREK channels, another study by Tulleuda and colleagues showed that a synthetic sanshool derivative isobutylalkylamide (IBA) produced a small but significant activation of TREK-1 channels (Tulleuda et al. 2011). In collaboration with colleagues at Pfizer Neusentis, I sought to investigate the mechanisms underlying the effects of spilanthol and IBA on TREK channels and to evaluate their analgesic potential.

We hypothesised that if alkylamides indeed do modulate TREK channels then by establishing their mechanism of action we may also provide insight into channel modulation by endogenous lipids whilst potentially explaining the bioactivity of alkylamide-containing folk medicines. Ultimately these investigations demonstrate that the effect of alkylamides of TREK channels are complex and assay-context dependent.

3. Results: Alkylamide modulation of K2P channels

3.1 Alkylamide activation of TREK-1 in TEVC

In two-electrode voltage clamp recordings of *Xenopus* oocytes expressing hTREK-1 spilanthol (100 μM) provoked a slow, yet marked current increase. TREK-1 currents recorded from voltage steps to -40mV from a holding potential of -80mV increased 3.99 ± 0.50 fold, with the mean time to maximal activation of 443 ± 30 s (n = 6), Figure 2. The activation of TREK-1 was dose dependent with 1 and 10 μM spilanthol increasing currents 1.1 ± 0.1 and 1.4 ± 0.2 fold respectively (n = 3), and fully reversible upon washout at all concentrations, Figure 2. Spilanthol activation occurred across the voltage range tested but appeared to be greatest at negative potentials; spilanthol increased currents at -40 mV 4.0 ± 0.5 fold (n = 6) compared with a 2.5 ± 0.1 fold increase at +40 mV (n = 3), Figure 2.

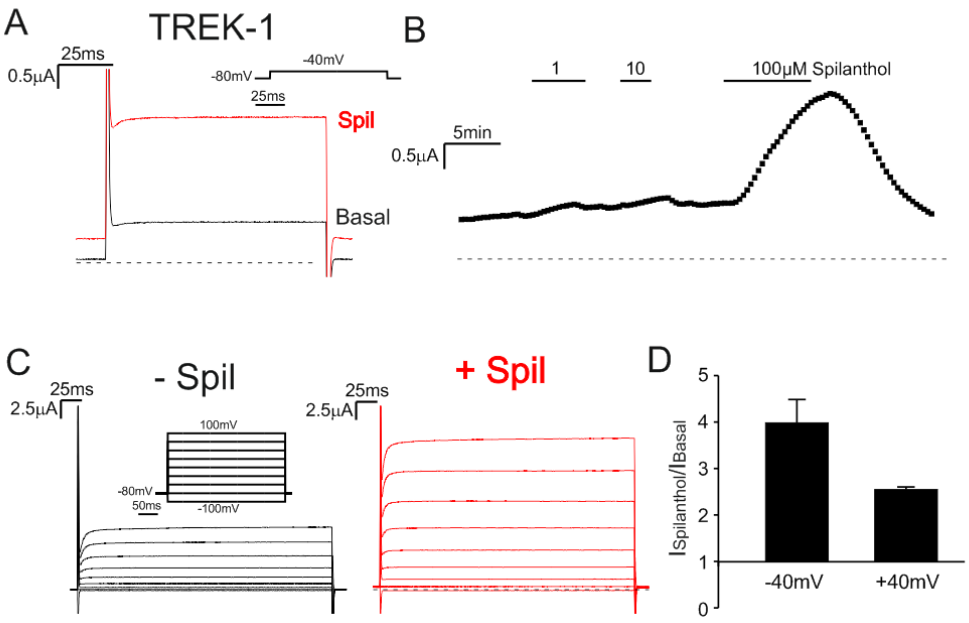

Figure 2: Spilanthol activates TREK-1 in TEVC recordings of whole *Xenopus* oocytes. *A) Example traces of TREK-1 currents held at -80 mV and stepped to -40mV (as in inset) in the absence (black trace) and presence (red trace) of 10 0µM spilanthol. B) I/t plot from example experiment showing spilanthol effect at 1, 10 and 100 µM. Cell held at -80mV and stepped to -40 mV every 5s. C) Cell expressing TREK-1 held at -80 mV and voltage stepped from -100 to +60 mV in 20 mV increments. I/V profile in the absence (left panel, black) and presence (right panel, red) of 100 µM spilanthol. D) Mean fold activation of TREK-1 currents by 100 µM spilanthol at either -40 mV (4.0 ± 0.5 fold, n = 6) or +40 mV (2.5 ± 0.1 fold, n =4).*

However, in marked contrast to TREK-1 no activation of the closely related TRAAK channel was observed during 100 µM spilanthol administration over the same time frame, currents after spilanthol administration were 1.0 ± 0.02 times basal levels (n = 7), see Figure 3 for details.

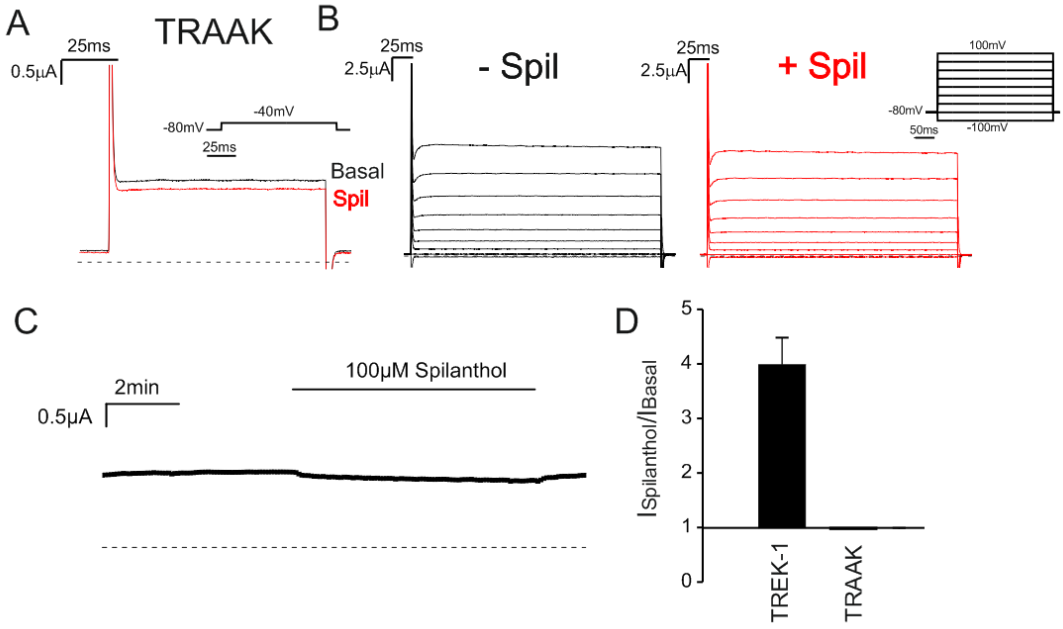

Figure 3: Spilanthol does not activate TRAAK in TEVC recordings of whole *Xenopus* oocytes. *A) Example traces of TRAAK currents held at -80 mV and stepped to -40 mV (as in inset) in the absence (black trace) and presence (red trace) of 100 µM spilanthol. B) Cell expressing TREK-1 held at -80 mV and voltage stepped from -100 to +60 mV in 20 mV increments. I/V profile in the absence (left panel, black) and presence (right panel, red) of 100 µM spilanthol. C) I/t plot from example experiment showing spilanthol effect at 100 µM. Cell held at -80 mV and stepped to -40 mV every 5 s. D) Mean fold activation of TREK-1 and TRAAK currents by 100 µM spilanthol at -40 mV (for TREK-1 spilanthol increased currents 4.0 ± 0.5 fold, n = 6; for TRAAK spilanthol were currents 1.0 ± 0.02 times basal current levels, n = 7).*

The effects of IBA were then tested for comparison. As with spilanthol, IBA provoked a slow but significant increase in TREK-1 current, with mean maximal activation 2.8 ± 0.4 fold after 536 ± 37s (n = 6), Figure 4. Again no activation of TRAAK was observed.

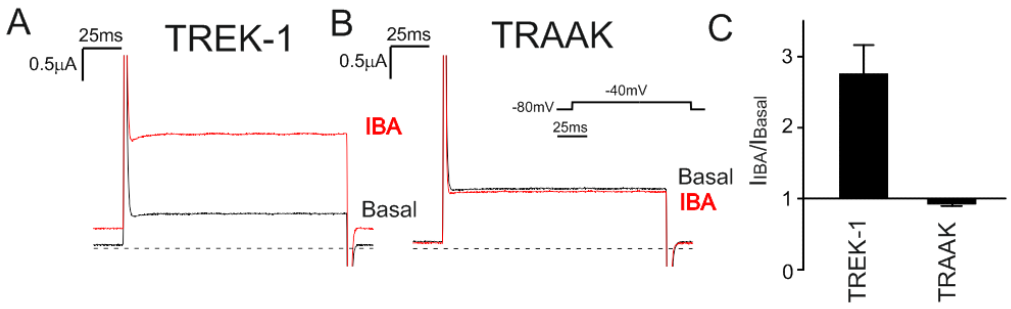

Figure 4: IBA selectively activates TREK-1 but not TRAAK in TEVC recordings of whole *Xenopus* oocytes. *A) Example traces of TREK-1 currents held at -80mV and stepped to -40mV (as in inset) in the absence (black trace) and presence (red trace) of 100μM IBA. B) Example traces of TRAAK currents held at -80mV and stepped to -40mV (as in inset) in the absence (black trace) and presence (red trace) of 100μM IBA. C) Mean fold activation of TREK-1 and TRAAK currents by 100μM IBA at -40mV (for TREK-1 IBA increased currents 2.8 ± 0.4 fold, n = 6; for TRAAK IBA currents were 0.93 ± 0.06 times basal currents, n = 6).*

These results indicate that both spilanthol and IBA evoke a significant activation of TREK-1 currents in whole cell recordings of *Xenopus* oocytes. However, parallel studies by our colleagues at Pfizer Neusentis saw strikingly different results in a series of whole cell patch clamp experiments on TREK-1 expressing HEK-293 cells.

3.2 Alkylamide inhibition of K^+ channels in whole cell patch clamp

Whole cell patch clamp studies of hTREK-1 in HEK-293 cells performed by Lishuang Cao and Alex Loucif (Pfizer Neusentis) showed a robust inhibition by 100μM IBA (currents in 100 μM IBA were 0.43 ± 0.04 times basal levels, n = 12), with a small but clear inhibition also provoked by 100 μM spilanthol (currents in 100μM spilanthol 0.82 ± 0.03 times basal levels, n = 6), see Figure 5.

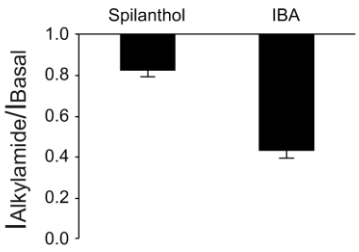

Figure 5: Spilanthol and IBA inhibit TREK-1 currents in whole cell patch clamp. *Currents were recorded from transiently transfected HEK293 cells. Inhibition of currents from voltage steps to 0mV reported (n = 6 for spilanthol and n = 16 for IBA). Data provided by Lishuang Cao and Alex Loucif, Neusentis.*

Interestingly further experiments showed that alkylamides have a non-specific inhibitory effect on a range of structurally diverse K^+ channels. For example spilanthol, IBA and sanshool decreased TRESK, $K_V1.1$ and $K_V4.3$ currents, see Figure 6.

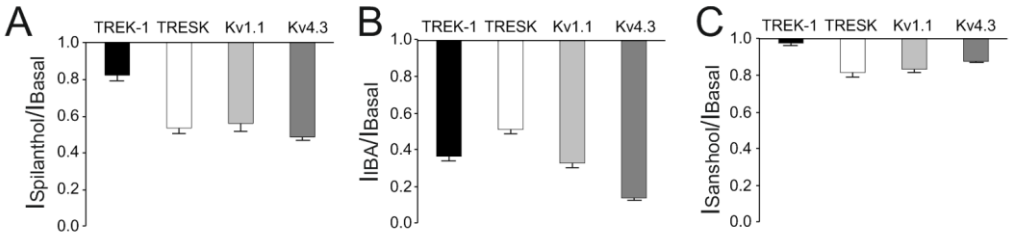

Figure 6: Alkylamides as broad spectrum potassium channel inhibitors. *Whole cell patch clamp recordings indicate that A) spilanthol, B) IBA and C) sanshool (all administered at 100μM) act as broad-spectrum potassium channel inhibitors. Inhibition recorded at current steps to 0 mV for K2P channels and steps to +30mV for K_V channels (data from Lishuang Cao and Alex Loucif, Neusentis).*

Plainly, therefore, a major discrepancy existed in the results of these seemingly similar TEVC and whole cell patch clamp experiments. A potential clue to the source of this different behaviour lay in the activation rate observed in TEVC experiments. As described above, activation of TREK-1 by spilanthol and IBA appeared to be extremely slow, with maximal effects often only reached after >5 minutes. This property often indicates an indirect mechanism of action, perhaps involving additional signalling cascades as opposed to a direct interaction with the

channel itself. A simple method to investigate whether the effect of a molecule on an ion channel is via direct interaction is to test its effects in excised patch clamp recordings. This method involves the excision and recording of a patch of membrane in isolation of the cell and its complex networks of signalling cascades. Therefore I tested the effects of spilanthol and IBA on TREK-1 currents in inside out patch clamp experiments.

3.3 Spilanthol and IBA directly inhibit TREK-1 in inside out patches

In inside-out patch clamp recordings of *Xenopus* oocytes expressing TREK-1 acute administration of 100 µM spilanthol provoked a small inhibition to 0.92 ± 0.05 times basal current levels (n = 5), whilst 100 µM IBA showed higher efficacy, inhibiting channels to 0.70 ±0.07 times basal current levels (n = 5), see Figure 7.

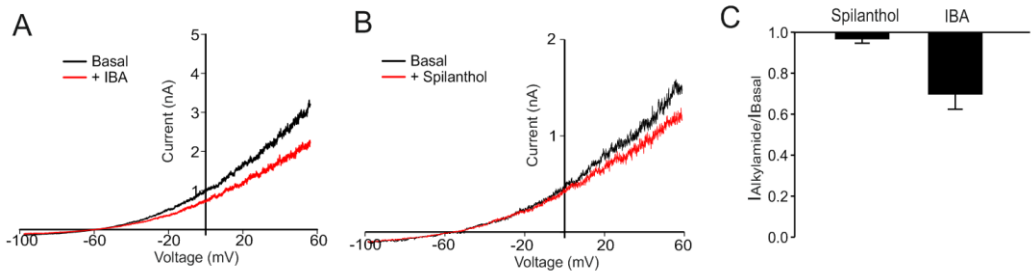

Figure 7: Spilanthol and IBA provoke slight inhibition of TREK-1 currents in inside-out patches from Xenopus oocytes. *A) Example traces for TREK-1 currents in the absence (black) and presence of 100µM IBA. B) Example traces for TREK-1 currents in the absence (black) and presence of 100µM spilanthol. C) Mean fold change of TREK-1 currents provoked by spilanthol (0.92 ± 0.05 times basal currents, n = 5) and IBA (0.70 ± 0.07 times basal currents, n = 5).*

These results demonstrate that when channels are isolated from the cellular environment alkylamides do not activate TREK-1 channels. In this way it appears that the whole cell patch clamp experiments provide a better representation of the

direct effects of the molecule than the TEVC experiments. This is perhaps expected as the whole cell configuration likely results in the dialysis of intracellular components and signalling molecules, which may be less extensive in TEVC recordings. This cytosolic dialysis may act to uncouple the TREK-1 channel from some regulatory pathways in whole cell patch clamp.

Thus, alkylamides exert a direct inhibitory effect on a range of K^+ channels, including TREK-1. However, when cellular integrity is maintained, as in whole cell two-electrode voltage clamp experiments of *Xenopus* oocytes, spilanthol and IBA activate channels by a secondary, presumably indirect mechanism.

We wished to elucidate this mechanism of activation. In order to do this I tested the effects of spilanthol on a series of chimeric, truncated and mutant channels to narrow down the modular regions responsible for the activatory effect.

3.4 Whole cell activation of TREK-1 requires the C-terminus

To investigate the difference in between TREK-1 and TRAAK, I engineered a series of chimeric channels in which the C-terminal was exchanged, Fig 8A. In cells expressing the chimeric channel comprised of the N-terminus and transmembrane domains of TREK-1 and the C-terminus of TRAAK, hereafter referred to as TREK-1(cTRAAK), no channel activation was provoked by spilanthol application, see Figure 8C. Conversely in chimeric channels comprised of the N-terminus and transmembrane domains of TRAAK and the C-terminus of TREK-1, hereafter referred to as TRAAK(cTREK-1), spilanthol provoked a fold increase in current of 3.4 ± 0.5, with a mean time to maximal activation of 533 ± 44 s (n = 8), see Figure 8C.

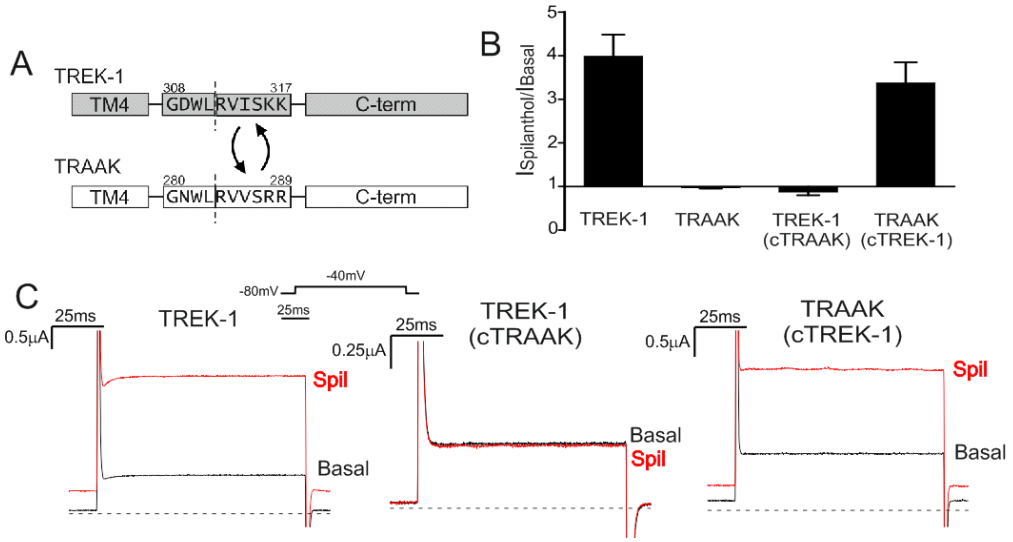

Figure 8: The C-terminus of TREK-1 is necessary and sufficient to confer sensitivity to spilanthol. *A) Chimeras made at a conserved sequence in the distal TM4 helix. B) Mean fold increase in current from steps to -40 mV for TREK-1 WT (4.0 ± 0.5 fold, n = 6), TRAAK WT (1.0 ± 0.02 times basal currents, n = 7), TREK-1(cTRAAK) (0.9 ± 0.1 times basal currents, n = 6) and TRAAK(cTREK-1) (3.4 ± 0.5 fold, n = 8). C) Example traces from cells expressing TREK-1, TREK-1(cTRAAK) (left) and TRAAK(cTREK-1) (right). Cells held at -80 mV and stepped to -40 mV.*

Therefore the intracellular C-terminal domain of TREK-1 was necessary and sufficient for spilanthol sensitivity. Notably both chimeras retained function and were activated by the non-selective TREK family activator BL-1249, Figure 9.

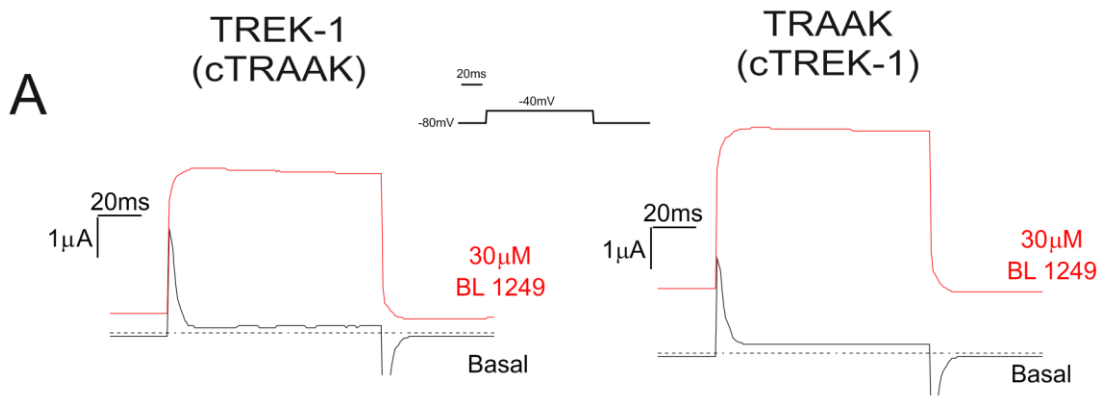

Figure 9: The TREK-1(cTRAAK) and TRAAK(cTREK-1) chimeras retain BL 1249 sensitivity. *A) Example traces showing whole cell TREK-1(cTRAAK) (left panel) and TRAAK(cTREK-1) (right panel) currents in the absence (black) and presence (red) of BL 1249, voltage protocol in inset. Note, large activation by BL-1249 masked the capacitance transients observed in black traces,*

The C-terminus of TREK-1 is over 100 amino acids long so in order to more accurately locate the critical region for spilanthol sensitivity a number of truncations were made in the TRAAK(cTREK-1) chimera. The distal 69 or 98 amino acids were truncated to form the TRAAK(cTREK-1)Δ69 and TRAAK(cTREK-1)Δ98 channels, see Figure 10A. Truncation of the final 69 amino acids appeared to decrease but not abolish spilanthol sensitivity and the channel was still significantly activated to 2.42 ± 0.28 times basal current levels, Figure 10C. Further truncation of the C-terminus in TRAAK(cTREK-1)Δ98 abolished spilanthol activation, Figure 10C.

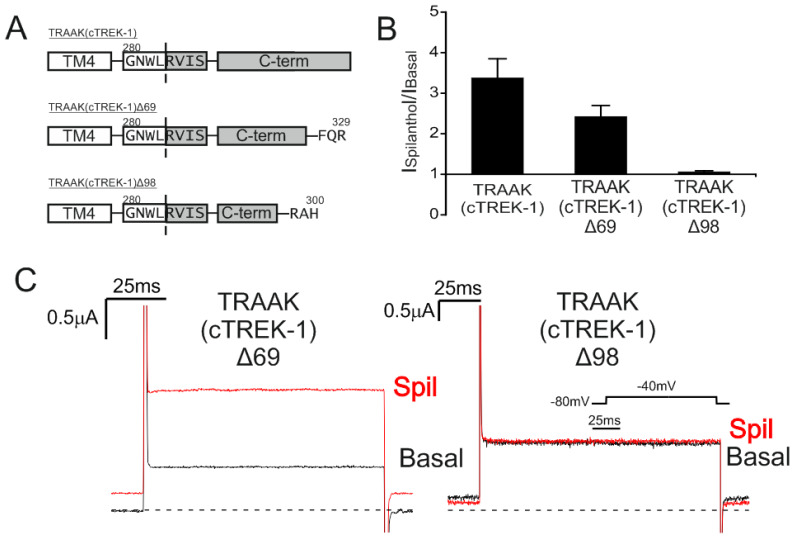

Figure 10: The effect of C-terminal truncations of alkylamide activation. *A) Truncations were made to the C-terminus of the TRAAK(cTREK-1) chimera, which flanked the PKA phosphorylation site S348A. B) Mean fold increase in current from steps to -40 mV for TRAAK(cTREK-1) (3.37 ± 0.47 fold, n = 8), TRAAK(cTREK-1)Δ69 (2.42 ± 0.73 fold, n = 7) and TRAAK(cTREK-1)Δ98 (1.06 ± 0.05 fold, n = 4). C) Example traces from cells expressing TRAAK(cTREK-1)Δ69 (left) and TRAAK(cTREK-1)Δ98 (right). Cells held at -80 mV and stepped to -40 mV.*

3.5 A C-terminal phosphorylation site is critical for alkylamide activation of TREK-1

Between H328 and R357 (the TREK-1 amino acids analogous to the site of truncation in TRAAK(cTREK-1)Δ98 and TRAAK(cTREK-1)Δ69 respectively) lies a

critical PKA phosphorylation site, S348 (Patel et al. 1998; Bockenhauer et al. 2001; Maingret et al. 2002).

Interestingly mutation of the serine to alanine in S348A completely abolished spilanthol activation altogether; current after spilanthol administration was 0.90 ± 0.08 times basal current, see Figure 11. Furthermore, as for spilanthol, activation by IBA was abolished in the TREK-1 S348A mutant; current after IBA administration was 0.86 ± 0.05 times basal current, see Figure 11.

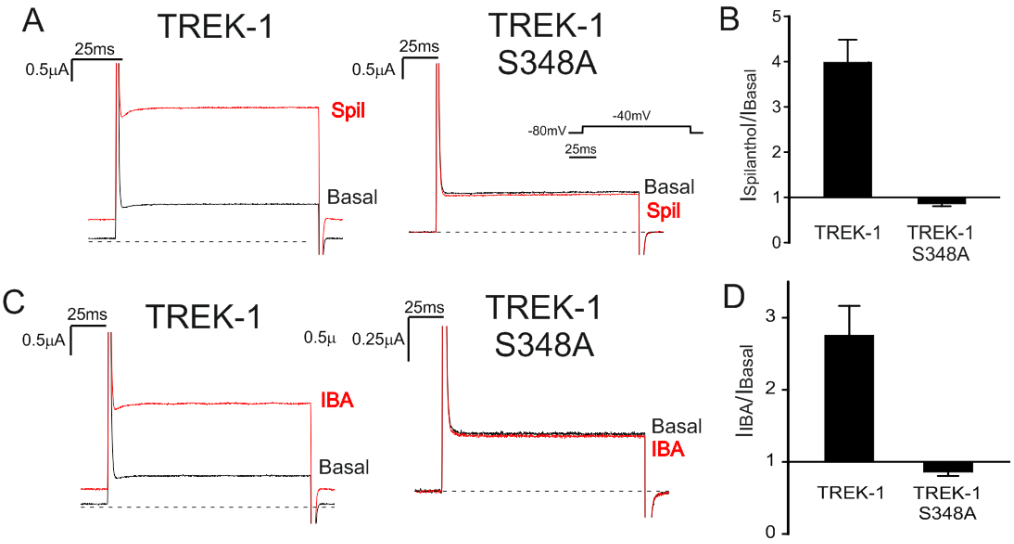

Figure 11: The C-terminus phosphorylation site S348 is critical for activatory alkylamide sensitivity in TREK-1 *A) Example traces from cells expressing TREK-1 (left panel) and TREK-1 S348A (right panel) showing currents in the absence (black) and presence (red) of 100 µM spilanthol, voltage protocol in inset. B) Mean fold increase in current upon spilanthol administration from steps to -40 mV for TREK-1 WT (3.99 ± 0.50 fold, n = 6) and TREK-1 S348A (0.90 ± 0.08 times basal currents, n = 5). C) Example traces from cells expressing TREK-1 (left panel) and TREK-1 S348A (right panel) showing currents in the absence (black) and presence (red) of 100 µM IBA, voltage protocol in inset. B) Mean fold increase in current upon IBA administration from steps to -40 mV for TREK-1 WT (2.76 ± 0.41 fold, n = 6) and TREK-1 S348A (0.86 ± 0.05 times basal currents, n = 6).*

Taken together, these results indicate that the indirect activation of TREK-1 in whole cell recordings of oocytes by alkylamides occurs via modulation of tonic inhibitory PKA-phosphorylation of S348.

3.6 Physiological implications of alkylamide modulation of TREK channels

Therefore, under certain circumstances alkylamides appear able to activate TREK-1. This could have important ramifications for the physiological effects of alkylamides. Activation of TREK-1 would be expected to hyperpolarise the resting membrane of a cell. As sensory neurones of the trigeminal and dorsal root ganglion have been shown to express TREK channels this could provide a possible explanation for the putative analgesic effects of alkylamide containing folk medicine preparations. However, it is unclear whether alkylamide activation of TREK channels actually relevant in somato-sensation, or is it a mere oocyte-specific phenomenon? To address this, our colleagues at Pfizer Neusentis used calcium imaging experiments to test the effects of alkylamide administration (in this case sanshool) on cultured mouse DRG neurones.

These experiments indicate that 100 μM sanshool administration increases intracellular calcium concentration in a subset of DRG neurones, Figure 12. This is consistent with the resting membrane potential of these cells becoming depolarised, leading to the activation of voltage gated calcium channels and the consequent influx of calcium, and is clearly in conflict with the idea that alkylamides activate K2P channels, which would be expected to hyperpolarise the resting membrane potential and would be more likely to decrease intracellular calcium concentrations.

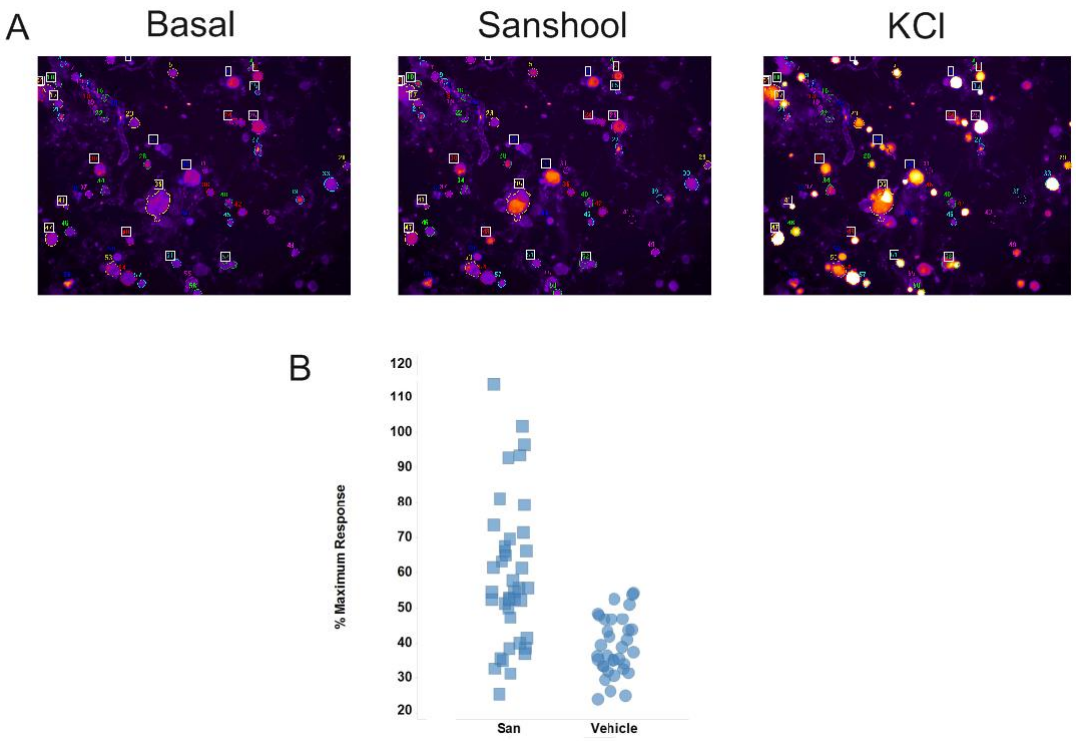

Figure 12: In cultured mouse DRG cells sanshool activates a subset of neurones in calcium imagining experiments (data and analysis from Lishuang Cao, Neusentis). *A) Example snapshot of cultured DRG cells prior to admin of sanshool (left panel), after 100μM sanshool (middle panel) and after activation by high K^+ (40mM KCl, right panel). B) Summary analysis of normalised sanshool response (percentage response relative to calcium influx induced by high K^+)*

Curiously, sanshool appeared the least effective alkylamide tested in inhibiting potassium channel activity (see Figure 6C), and therefore it is possible that elevations in intracellular calcium could instead be attributed to the previously reported activation of TRP channels by alklyamides (Koo et al. 2007; Riera et al. 2009).

In contrast, the TREK channel activation I observed in TEVC recordings may be of little significance in these cells. This could be due to differences in various pathways between oocytes and DRG cells, or it could reflect the fact that the hyperpolarising effect of TREK channel activation by sanshool is counteracted by the depolarising effect of non-specific inhibition of other K+ channels by sanshool.

4. Summary: The complex nature of alkylamide effects

Alkylamides have been shown to provoke varied somatosensory effects including tingling paraesthesia and analgesia (Lennertz et al. 2010; Tulleuda et al. 2011; Tsunozaki et al. 2013). These two effects appear conflicting, with neuronal excitation presumably underlying tingling and decreased neuronal excitability presumably underlying analgesia. Therefore it is likely that alkylamides provoke a complex myriad of effects on a range of molecular targets. Considering the activation of TREK-1 by spilanthol and IBA in TEVC experiments it is possible that this may dampen neuronal excitability in TREK-1 expressing cells and contribute to the physiological effects of alkylamides.

Elsewhere the excitatory effects of hydroxy-α-sanshool have previously been attributed to either TRP channel activation or K2P potassium channel inhibition whilst its analgesic effects were reported to be due to inhibition of voltage gated sodium channels (Koo et al. 2007; Riera et al. 2009; Bautista et al. 2008; Tulleuda et al. 2011; Tsunozaki et al. 2013). These multiple interactions indicate that hydroxy-α-sanshool is a promiscuous modulator of a range of ion channels and it is likely that other alkylamides share this property.

Comparison of the effect of spilanthol and IBA in two-electrode voltage clamp and whole cell patch clamp studies demonstrate that the effects of alkylamides on the TREK subfamily of K2P channels appear complex and assay-context specific. This complexity, alongside the non-specific nature of their activity in inhibiting a broad range of K^+ channels ultimately makes the molecules unattractive for further study as potential analgesics.

Chapter 4: Functional studies of crystallographic TREK-2 states

1. Introduction

The structural mechanisms by which K2P channels gate remain mysterious. The recent resolution of crystal structures for a number of K2P channels has given vital insight into potential stable conformations of the channels, and provide static snapshots of the channels (Miller & Long 2012; Brohawn et al. 2012; Brohawn et al. 2013). Through the convergence of data from structural, functional and computational studies we can begin to unravel the complexity of gating movements. Recently the crystal structure of the TREK-2 channel in two distinct conformations, and bound by the state-dependent inhibitor norfluoxetine were solved by colleagues in the Elizabeth Carpenter group at the Structural Genomics Consortium, Oxford. These developments provided a crucial catalyst for investigations into the gating mechanisms of TREK K2P channels, but the functional relevance of these structures was not clear. In this chapter I describe how functional analysis of TREK-2 has provided insight into the significance of these structures, and the mechanisms of gating in TREK-2.

2. The crystal structure of TREK-2

Yin Yao Dong and Ashley Pike within the Carpenter group solved structures for TREK-2 in what we have termed “down” (PDB code 4XBJ) and “up” (4BW5) conformations at 3.9 and 3.4Å, respectively, see Figure 1. These structures showed

significant similarities to the published TWIK-1 and TRAAK structures and demonstrated that TREK-2 forms as a domain-swapped dimeric channel with a distinctive intramembrane fenestrations and a pseudo symmetrical central pore beneath the characteristic K2P helical cap domain (Dong et al. 2015).

Intriguingly the structures differ in two crucial ways: firstly, a concerted movement of the M2, M3 and M4 transmembrane helices between the down and up conformations closes the intramembrane fenestration, and secondly, different ion occupancies are observed in the selectivity filter for the two structures.

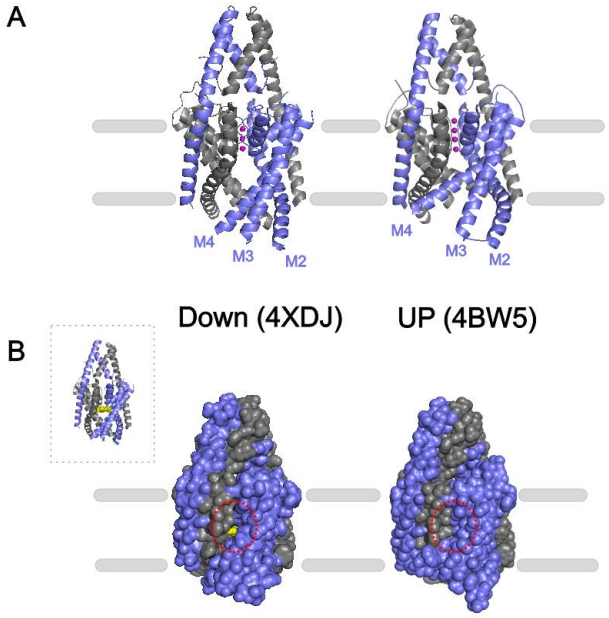

Figure 1: The crystal structure of TREK-2 in two distinct conformations. *A) The down (left) and up (right) conformations of TREK-2. B) A surface representation of the down and up conformations shows that the intramembrane fenestration (circled in red) is closed in the up conformation. In the down conformation this fenestration is occupied by an undefined tubular electron density (shown in inset in yellow).*

In the down conformation the M2/M3 linker region hangs below the predicted plane of the phospholipid bilayer whilst M4 lies almost perpendicular to the plane of the membrane. This helical arrangement results in notable lateral fenestrations within the transmembrane domain. In contrast, in the up conformation the M2/M3 linker region is predicted to interface with the inner leaflet of the phospholipid

bilayer, whilst M4 undergoes kinking and a 30° rotation moving further up into the membrane. This upward movement of M4 brings it in close proximity to M2 and closes the lateral fenestrations.

2.1 The lack of a bundle-crossing gate in K2P channels

Notably both conformations retained an open conduction pathway at the intracellular region of the channel (see Figure 2). This region is analogous to the "bundle-crossing" gate region existent in the other families of mammalian potassium channels, voltage gated- and inwardly rectifying potassium channels. In K_V and Kir channels this bundle-crossing gate is a crucial in determining whether the channel is open and conductive, with radial movements of the pore lining helices opening the channel (Doyle et al. 1998; Holmgren et al. 1998; Kuo et al. 2003; Bavro et al. 2012).

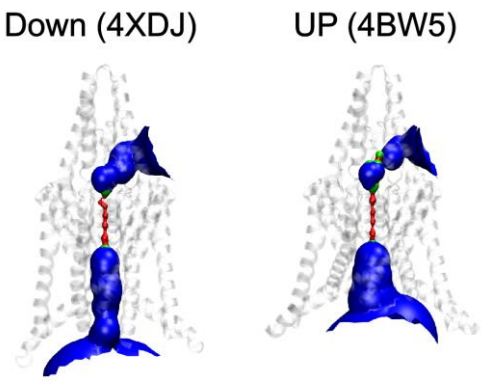

Figure 2: Both the down and up state include an open bundle crossing gate. *The solvent accessible region of the central conduction pathway for the down and up state is shown in blue and demonstrates that solvent access is unimpeded at the cytoplasmic region.*

The predicted lack of the bundle-crossing gate prompted the suggestion that K2P channels may gate primarily at the selectivity filter (Piechotta et al. 2011; Rapedius et al. 2012). With this in mind it was fascinating to note that ion occupancy within the selectivity filter varied between the distinct conformations: in the up

conformation electron density for 4 potassium ions was clearly observed, yet in the down conformation three ions were observed, with an absence of electron density in the S1 site, see Figure 1. This suggests that movement of the TM helices may gate the channel, but at the selectivity filter gate and not the helix bundle crossing.

2.2 What functional states do these conformations represent?

Taken together these differences between the conformations presented a testable hypothesis, namely that the up conformation represented an open, conductive channel whilst the down conformation represents a closed, non-conductive conformation. This prediction follows two separate lines of reasoning: firstly, it has been suggested that 4 ions in a selectivity filter of a potassium channel are required for permeation, and that deviation from this results in a non-conductive channel (Bernèche & Roux 2005; Cuello et al. 2010; Ostmeyer et al. 2013; Köpfer et al. 2014), and secondly, it has been proposed that activation of TREK channels involves a coupling of the proximal C-terminus with the phospholipid bilayer (Bagriantsev et al. 2011; Bagriantsev et al. 2012; Sandoz et al. 2011). It would be predicted that this movement would require an upward movement of M4 for transduction of activatory stimuli to the selectivity filter gate.

3. Results: Critical domains for TREK-2 channel gating

3.1 The hinge and zipper regions

We sought to test the effects of mutations in TREK-2 in the regions that appeared to be critical for inter-conversion from one crystallised conformation to the other.

Residues selected for mutation were either in the "hinge" region (F215, F244, I245, and Y315) or the "zipper" region (R237, M322, and W326), see Figure 3. The hinge consisted of packed aromatic and hydrophobic residues which appear to rearrange between conformations. It is difficult to confidently predict hydrogen bond interactions in structures at such low resolution but the models suggest Y315 could act as a ratchet in making hydrogen bonds to the peptide backbone of I245 in the down state and switches to the backbone of F244 in the up state.

Meanwhile, the zipper region is formed by R237 of M3 packing with M322 and W326 of M4 in the down conformation. This interaction is disrupted in the up state as M3 and M4 move apart. Gain-of-function (GoF) mutations in residues homologous to these residues in the related TREK-1 channel have previously been observed from random mutation yeast screen assays performed in the Tucker lab (Chetan Sharma, unpublished).

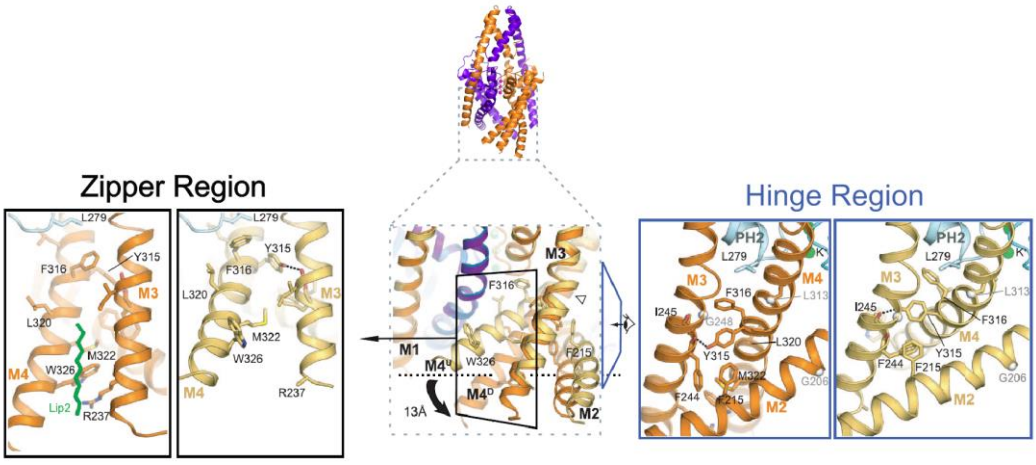

Figure 3: Cartoon representations of the "hinge" and "zipper" regions of TREK-2. *The zipper (left panels) is formed of interactions between R237 and M322 and W326 in the down state (orange) which are broken by an upward translocation of TM4 in he up conformation (yellow). The hinge (right panels) is formed by hydrophobic interactions between the aromatic sidechains of F215, F244 and Y315.*

3.2 Alanine mutagenesis of the hinge and zipper

When these residues were mutated to alanine to disrupt sidechain interactions increases in whole cell currents were observed. Cells were injected with 4ng of RNA and incubated for 24h prior to measurement of basal channel activity which was assayed by whole cell TEVC recording. As can be seen from Figure 4 and Table 1, mutation of both hinge and zipper residues increased whole cell currents. Interestingly the largest increases in whole cell currents for the hinge mutant (Y315A) and the zipper mutant (W326A) were comparable to the E337A mutation which has previously been shown to activate TREK channels (Honoré et al. 2002).

.

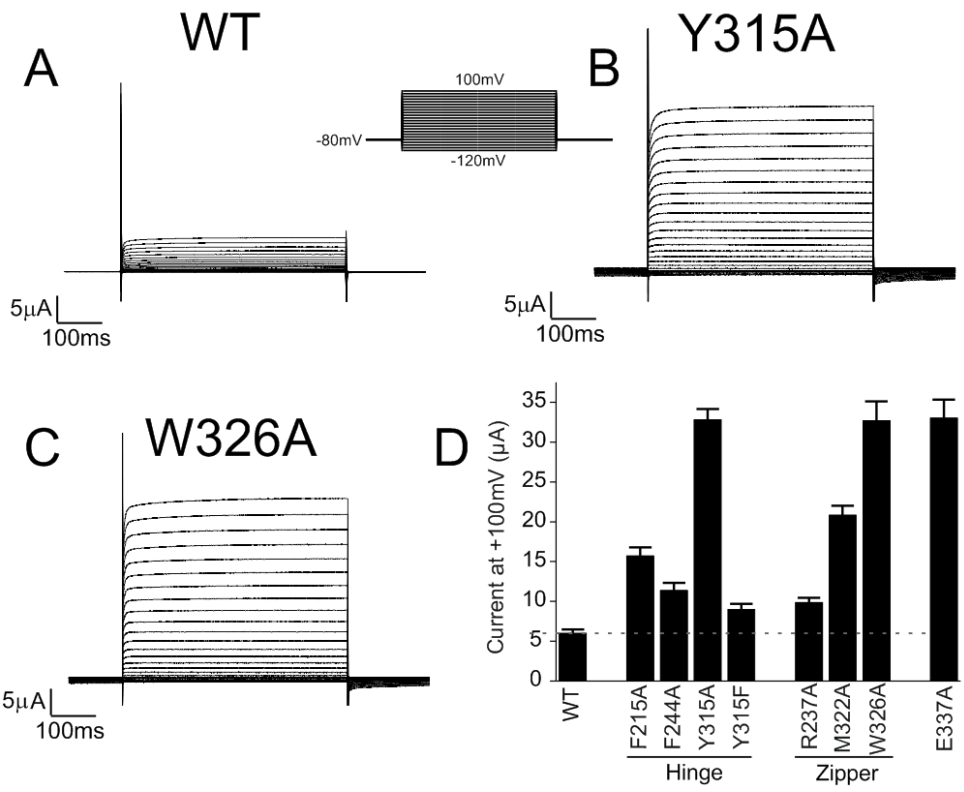

Figure 4: Mutations in the hinge and zipper regions of TREK-2 increase basal whole cell currents. *A-C) Example traces of TEVC recordings from oocytes expressing TREK-2 wild type, Y315A and W326A showing currents at voltage steps as indicated in inset. D) Summary of mean basal current at +100 mV step for TREK-2 wild type, hinge and zipper mutants and E337A.*

Channel	Peak Current (μA)
WT	6.0 ± 0.5 (n=30)
F215A	15.7 ± 1.1* (n=22)
F244A	11.4 ± 1.0* (n=23)
Y315A	32.8 ± 1.4* (n=28)
Y315F	9.0 ± 0.6* (n=23)
R237A	9.9 ± 0.6* (n=24)
M322A	20.8 ± 1.2* (n=22)
W326A	32.7 ± 2.4* (n=17)
E337A	33.0 ± 2.3* (n=25)

Table 1: Mean peak current at +100mV for hinge and zipper mutants (* p-value < 0.01, unpaired T-test).

The observed increases in whole cell basal currents could be due to increased expression of channels at the plasma membrane (n), open probability (P_o) or single channel conductance (g). Ideally one would use single channel analysis to unequivocally demonstrate that macroscopic current increases are due to increased open probability. However TREK single channel behaviour has proven to be difficult to analyse quantitatively due to their extremely low basal open probability, so in order to demonstrate that mutant channels did indeed exhibit increased open probability the mutants were tested for their mechano-activation.

3.3 Hinge and zipper mutations disrupt stretch activation

Inside-out giant patches were subjected to negative pressure (-11 mmHg) applied via the patch pipette to provoke stretch activation. In wild type channels this pressure application increased currents 14.4 ± 4.6 fold. Notably, marked decreases in stretch activation were observed in a number of the hinge and zipper mutants. For example activation of Y315A was 1.1 ± 0.1 fold; whilst W326A exhibited 1.7 ± 0.3 fold activation upon stretch activation, see Figure 5 and Table 2. Again this effect was comparable to the E337A mutation, which reduced stretch activation to 2.3 ± 0.3 fold. Furthermore statistically significant decreases in stretch activation

were seen in the F215A, R237A, Y315F and M322A mutants (for summary see Table 2). A reduction in the extent of mean fold activation was also observed for F244A but this effect was not statistically significant (p = 0.27).

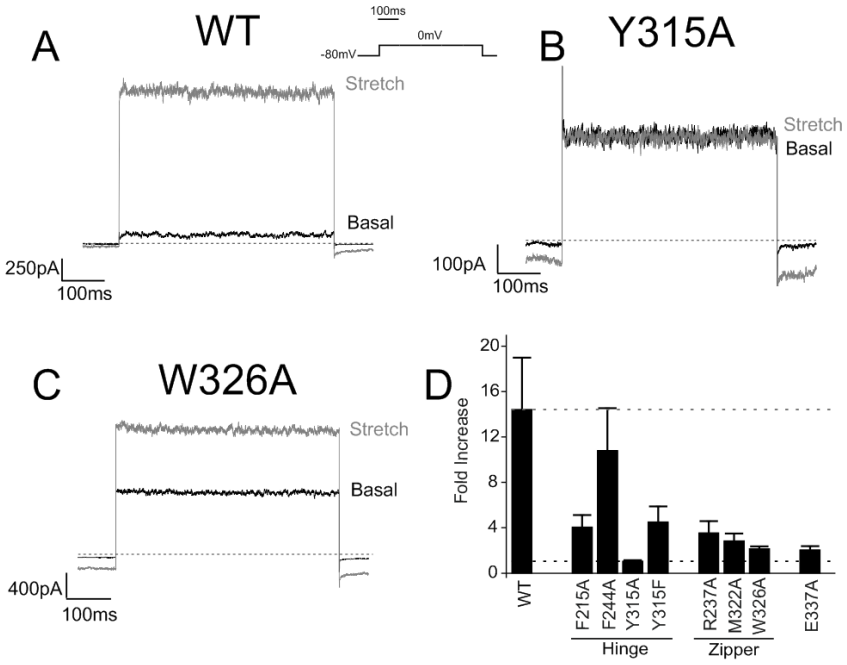

Figure 5: Mutations in the hinge and zipper regions of TREK-2 decrease stretch activation in excised inside-out patch clamps recordings. *A-C) Example traces of wild type, Y315A and W326A currents in the absence (black traces) and presence (grey traces) of -11 mmHg suction. D) Summary of mean fold activation induced by -11 mmHg pressure application for TREK-2 wild type, hinge and zipper mutants and E337A.*

Channel	Fold Increase
WT	14.4 ± 4.6 (n=8)
F215A	4.1 ± 1.0* (n=8)
F244A	10.8 ± 3.7 (n=9)
Y315A	1.1 ± 0.1* (n=5)
Y315F	4.5 ± 1.4* (n=9)
R237A	3.6 ± 1.0* (n=8)
M322A	2.8 ± 0.7* (n=7)
W326A	1.7 ± 0.3* (n=6)
E337A	2.3 ± 0.3* (n=5)

Table 2: Mean fold activation by -11mmHg for hinge and zipper mutants (* p-value < 0.05, Wilcoxon Rank Sum Test).

This apparent decrease in mechano-activation could be the result of either simple elevations in basal open probability, or perhaps counter-intuitively, *increased*

stretch sensitivity. It is well known that the formation of the giga-Ohm seal required for low noise patch clamp recording involves annealing of membrane lipids to the pipette glass (Opsahl & Webb 1994). This lipid-glass interaction increases basal tension in the membrane of the patches such that upon seal formation and patch excision channels are subject to significant lateral tensions, close to the lytic tensions (patch tensions are estimated to be 0.5-4mN/m whereas lytic tension is estimated to be ~10mN/m) (Opsahl & Webb 1994; Sokabe et al. 1991; Suchyna et al. 2009).

Basal currents in excised patches therefore represent channel activity at this elevated tension. Mutations which provoke a blunting of stretch activation upon administration of additional membrane tension (via increased suction) may indicate that the mutation shifts the tension-activation curve to such an extent that channels show high levels of activation from the basal patch tension alone, which cannot be increased further. Regardless, whether the decreased stretch activation is a result of elevated basal open probability in the absence of membrane stretch or due to an increased sensitivity to membrane stretch does not affect the conclusion that these mutations increase basal channel activity in patches.

3.4 Structural interpretation of the effects of mutating the hinge and zipper regions

Therefore the R237A, M322A and W326A mutations, which would all be predicted to disrupt the zipper region formed in the down conformation (and thereby destabilise the down state), all increase channel activity. It is perhaps more difficult to predict the structural consequence of mutations in the hinge region, but it is clear that disruption in this site also favours channel activation and therefore likely destabilises the closed state. The Y315A mutation profoundly increases channel

activity whilst the more conservative Y315F mutation exhibits an intermediate phenotype. This suggests that the hydrogen bonding between M3 and M4 contributes to stabilisation of the down state but that this interaction is not exclusively responsible, with the aromatic ring also being important.

These results are consistent with the notion that the down conformation may represent a closed state. However as the deleterious effects of single amino acid changes can be wide ranging interpretation of mutagenesis data is notoriously difficult. Consequently further evidence was required to consolidate the TREK-2 gating model.

4. Results: The norfluoxetine binding site in TREK-2

A crucial further advance in our understanding of what the different TREK-2 conformations represent was brought about by co-crystallisation of the channel with norfluoxetine and a bromine-labelled fluoxetine derivative (the work of Alexandra Mackenzie and Yin Yao Dong).

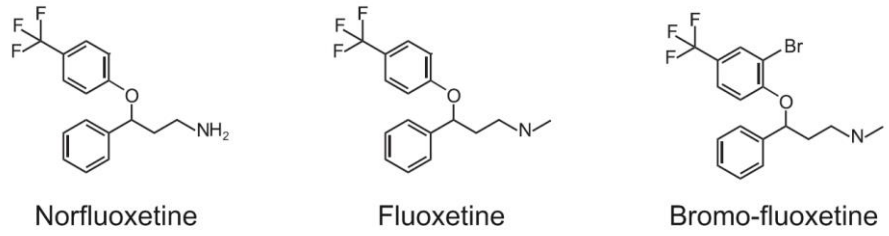

Figure 6: The chemical structures of norfluoxetine, fluoxetine and bromo-fluoxetine.

Fluoxetine, originally developed as a selective serotonin reuptake inhibitor, and its active metabolite norfluoxetine have previously been shown to be inhibitors of TREK-1 and TREK-2 (Kennard et al. 2005; Kang et al. 2008). Whilst the mechanism

of action of these molecules at TREK channels was hitherto unknown, Kennard and colleagues have demonstrated that fluoxetine acts as a state dependent inhibitor, at least for TREK-1 (Kennard et al. 2005). This conclusion was drawn from the finding that fluoxetine inhibition, at the single concentration tested, was decreased in the TREK-1 E306A GoF mutation (analogous to E337A in TREK-2).

4.1 The fenestration binding site

In light of this known state-dependent mechanism of fluoxetine inhibition we were fascinated to observe that the crystallographic binding site was within the hydrophobic pocket of the lateral fenestrations, a site only accessible in the down conformation, Figure 7.

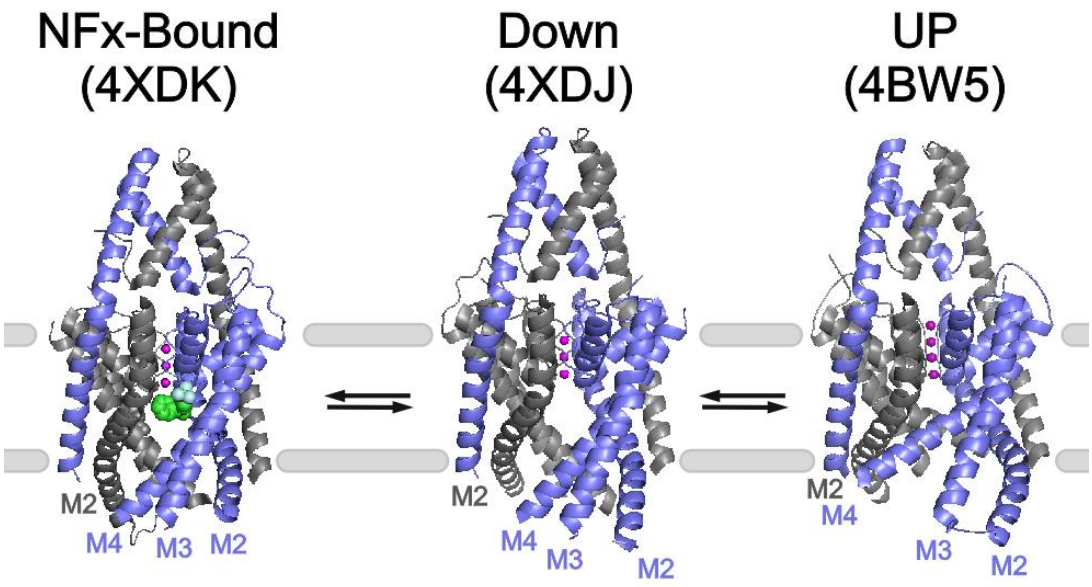

Figure 7: The norfluoxetine/fluoxetine binding site in TREK-2. *Norfluoxetine (shown in green, left panel) and fluoxetine bind in the fenestration. This site is only available in the down conformation (middle panel) and not the up conformation (right panel) where an upward movement of TM4 abolishes the site.*

As described above, transmembrane helix rearrangements in the up conformation close the fenestrations, completely distorting the putative binding site. This finding

immediately provides a potential explanation for the state-dependence of inhibition, because shifting the equilibrium from the down conformation (where the binding site is accessible) to the up conformation (where the binding site is inaccessible) would be expected to decrease potency. This then presents a testable hypothesis: if channel activation by modulatory stimuli involves conformational changes from the down to the up conformation activation should decrease inhibitor potency. In order to test this hypothesis I first attempted to confirm TREK-2 inhibition by fluoxetine and norfluoxetine.

4.2 TREK-2 inhibition by fluoxetine and norfluoxetine

The effects of fluoxetine and norfluoxetine were tested in excised inside out patch clamp recordings from oocytes expressing TREK-2. Both compounds significantly inhibited TREK-2: At 0 mV 30 μM fluoxetine provoked a 77.1 ± 7.6% inhibition whilst norfluoxetine provoked an 84.6 ± 3.7% inhibition of basal currents. In the course of these experiments it was observed that high concentrations of fluoxetine also had additional effects on membrane patches. Specifically it appeared that 30 and 100 μM fluoxetine occasionally induced activation of non-TREK-2 currents, even in uninjected oocytes. Interestingly the IV profile of these endogenous currents appeared qualitatively similar to endogenous stretch-activated currents, with currents reversing around 0mV, Figure 8. This undesired, off-target effect was not observed as frequently for norfluoxetine. Perhaps the slight difference in chemical structure with the additional methyl group conferring greater hydrophobicity to fluoxetine affects membrane partitioning and this in turn may alter membrane dynamics, inducing stretch activation of endogenous channels (Lundbaek et al. 2010).

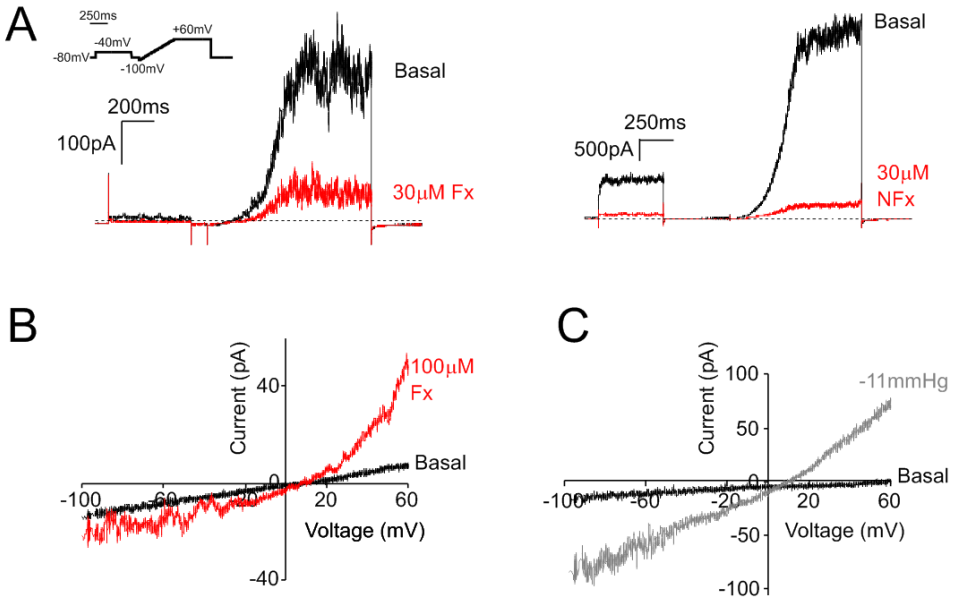

Figure 8: Fluoxetine and norfluoxetine inhibition of TREK-2. *A) Example traces from an inside-out patch showing inhibition of TREK-2 WT by 30μM fluoxetine (left panel) and 30μM norfluoxetine (right panel), voltage protocol in inset. B) Example traces from voltage ramps of an inside out patches from an uninjected oocyte in the absence (black) and presence of 100μM fluoxetine. C) Example traces from voltage ramps of an inside out patches from an uninjected oocyte in the absence (black) and presence of -11mmHg pressure.*

For studies of mechano-sensitivity we therefore focussed on norfluoxetine to avoid potential confounds of high concentrations of fluoxetine altering membrane dynamics. Importantly both norfluoxetine and bromo-fluoxetine appeared bound in the same site in the crystal structures and thus we assume the mechanism of action will be shared for both molecules. As shown in Figure 9 norfluoxetine induced a clear dose-dependent inhibition of TREK-2 (IC_{50} 4.9 ± 0.5 μM, Hill coefficient 1.2 ± 0.1, n = 15). As shown previously for TREK-1, this inhibition was voltage-insensitive across the range tested (see Figure 9D).

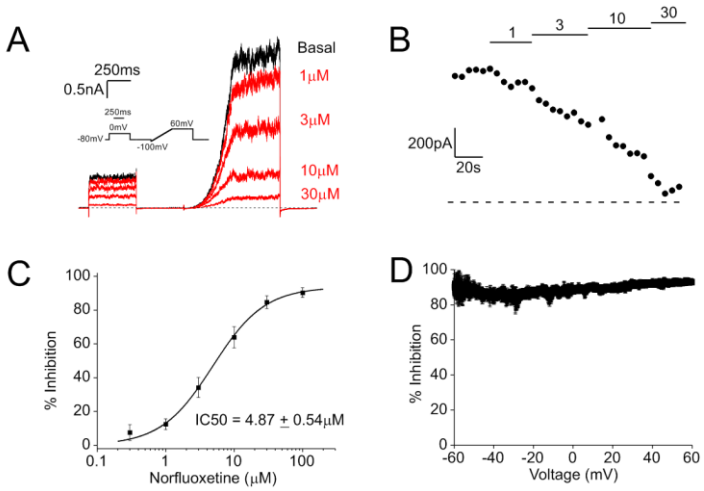

Figure 9: Norfluoxetine inhibition of TREK-2. *A) Example traces from an inside-out patch showing dose dependent inhibition of TREK-2 WT by norfluoxetine (voltage protocol in inset). B) I/t plot showing currents recorded from 0mV steps at a 5s intervals at increasing concentration of norfluoxetine (administration periods denoted by horizontal lines, concentration in μM). C) Summary dose response curve for norfluoxetine inhibition of TREK-2 (IC_{50} 4.9 ± 0.5 μM, Hill coefficient 1.2 ± 0.1, n = 15). D) Percentage inhibition by 30μM norfluoxetine as a function of voltage (mean ± standard deviation, n = 3).*

4.3 Validating the crystallographic binding site: The crystal construct retains norfluoxetine sensitivity

In order to validate the crystallographic binding site, norfluoxetine was first tested for inhibition against the truncated "crystal construct" TREK-2 channel used in the co-crystallisation trials. The crystal construct tested, which was truncated at the N-terminus by 71 amino acids and at the C-terminus by 213 amino acids consisted of the transmembrane, pore and extracellular regions of the channel along with the proximal C-terminus, and retained sensitivity to stretch and flufenamic acid (FFA) activation and tetrapentylammonium (TPenA) inhibition, see Figure 10.

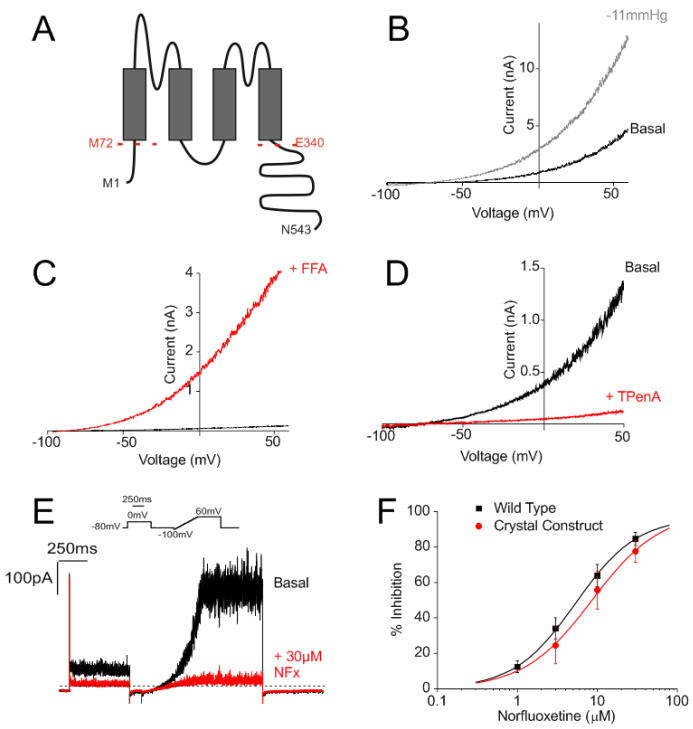

Figure 10: Function and norfluoxetine sensitivity of the truncated TREK-2 crystal construct protein. *A) Schematic showing TREK-2 wild type with truncation sites of the crystal construct indicated by red dashed lines. B) Example traces from an inside-out patch clamp experiments showing activation of crystal construct TREK-2 by -11mmHg pressure application (grey trace). C) Example traces from an inside-out patch clamp experiments showing activation of crystal construct TREK-2 by 1mM flufenamic acid (red trace). B) Example traces from an inside-out patch clamp experiments showing inhibition of crystal construct TREK-2 by 1mM TPenA (red trace). E) Example traces showing norfluoxetine inhibition (red trace) of crystal construct TREK-2 (voltage protocol in inset). F) Summary dose response for norfluoxetine inhibition of wild type TREK-2 (black squares) and crystal construct TREK-2 (crystal construct in red circles, IC_{50} 8.6 ± 0.5µM, Hill coefficient 1.0 ± 0.1, n = 4).*

As can be seen in Figure 10, sensitivity to inhibition by norfluoxetine was retained in the crystal construct (inhibition at 30 µM 77.6 ± 6.3%, IC_{50} 8.6 ± 0.5 µM, Hill coefficient 1.0 ± 0.1, n = 4). Importantly this result demonstrates that the norfluoxetine binding site must be within the structures retained in the crystal construct, ruling out a binding site formed by the N-terminus or the C-terminus beyond glutamate 340. In a previous study it was suggested that fluoxetine inhibition of TREK-1 requires the C-terminus (Sandoz et al. 2011). This conclusion was based upon results from an innovative optical approach in which coupling of

the isolated C-terminus with the membrane was measured optically using a fluorescent GFP-labelled tag. Here the assertion was that coupling of the C-terminus acted as a surrogate readout for TREK-1 activity and this coupling was impaired by a high concentration (100 μM) of fluoxetine. Sixteen amino acids included in the proximal C-terminus of the TREK-2 crystal construct were also present in the isolated C-terminus used by Sandoz and colleagues therefore it is possible that this region is responsible for the interaction. However the crystallographic binding site is far removed from the C-terminus making a critical C-terminus interaction unlikely. Perhaps the effect of fluoxetine on the optical coupling of the fluorescent probe in the report from Sandoz and colleagues can be explained by the high concentration of the drug having additional, non-specific effects. It would be telling to establish whether similar effects were seen at lower concentrations.

4.4 Validating the crystallographic binding site: A binding site mutation shifts sensitivity

In order to further validate the crystallographic binding site a mutation within the fenestration region was made and tested for norfluoxetine sensitivity. L320 lines the fenestration, as can be seen in Figure 11. Introduction of a bulky tryptophan at this site was predicted to impair binding either by steric hindrance or changes in side chain-drug electrostatic interactions. When tested in inside-out patch experiments norfluoxetine potency was indeed decreased in the L320W mutant, with the IC_{50} increased to 10.9 ± 1.6 μM (Hill coefficient 1.4 ± 0.2, n = 8), Figure 11. Critically the mutation alone did not appear to significantly alter basal open probability as whole cell currents and stretch activation was comparable with wild type, Figure 11. This is important because, as reported for the TREK-1 E306A

mutation and as discussed in detail in Chapter 7, mutations which increase open probability may reduce the potency of a state dependent inhibitor by shifting the equilibrium between the open and closed conformations rather than by directly affecting binding energy. Therefore, that this mutation within the putative binding site shifts norfluoxetine potency without affecting normal gating behaviour provides validation of the binding site identified in the co-crystallisation study.

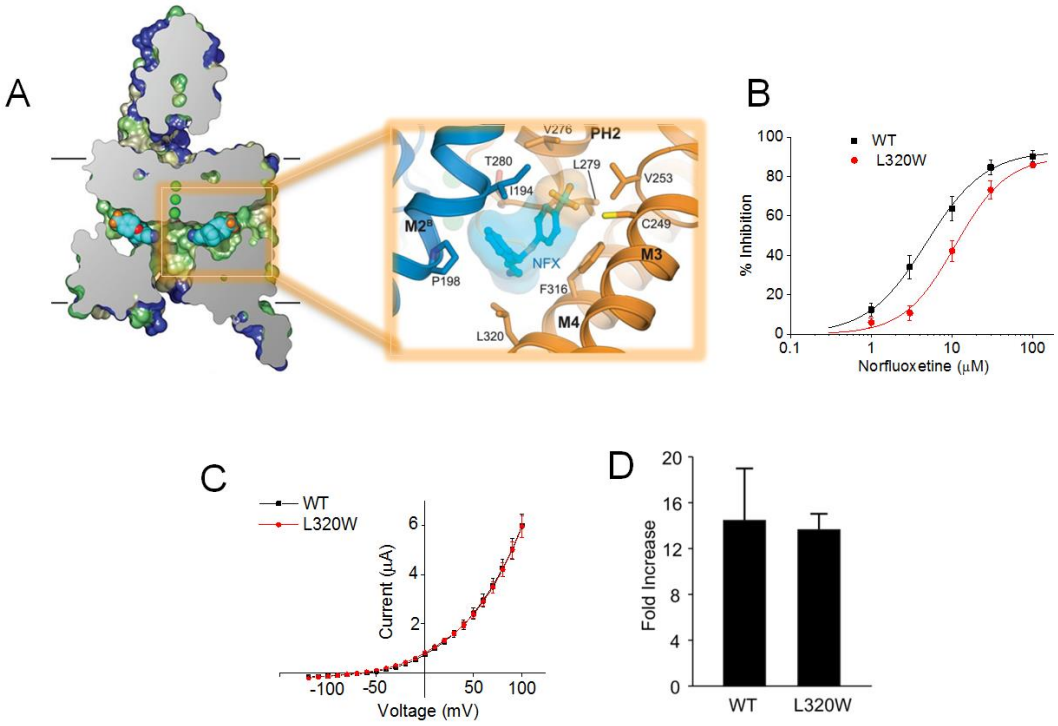

Figure 11: Functional validation of the crystallographic norfluoxetine binding site. *A) Representation of norfluoxetine in the fenestration binding site, expanded in orange box to show surrounding sides chains including L320 (image created by ACW Pike and EP Carpenter). B) Dose response curve for norfluoxetine inhibition or wild type TREK-2 (black squares) and the L320W mutant (red circles; IC_{50} increased to 10.9 ± 1.6 μM, Hill coefficient 1.4 ± 0.2, n = 8). C) Mean basal whole cell currents from TEVC recordings of oocytes expressing wild type (black squares) and L320W TREK-2 (red circles) (WT current at +100 mV 6.0 ± 0.5μA, n=30; L320W 5.9 ± 0.4μA, n=30; p = 0.79). D) Mean fold activation of wild type and L320W TREK-2 currents by -11 mmHg of pressure in inside-out patches (fold activation of WT 14.4 ± 4.6, n=8; L320W 13.6 ± 1.4, n=5; p = 0.71).*

5. Insights from novel TREK-2 crystal structures

These results therefore provide novel insights into structure and function of TREK-2. Crystal structures reveal two distinct conformations for the channel, the up and down conformations. Mutagenesis of residues which are well placed to stabilise the down conformation appear to activate the channel, which leads us to propose that the down state likely represents a closed channel. Fascinatingly, the co-crystallisation of norfluoxetine to the down structure provides a testable hypothesis for state-dependent inhibition, i.e.: the drug binding site is only accessible in the down conformation and so conversion to the up confirmation would decrease accessibility and therefore potency. In the following chapter I describe how we can use this observation to further probe the functional significance of the up and down conformations.

Chapter 5: The structural basis of mechano- and temperature-activation in TREK-2

1. Introduction

As described in Chapter 4, the state dependent inhibitor norfluoxetine can be used to probe the structural mechanisms of polymodal gating in TREK-2. With the newly gained knowledge of how norfluoxetine binds to the channel we can predict that shifting the channel from states resembling the crystallised down conformation to states resembling the up conformation would decrease norfluoxetine accessibility. So are there regulatory stimuli which induce such shifts, and if so which ones?

By addressing these questions we can test the assertion that the up conformation likely represents an open channel, whilst the down conformation likely represents a closed channel. Secondly we can infer the structural movements involved in TREK channel activation by different stimuli, such as mechanical force and temperature.

2. Mechano-activation

Molecular mechano-sensitivity exists in every kingdom of life. From protists, bacteria and yeasts to plants and metazoa mechano-sensitive (MS) ions channels are critical for the integration of physical cues into developmental and behavioural responses. MS channels have been implicated in a wide array of functions, including regulation of cell turgor in bacteria, yeast and plants, gravity-sensing in plants and locomotion of paramecium (Berrier et al. 1992; Levina et al. 1999; Zhou et al. 2003;

Monshausen & Haswell 2013; Naitoh & Eckert 1969; Prole & Taylor 2013; Salmi et al. 2011). In animals mechano-sensation is vital for many functions, ranging from touch perception and hearing to bone remodelling, blood pressure regulation, mechano-electrical feedback in the heart, and stem cell differentiation (Delmas et al. 2014; Delmas et al. 2011; Pathak et al. 2014).

TREK channels

The mechano-sensitivity of TREK channels is likely to be critical in numerous physiological contexts. For example knock out mice models have implicated the channels in noxious and innocuous touch sensation, where TREK activation likely counteracts and fine-tunes the excitatory effect of mechanically-activated cation channels, including Piezo 2 (Ranade et al. 2014; Pereira et al. 2014; Alloui et al. 2006; Noël et al. 2009). Elsewhere TREK-1, TREK-2 and TRAAK channel expression has been reported in osteoblasts where blockade by bupivacaine increased cell proliferation prompting authors to propose a role for TREK-1 channels in load-sensing and bone regeneration (Hughes et al. 2006).

Furthermore, the expression of TREK-1 in the cardiac myocytes of both the atria and ventricles has led to the suggestion that the channel may be involved in mechano-electrical feedback (MEF), the effect of mechanical forces within the myocardium on electrophysiology (Kelly et al. 2006). Interestingly, immunofluorescent staining for TREK-1 showed a remarkable striated pattern of expression, which may position the channels perfectly for sensing longitudinal stretch, yet whether TREK channels play a role in MEF remains to be definitively established (Xian et al. 2006; Kelly et al. 2006), and the TREK-1 knockout mouse showed no significant alterations in cardiac output (Namiranian et al. 2010).

Other mechanosensitive channels

Many ion channels have been suggested to be directly gated by mechanical forces, including bacterial MscL and MscS channels, the acid sensing channels degenerin-epithelial Na^+ channels, TRPs, Piezo proteins, and chloride channels (Delmas et al. 2011; Imai et al. 2000; Poole et al. 2014). Furthermore in numerous other channels, including voltage gated potassium channels, membrane tension appears to modulate regulation by other stimuli (e.g. voltage)

Changes in ion channel behaviour by mechanical forces is not restricted to any archetypal mechano-receptor, and there is no known conserved, canonical mechano-sensor domain, rather it is likely that changes in membrane properties can *ipso facto* affect membrane protein function (Teng et al. 2014). But how are mechanical forces sensed by channels, and how is this transduced to gating?

2.1 Mechanisms of mechano-sensation

Proposed mechanisms for mechano-sensation in ion channels can roughly be divided into two categories: regulation via a molecular tether or regulation via forces exerted through the lipid membrane (the Force-From-Lipid principle), as shown in Figure 1.

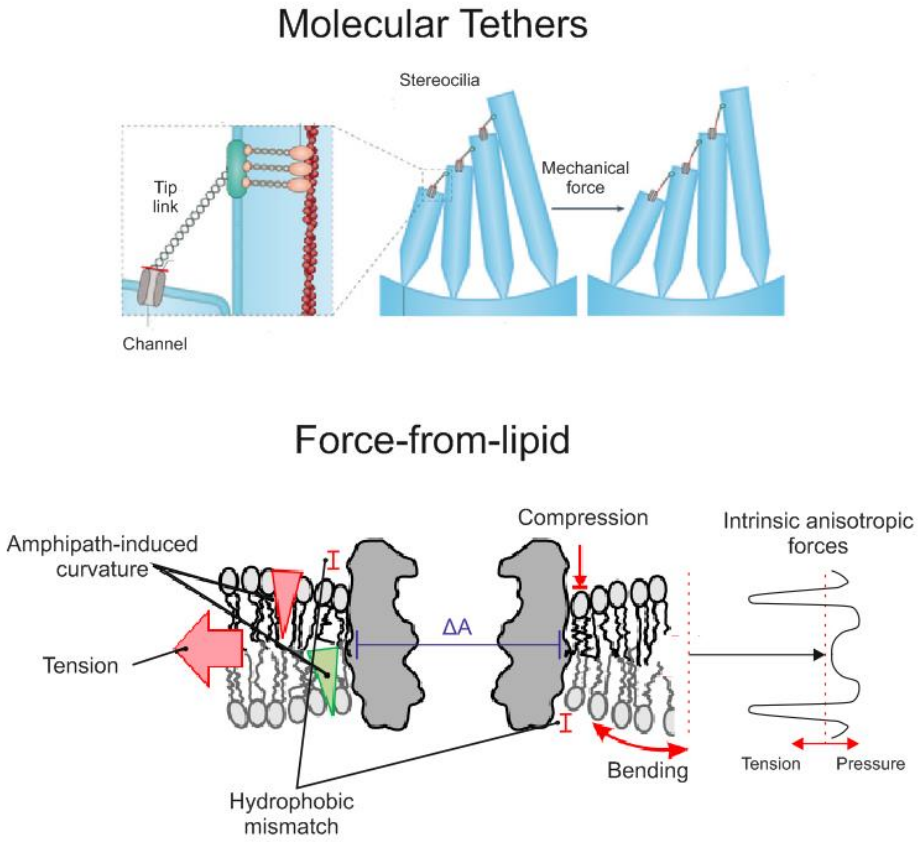

Figure 1: Models of mechanical activation of ion channels. *Top: the molecular tether model as conceived for cochlear hairs cells. Mechanical displacement of stereocilia increases tension on the tip link, which gates the channel (figured modified from* Hudspeth 2014) *Bottom: the force-from-lipid principle for bilayer-mediated mechano-activation. Membrane deformation can be induced by amphipaths, lateral tension or embedded proteins. Hydrophobic mismatch between the channel and the membrane, the membrane deformation energy (which includes the compression- and bending-moduli of the membrane), and intrinsic anisotropic forces contribute to the total free energy. Adaptive changes in cross-sectional area (ΔA) of the embedded protein can act to minimise hydrophobic mismatch and hence free energy (figure modified from* Anishkin et al. 2014).

The tether mechanism of mechano-sensing

The molecular tether concept involves the complexing of the channel to the cytoskeleton, the membrane, the extracellular matrix or another secondary protein via a linker (Martinac et al. 2014). Examples of such a complexes are the cochlear hair cell, the *C. elegans* MEC complex, and mammalian rapidly-adapting low

threshold mechanoreceptors (Laitko et al. 2006; Söllner et al. 2004; Siemens et al. 2004; Hamill & McBride 1996; Hu et al. 2010; Ranade et al. 2014).

2.2 The Force-From-Lipid Principle for mechano-sensing in membrane proteins

The force-from-lipid (FFL) principle describes the physicochemical relationship between the lipid membrane and embedded proteins. The self-assembly of a lipid bilayer, and the expression of proteins within it, creates intrinsic anisotropic forces. Additional forces exerted upon the membrane can alter these intrinsic force vectors (in both magnitude and direction), and thereby change the energies of specific membrane protein conformations. Adaptive changes in protein conformation allow for minimisation of the energy in the new lipid environment, see Figure 1. This principle can provide a unifying theory of mechano-sensation in membrane proteins.

Hydrophobic Mismatch

The geometric relationship between the bilayer and embedded proteins is governed by a number of major factors. One of which is the energetic cost of hydrophobic mismatch i.e. the energy of solvating hydrophobic regions of a protein in a hydrophilic environment. To illustrate the significance of this energy Lundbaek and colleagues state that for a protein of 20nm radius the energetic cost of exposing one amino acid in an α-helix to water would be approximately 9 kcal mol^{-1} (for context the hydrolysis of ATP to ADP releases ~13 kcal mol^{-1}) (Veech et al. 1979; Lundbaek et al. 2010). This significant energetic cost means that minimising hydrophobic mismatch is critical for protein stability in the bilayer and proteins preferentially

orientate themselves with hydrophobic regions buried within the membrane. However, of course, the hydrophobic length of a protein can exceed bilayer thickness. In this situation the second major factor is revealed, that is the energy of membrane deformation.

Membrane deformation

Upon the application of an exogenous force the bilayer will deform, and in the case of stretch or pressure this results in a thinning of the membrane. Clearly, a decrease in membrane thickness would increase the exposure of previously buried hydrophobic amino acids. This cost can be minimised by either the protein changing conformation, or by the membrane deforming to minimise hydrophobic mismatch, which can only occur if the membrane deformation energy allows. Therefore the stability of a conformation state in the stretched bilayer is dependent on both the hydrophobic length of the protein and the membrane deformation energy of the bilayer.

Intrinsic membrane forces

Additionally, the tension at the lipid/water interface exerts large lateral forces upon any transmembrane protein (Cantor 1997; Gullingsrud & Schulten 2004). The tension arises from contraction of the lipid head groups preventing solvent from accessing the lipid core which in balanced by the repulsive force of the lipid tails which tend towards occupying a large volume to maximise their entropy. Tensions can hereby reach hundreds of mN/m at the head group/tail interface (Anishkin et al. 2014). These anisotropic forces vary in magnitude and direction across the

membrane and so a transmembrane protein is subject to a numerous different stresses in different domains, see Figure 1.

Molecular dynamics simulations have also shown that stretch significantly alters the intrinsic lateral forces in terms of both magnitude and direction across the height of the membrane (Gullingsrud & Schulten 2004). Therefore a protein would be subject to a very different stress profile in a stretched membrane compared to an unstressed membrane. An adaptive change in protein conformation may then minimise the free energy of the protein in this new, stretched system. In fact considering these principles, any membrane protein would be subject to changes in total free energy if membrane properties or geometry are altered. Therefore in this sense "mechano-sensitive" proteins are simply those which convert the inevitable change in free energy into a measureable change in function.

2.3 Support for the FFL Principle

Experimental support for the force-from-lipid principle was first provided by studies of the bacterial mechanosensitive channels purified from *E. Coli* and reconstituted into lipid bilayers (Sukharev et al. 1997; Martinac et al. 1990; Martinac et al. 1987). The reconstituted channels retained mechano-sensitivity in this reductionist paradigm proving that the channels must be activated directly by the membrane (Anishkin et al. 2014). Furthermore, the authors demonstrated that the channels were activated by anionic, cationic and neutral amphipaths leading to the postulation that insertion of amphipaths and consequent increases in membrane tension resulted in activation (Martinac et al. 1990).

Further investigation of MscL showed that mechano-activation was not dependent on the lipid composition nor upon membrane curvature *per se,* but rather by tension within the membrane (Moe & Blount 2005).

The FFL principle in K2P channels

The force-from-lipid principle was generalised for eukaryotic channels with the recent demonstration that TREK-1, TRAAK and TREK-2 can be activated by stretch after reconstitution into bilayers (Brohawn et al. 2014; Michael Clausen - unpublished).

Importantly however, whilst reconstitution experiments show that mechano-sensitivity is intrinsic to the proteins, it does not rule out the involvement of additional cellular elements in the modulation or sensitisation of mechano-sensation and indeed the cytoskeleton likely modulates TREK channel mechano-sensation (Honoré et al. 2006; Lauritzen et al. 2005; Maksaev et al. 2011).

What is the structural basis for mechano- activation in TREK-2?

Therefore, TREK channels are gated by changes in mechanical forces within the lipid bilayer, but it was not known how the channel senses these forces, and what conformational changes were involved in mechano-activation. I sought to use the state-dependent inhibitor norfluoxetine to probe this.

3. Results: Investigating the structural basis for mechano-activation

3.1 Mechano-activation decreases norfluoxetine potency

Mechano-activation was provoked by application of negative pressure (suction) via the patch pipette in inside-out patches. As can be seen in Figure 2, mechano-

activation of TREK-2 significantly decreases norfluoxetine potency, for channels activated by -11mmHg of suction the norfluoxetine IC_{50} was increased to beyond 30 μM (inhibition at 30μM 30.2 ± 4.5%, n = 8). The potency of the pore blocker TPenA was unchanged by mechano-activation, as expected, see Figure 2. These results indicate that the accessibility or binding energy for norfluoxetine is decreased in the mechano-activated conformation of TREK-2.

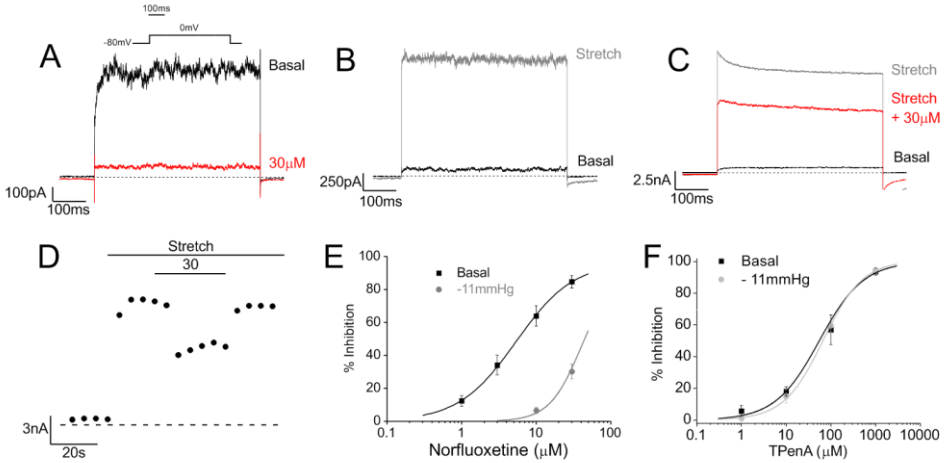

Figure 2: Mechano-activation decreases norfluoxetine potency in inside-out patches. *A) Example traces showing 30 μM norfluoxetine inhibition (red trace) of basal TREK-2 currents (black trace) (voltage step to 0mV as shown in inset). B) Example traces showing -11 mmHg pressure activation of TREK-2 (grey trace). C) Example traces pressure activation (grey trace) and subsequent co-administration of pressure with norfluoxetine (red trace). D) I/t plot showing TREK-2 currents recorded from 0 mV steps at a 5 s intervals upon stretch and norfluoxetine administration (administration periods denoted by horizontal lines, concentration in μM). E) Summary dose response curves for norfluoxetine inhibition in the absence (black squares) and presence (grey circles) of -11 mmHg pressure (IC_{50} for stretch-activated currents >30 μM, n=8). F) Summary dose response curves for TPenA inhibition in the absence (black squares) and presence (grey circles) of -11 mmHg pressure (IC_{50} for basal currents 55.0 ± 7.5 μM, Hill coefficient 0.9± 0.1, n=4; IC_{50} for stretch-activated currents 65.1 ± 3.7 μM, Hill coefficient 1.0 ± 0.1, n=8).*

This is consistent with the mechano-activated state resembling the crystallised up conformation, a structure where the norfluoxetine binding site has been abolished. Increasing the probability of the channel adopting this conformation as the equilibrium is shifted towards the mechano-activated state results in a decreased

probability of norfluoxetine binding to the channel and thereby decreases steady state inhibition. In turn this model predicts that norfluoxetine acts by binding to channels in the down conformation and preventing conversion into the activated state. This prediction can be tested by analysing the kinetics of mechano-activation (which are usually extremely rapid) in the absence and presence of norfluoxetine. Here the rate at which the channel was activated in patches pre-administered with 10μM norfluoxetine was compared to patches in the absence of norfluoxetine.

3.2 Norfluoxetine locks channels in the closed state

As one can see in Figure 3, in the absence of norfluoxetine channels open rapidly upon administration of suction with a 20-80% rise time of 2.8 ± 0.4 ms (n=6), before a slight inactivation to a steady state level. Meanwhile in the presence of norfluoxetine the kinetics of activation are strikingly different Figure 3A. Here, initially, a rapid component of activation is again observed, which likely represents the proportion of channels unbound by the inhibitor at this concentration (the latency of this component is not significantly different, 20-80% rise time of 4.8 ± 1.4ms p = 0.42). However the response differs in patches administered with norfluoxetine in the emergence of a secondary, slow component of activation which ultimately reaches steady state on a second time scale. The rise time for this component is increased by roughly three orders of magnitude to 3186 ± 1897ms (n = 5), see Figure 3B. This slower mechano-activation can be explained by channels being initially bound and inhibited by norfluoxetine which prevents conversion to the stretch activated conformation, which in turn can only occur after the drug dissociates from the channel, an event which occurs on the second time scale.

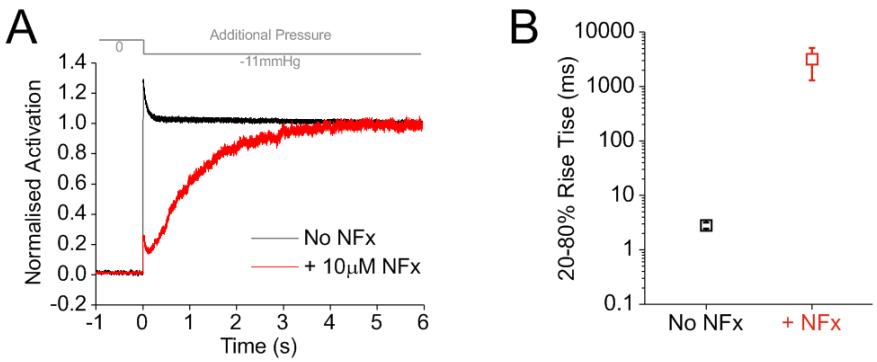

Figure 3: Mechano-activation kinetics are changed in the presence of norfluoxetine. *A) Example traces showing stretch activation in the absence (black) and presence (red) of 10 μM norfluoxetine (n = 5 for both). Stretch responses normalised to steady state current levels. Pressure (-11 mmHg) was applied at 0 s as denoted in grey inset protocol. B) Mean 20-80% rise time for currents in the absence (black) and presence (red) of 10 μM norfluoxetine.*

This suggests that the mechanism by which norfluoxetine inhibits TREK channels involves the drug binding preferentially to closed channels, likely in some variation of the crystallised down conformation.

3.3 A structural model for mechano-activation in TREK-2

To summarise, these results demonstrate for the first time that mechano-activation decreases norfluoxetine potency which in turn suggests that the mechano-activated state exhibits decreased affinity for the inhibitor. This leads us to the proposition that the mechano-activated state resembles the up conformation and is consistent with the emerging structural model where the up conformation represents a conductive channel whilst the down conformation represents a closed channel, see Figure 4.

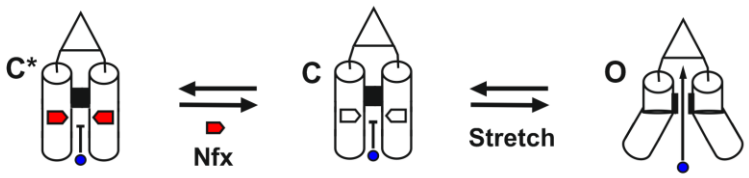

Figure 4: Proposed gating scheme for mechano-activation and norfluoxetine inhibition of TREK-2. *Channels in the closed state (C) are impermeable to potassium ions (blue circle) due to closure of the selectivity filter gate. Norfluoxetine can bind within intramembrane fenestrations (empty pentagonal boxes) to lock channel in drug-bound closed state (C*). Conversely stretch can activate the channel from C to an open state (O) via a conformational change which abolishes the fenestration binding site.*

As stated, TREK channels are polymodal sensors regulated by a diverse range of stimuli, yet it is not known whether these different regulatory inputs involve the same structural responses. With this in mind attention was turned to the structural mechanism of temperature activation.

4. Temperature activation of TREK channels

Clearly all biochemical processes are temperature dependent to some degree, for ion channels this is apparent from the Boltzmann equation of statistical mechanics which can be used to describe the relationship between open probability and free energy difference and includes a term for temperature (Qin 2014):

$$P_o = 1/(1+e^{(\Delta G/RT)})$$

Where ΔG is the free energy difference (and ΔG = Δenthalpy – TΔentropy), R is the gas constant and T is temperature.

Despite this universal effect some ion channels display markedly higher temperature dependence than many others, including TREK channels which display

5-10 fold activation for 10°C temperature elevation around 37°C due to increases in open probability (Bagriantsev et al. 2012; Kang et al. 2005; Maingret et al. 2000).

The mechanisms by which the TREK channels, and indeed other ion channels in general, sense temperature remain mysterious. The temperature dependence of TRP channels has been studied far more exhaustively and yet here, still, temperature activation remains a mystery (Schneider et al. 2014; Feng 2014). The first mechanistic question to ask is: is temperature dependence intrinsic to the protein or mediated via an indirect mechanism?

4.1 Indirect or direct temperature activation

One possible explanation for temperature sensitivity in TREK channels could be temperature dependent changes in the biophysical properties of the membrane, such as fluidity and thickness (Islas 2014; Cossins & Prosser 1978; Meves 2008; Cybulski et al. 2015). This remains to be explored and could be tested by future investigations of the temperature dependence of reconstituted TREK channels.

Interestingly temperature activation appears to be lost upon patch excision, which may indicate the requirement of additional mediators (Kang et al. 2005; Maingret et al. 2000).

The physical basis for intrinsic temperature-activation in ion channels is contentious, but a number of models have been suggested. It has been discussed that the large enthalpic changes involved could possibly arise due to conformational changes (Qin 2013; Jara-Oseguera & Islas 2013), or alternatively, due to changes in specific heat capacity between the open and closed states (Clapham & Miller 2011; Chowdhury et al. 2014), whilst transduction of sensing to gating has been described by models of allosteric coupling (Jara-Oseguera & Islas 2013). The complexity of

the stimulus means that establishing a generalised thermodynamic framework has proven difficult and remains a topic of active debate.

4.2 Temperature activation of TREK channels

Previously it has been suggested that the C-terminus of TREK-1 necessary for temperature activation (Maingret et al. 2000; Bagriantsev et al. 2012). Uncoupling the C-terminus by inserting a tri-glycine (or tri-alanine motif in the distal M4 region) abrogates temperature activation of TREK-1, and does so in each chain in an additive manner (Bagriantsev et al. 2012).

Interestingly the C-terminus of TREK-2 did not appear to be as critical as replacement by the TASK-3 C-terminus only slightly reduced temperature activation (Kang et al. 2005). The role of the C-terminus for temperature activation of TRAAK is currently unreported. Therefore whether the C-terminus is involved in temperature activation for all TREK channels in the same way is contentious.

In theory TREK channel activation by temperature could involve non-specific membrane effects, conformational changes, heat capacity changes and allosteric coupling between distinct sensor- and gating-domains. I sought to probe the structural basis of temperature activation in TREK-2 using state-dependent inhibitors.

5. Results: Investigating temperature-activation of TREK-2 using norfluoxetine

5.1 Temperature activation of TREK-2 in TEVC recordings

In light of a published report demonstrating that temperature sensitivity was lost in excised patches expressing TREK-1, investigation of temperature activation on TREK-2 was performed using TEVC. Here robust increases in whole cell current were observed upon raising the bath temperature with currents at 37°C to 17.2 ± 1.8 fold that observed at 22°C (n = 8), see Figure 5A. This marked temperature sensitivity was not observed for the crystal construct TREK-2 truncation (currents at 37°C were 1.7 ± 0.1 fold that at 22°C, n = 8), see Figure 5B. As the crystal construct retains mechano-sensitivity this result indicates that the sensing element for stretch and temperature activation is different. This finding is consistent with a previous study that suggested that the C-terminus of TREK-1 was critical for temperature sensation (Maingret et al. 2000), yet was contradictory with a further study on TREK-2 which suggested that the C-terminus was not required (Kang et al. 2005). In this regard the temperature sensing element remains unknown, however by testing for the effect of temperature activation on norfluoxetine potency we can determine whether temperature activation involves similar conformational rearrangements to those proposed for stretch activation.

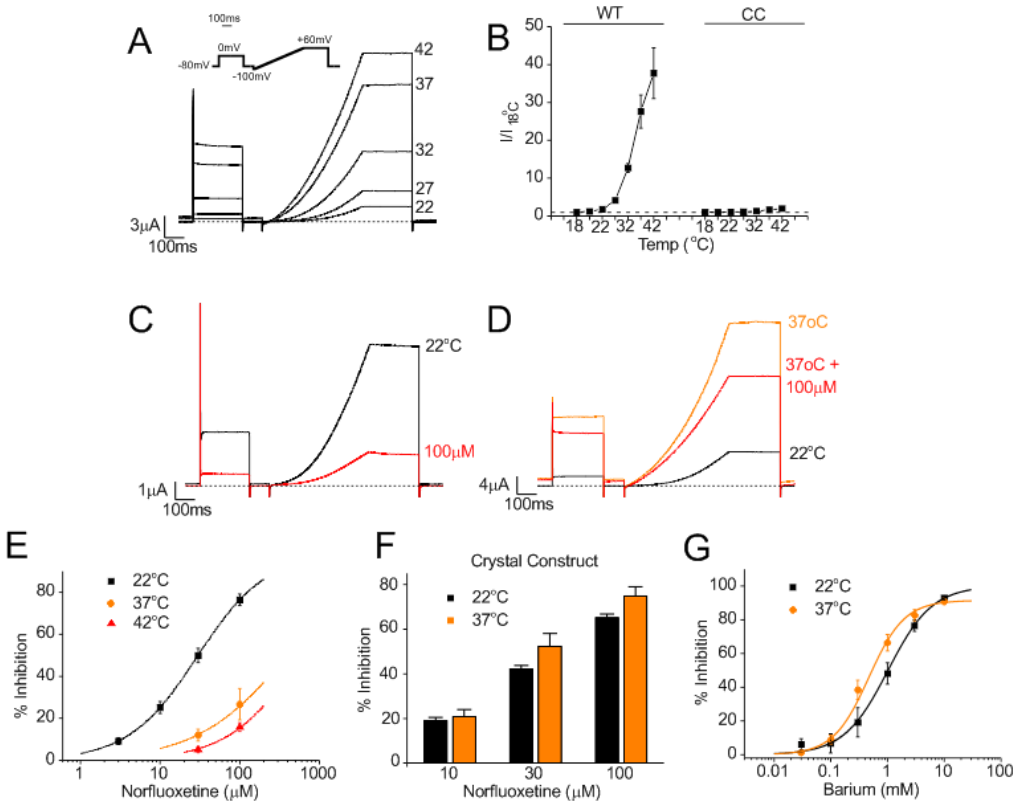

Figure 5: Temperature activation decreases norfluoxetine potency in whole cell TEVC recording of oocytes expressing TREK-2. *A) Example traces showing temperature activation of TREK-2 (temperature in °C as indicated; voltage protocol in inset). B) Temperature activation of wild type (n=5) and crystal construct (n=3) TREK-2 normalised to current levels at 18°C, currents recorded from 0mV steps. C) Example traces showing inhibition of whole cell currents (black trace) by 100 μM norfluoxetine (red trace) at 22°C. D) Example traces showing activation of currents by elevation of bath temperature from 22°C (black trace) to 37°C (orange trace), and subsequent inhibition by 100 μM norfluoxetine at 37°C (red trace). E) Summary dose response curves for norfluoxetine inhibition of whole cell currents at 22 (black squares), 37 (orange circles) and 42°C (red triangles) (IC_{50} at 22 °C 29.4 ± 0.1μM, Hill coefficient 1.0± 0.1, n=16; IC_{50} at 37 and 42 °C >100 μM, n=11 and n=6 respectively. F) Norfluoxetine inhibition of TREK-2 crystal construct currents at 22 and 37°C. G) Summary dose response curves for barium inhibition of whole cell currents at 22 (black squares) and 37 °C (orange circles) (IC_{50} at 22 °C 1022.2 ± 91.9 μM, Hill coefficient 1.1± 0.1, n=6; IC_{50} at 22 °C 468.8 ± 57.9 μM, Hill coefficient 1.4± 0.1, n=5).*

5.2 Norfluoxetine inhibition of temperature activated TREK-2 channel

As expected, norfluoxetine displayed decreased potency in TEVC experiments as compared to excised patches. Whilst the IC_{50} was measured to be 4.9 ± 0.5 μM in

excised patch experiments it increased to 29.4 ± 0.1 μM in TEVC recordings (n=16), see Figure 5E. This decreased potency in TEVC compared to excised patches is commonly observed for a wide range of small molecules in different paradigms, and may be attributed to the presence of the vitelline membrane or the vast hydrophobic, protein filled yolk of the oocyte (Goldin 2006; Kiehn et al. 1996; Papke & Smith-Maxwell 2009). Irrespective of this, a marked decrease in potency of norfluoxetine was observed in TEVC experiments when the bath temperature was increased to 37 or 42 °C. At these elevated temperatures norfluoxetine IC_{50} was not resolved and 50 % inhibition was increased above the maximal concentration tested (100 μM), see Figure 5E.

Importantly norfluoxetine inhibition of the temperature-insensitive crystal construct was not decreased at elevated bath temperature. At 22 °C the crystal construct was inhibited by 10, 30 and 100 μM norfluoxetine by 19.0 ± 1.5, 42.1 ± 1.7 and 65.0 ± 1.7% respectively (n = 6), whilst at 37 °C inhibition at 10, 30 and 100 μM norfluoxetine was 20.8 ± 3.2, 52.3 ± 5.8 and 74.8 ± 4.2 % respectively (n = 6), see Figure 5F. These results provide reassurance that the effect of temperature on norfluoxetine potency seen in the full length channel is not due to physicochemical effects on the drug itself, or perhaps on temperature dependent effects on binding energies. Rather, the potency shift only occurs when the channel is temperature-activated.

Meanwhile, in contrast to norfluoxetine the potency of barium (Ba^{2+}) inhibition of WT TREK-2 was not decreased at elevated temperatures, but rather was slightly increased (IC_{50} for Ba^{2+} at 22 °C was 1.0 ± 0.01 mM, n = 6; whilst at 37 °C the IC50 was 0.5 ± 0.01 mM, n = 5), see Figure 5G. This slight increase may be expected for a permeant ion blocker which requires an open selectivity filter gate in order to access its binding site when applied from the outside (Ma et al. 2011). That there was no decrease barium potency was expected as the global conformational

changes proposed for temperature activation on the basis of the norfluoxetine results would not be expected to decrease barium binding.

5.3 Temperature activation of TREK-2

Taken together these results indicate that temperature activation of TREK-2 involves structural rearrangements which decrease the affinity for norfluoxetine. Further these results indicate that whilst the sensing element for temperature- and mechano-sensation may differ the structural mechanisms by which the activation is transduced to gating may be conserved. In addition these results imply that norfluoxetine inhibition of TREK channels *in vivo* may be less significant than previously believed. The potency of the drug *in vivo* will be inversely proportional to the time that the channel exists in the stretch or temperature activated state. This property could be prone to variation depending on the cellular context, including lipid environment and phosphorylation state but is likely to be higher at physiological temperature than room temperature. Therefore relating fluoxetine/norfluoxetine inhibition of TREK channels to clinical effects requires consideration of all these factors, and simple extrapolation of potency from room temperature assays is problematic.

Ultimately it is clear that certain diverse stimuli employ similar structural mechanisms in TREK channel activation and that both stretch- and temperature-activation involves conformational changes which impair norfluoxetine inhibition.

Interestingly this effect is also observed for activation of TREK-2 by the polyunsaturated fatty acid, arachidonic acid.

6. Results: Arachidonic acid activation of TREK-2 decreases norfluoxetine potency

Arachidonic acid (AA) is a potent and efficacious activator of TREK channels and in inside-out patches expressing TREK-2 here currents were increased 28.6 ± 8.6 fold upon administration of 10 μM AA (n=13), whilst the EC50 was 0.9 ± 0.1 μM (Hill coefficient 2.6 ± 0.2, n = 5), see Figure 6. As can be seen from Figure 16 activation of channels by arachidonic acid right shifted norfluoxetine potency in a dose dependent manner such that after activation by 10 μM AA norfluoxetine IC_{50} was increased to >30 μM. In this regard arachidonic acid activation is comparable to stretch and temperature activation and it would be tempting to propose that AA mediates its activatory effect via a similar structural mechanism.

However this cannot be reliably deduced from this data alone, whilst temperature and stretch activation are likely mediated by ligand free mechanisms AA most probably exerts its effect via a direct interaction with the channel. As such it is possible that the shift in norfluoxetine potency is due to simple competitive binding for a common binding site as opposed to any allosteric competition.

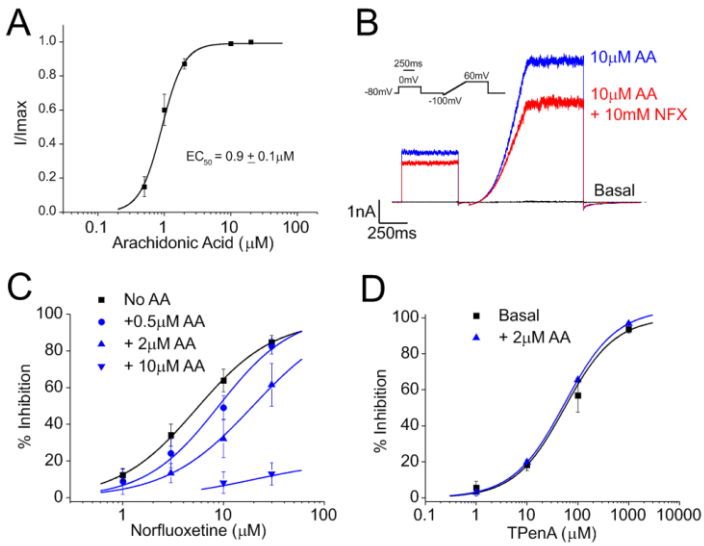

Figure 6: Arachidonic acid activation decreases norfluoxetine potency in inside-out patches expressing TREK-2. *A) Dose response curve for arachidonic acid activation of wild type TREK-2 currents recorded from 0mV steps, responses normalised to maximal activation (EC_{50} 0.9 ± 0.1 µM, Hill coefficient 2.6 ± 0.2, n=5). B) Example traces showing arachidonic acid activation (blue trace) of basal currents (black trace) and subsequent inhibition by co-administration of norfluoxetine with arachidonic acid (red trace) (voltage protocol in inset). C) Summary dose response curves for norfluoxetine inhibition of currents in the absence (black squares) and presence of 0.5 (blue circles), 2 (blue upward triangles), and 10µM arachidonic acid (blue downward triangles) (IC_{50} in the absence of AA 4.9 ± 0.5 µM, Hill coefficient 1.2 ± 0.1, n = 15; in 0.5µM AA 8.9 ± 0.9 µM, Hill coefficient 1.2 ± 0.1, n = 7; in 2µM AA 19.6 ± 1.2 µM, Hill coefficient 1.0 ± 0.1, n = 6; in 10 µM AA >30µM, n = 6). D) Summary dose response curves for TPenA inhibition of currents in the absence (black squares) and presence of 2µM (blue triangles) arachidonic acid (IC_{50} in the absence of AA 55.0 ± 7.5 µM, Hill coefficient 0.9 ± 0.1, n=4; IC50 in the presence of 2 µM AA 65.2 ± 3.7µM, Hill coefficient 1.0 ± 0.1, n=5)*

Interestingly, AA activation does not appear to shift TPenA potency, see Figure 6. The predicted binding site for TPenA is expected to overlap with the crystallographic norfluoxetine binding site and preliminary studies indicate that quaternary ammonium inhibitors may compete with fluoxetine (Thomas Baukrowitz lab, unpublished data). So if AA competed with norfluoxetine for a binding site it may be expected to also compete with TPenA. The lack of any shift in TPenA sensitivity in AA-activated channels argues against competition, which may in turn argue against AA/norfluoxetine competition. However, it is of course possible that the TPenA/norfluoxetine binding site overlap is spatially distinct from a possible AA/norfluoxetine binding site overlap. With these multiple

complications it is difficult to conclusively determine the mechanism by which AA activates TREK-2 at this stage, and further work is warranted.

6.1 The mechanism of PUFA-activation in TREK channels

Poly *cis*-unsaturated fatty acids (including arachidonic acid) have been reported to increase membrane fluidity (decrease in stiffness), which clearly could have a significant effect on transmembrane protein activity (Meves 1994; Meves 2008; Klausner et al. 1980; Richieri et al. 1990; Lundbaek et al. 2010). Therefore it is possible that PUFAs exert their effects on TREK/TRAAK channels exclusively via changes in the membrane properties.

However, AA activation has been reported to be via a specific C-terminal region which may indicate a direct interaction (Patel et al. 1998; Kim 2001). Yet, curiously the C-terminus is not required for AA activation of TRAAK (Kim, et al. 2001). Therefore it is possible that AA and PUFAs activate the TREK and TRAAK channels differently or perhaps in multiple ways.

The structural mechanism for activation by arachidonic acid

Whatever the cause of AA-induced activation of TREK-2 the effect of AA-activation on norfluoxetine sensitivity is clear. As I show, the presence of AA decreases norfluoxetine inhibition in TREK-2. This may indicate that the gating equilibrium shifts towards an open conformation in which the norfluoxetine binding site is abolished, as suggested for stretch and temperature activation. This would be consistent with AA decreasing the energy for the up state, which may arise from effects of PUFAs on membrane fluidity. By increasing membrane fluidity AA could

shift channel gating in favour of the up state. This may provide an explanation for a possible indirect mechanism of AA modulation of TREK channels.

Alternatively the AA-induced shift in norfluoxetine potency could also be explained by a simple competition for a common binding site. In this case AA would necessarily interact directly with the channel.

Therefore how arachidonic acid modulates TREK and TRAAK channels remains to be fully established.

7. Developing a structural scheme for TREK-2 gating

Together these results provide new insights into the conformational changes in TREK-2 gating. Further, they show that activation by membrane stretch and elevated temperature (and possibly arachidonic acid) provokes conversion to a state in which norfluoxetine sensitivity is markedly reduced. Coupling this functional data with the crystal structures leads me to postulate that activation by these mechanisms involves conversion from the closed down conformation to the open and conductive up conformation, see Figure 7. Norfluoxetine is able to access its binding site in the down conformation only, and therefore acts as a closed-channel blocker. The binding of the drug locks the channel closed and prevents activation.

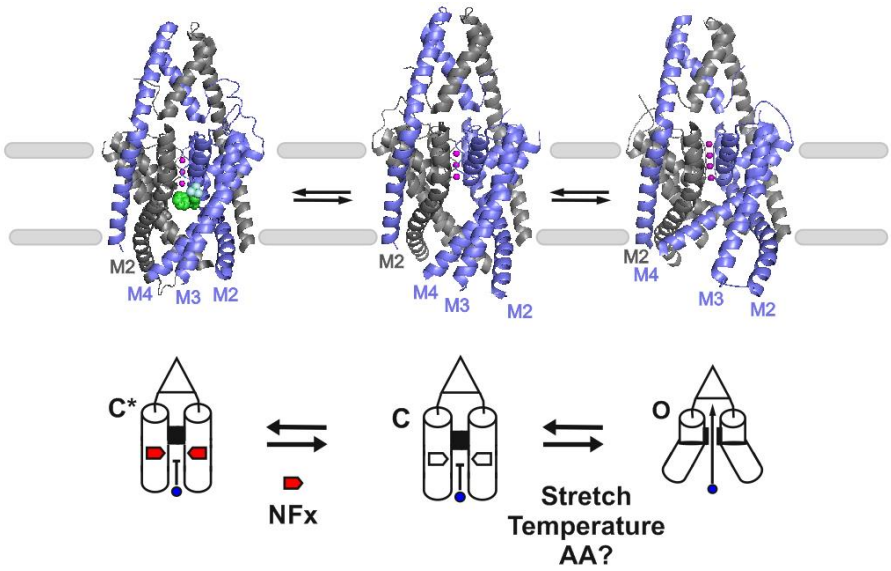

Figure 7: Extension of gating scheme from Figure 4. *Temperature activation activates TREK-2 (C → O) in a mechanism which also decreases norfluoxetine potency, similar to the mechanism proposed for mechano-activation.*

8. Results: Carvedilol and fluphenazine act as state dependent inhibitors of TREK-2

Following the elucidation of the norfluoxetine binding site, and the underlying basis of state-dependent inhibition I sought to explore if this mechanism was common to other TREK channel inhibitors. A number of other clinically used drugs have been identified as TREK channel inhibitors including carvedilol and fluphenazine (Kisselbach et al. 2014; Thümmler et al. 2007). The mechanism by which these drugs exert their effects on TREK channels was unknown and we hypothesised that these molecules could behave similarly to norfluoxetine.

8.1 Carvedilol and fluphenazine inhibit TREK-2

Firstly, carvedilol was tested for inhibition of wild type TREK-2 currents in inside-out patches. As can be seen below in Figure 8 carvedilol provoked a dose dependent decrease in basal currents with an IC_{50} 6.6 ± 0.5 μM (Hill coefficient 1.7 ± 0.1, n = 8).

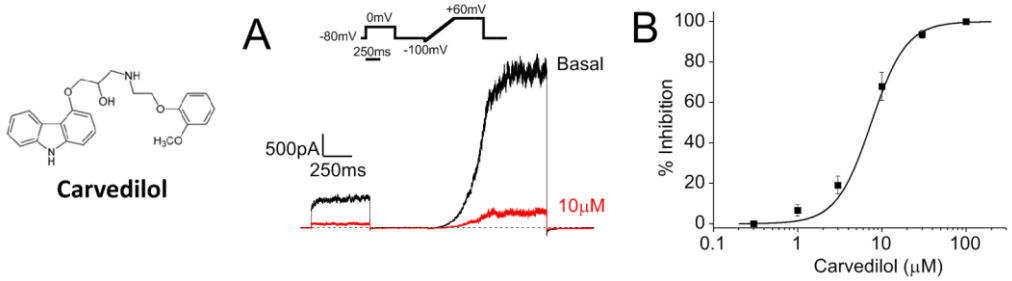

Figure 8: Carvedilol inhibition of TREK-2. *A) Example traces of an inside out patch clamp recording of TREK-2 showing inhibition of basal currents (black) by 10 μM carvedilol, voltage protocol in inset. B) Summary dose response curve for carvedilol block of TREK-2, IC_{50} 6.6 ± 0.5 μM (Hill coefficient 1.7 ± 0.1, n = 8). Mean percentage inhibition calculated from voltage steps to 0mV.*

Meanwhile fluphenazine displayed similar properties, with an IC50 of 3.8 ± 0.5 μM (Hill coefficient 1.1 ± 0.1, n = 8), see Figure 9.

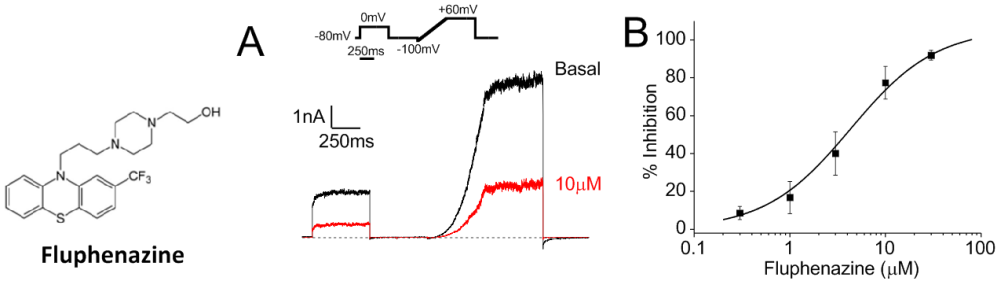

Figure 9: Fluphenazine inhibition of TREK-2. *A) Example traces of an inside out patch clamp recording of TREK-2 showing inhibition of basal currents (black) by 10 μM fluphenazine, voltage protocol in inset. B) Summary dose response curve for fluphenazine block of TREK-2, IC_{50} 3.8 ± 0.5 μM (Hill coefficient 1.1 ± 0.1, n = 8). Mean percentage inhibition calculated from voltage steps to 0 mV.*

8.2 Carvedilol and fluphenazine both act as state dependent inhibitors

As previously observed for norfluoxetine the potency for both carvedilol and fluphenazine was markedly decreased in patches in which TREK-2 was activated by pressure. Figure 10 shows that the IC_{50} for both inhibitors was shifted to above 30 μM in the presence of -11 mmHg suction (carvedilol n = 10; fluphenazine n = 9).

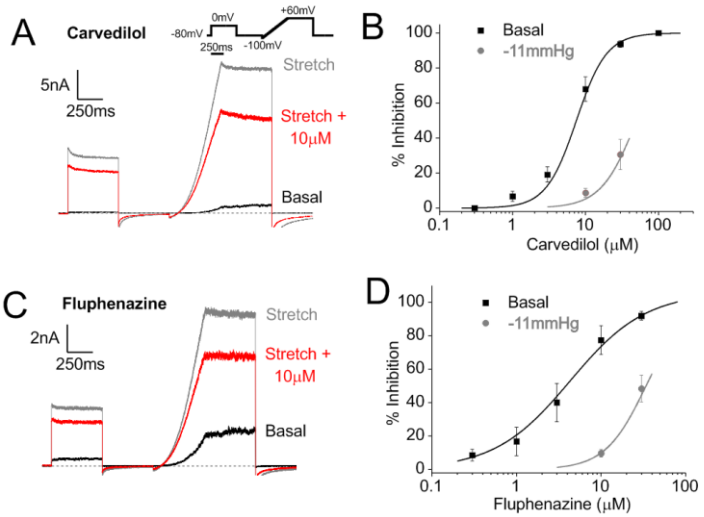

Figure 10: Inhibition of TREK-2 by carvedilol and fluphenazine is decreased in mechano-activated channels. *A) Example traces from an inside out patch clamp recording of TREK-2 showing activation of basal currents (black) by application of suction (-11mmHg, grey) and subsequent co-administration of carvedilol with suction (red), voltage protocol in inset. B) Summary dose curves for carvedilol inhibition in the absence (black squares) and presence (grey circles, IC50 > 30 μM, n = 10) of stretch. C) Example traces from an inside out patch clamp recording of TREK-2 showing activation of basal currents (black) by application of stretch (-11 mmHg, grey) and subsequent co-administration of fluphenazine with stretch (red), voltage protocol as above for carvedilol. D) Summary dose curves for fluphenazine inhibition in the absence (black squares) and presence (grey circles, IC50 > 30 μM, n = 9) of stretch.*

Clearly therefore mechano-activation involves conformational changes which decreases either the binding energy of accessibility of carvedilol and fluphenazine for their binding site.

Similarly, temperature activation also clearly decreased TREK-2 sensitivity to both inhibitors. In TEVC recordings at 22°C 30 μM carvedilol provoked a 63.9 ± 5.8% (n = 5) inhibition which was decreased to 31.4 ± 4.5% (n = 5) and 19.4 ± 5.0% (n = 5) at 37 and 42°C respectively, see Figure 11. Likewise 30μM fluphenazine inhibition was reduced from 51.4 ± 2.7% at 22°C (n = 8) to 30.9 ± 1.0% (n = 6) and 9.5 ± 1.8% (n = 7) at 37 and 42°C, see Figure 11. Importantly no temperature dependent effects on carvedilol potency were observed for inhibition of the temperature-insensitive TASK-1 channel, see Figure 11D. This provides assurance that temperature elevation does not

significantly affect the physico-chemical properties of the drug and indicates that the shift seen for TREK-2 is most likely due to temperature-dependent gating changes.

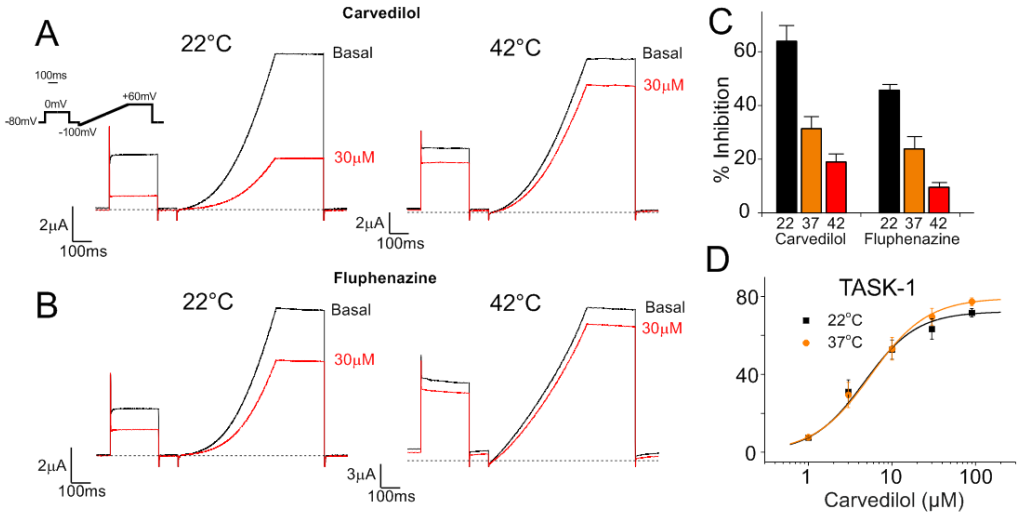

Figure 11: Temperature activation of TREK-2 channels decreases sensitivity to inhibition by carvedilol and fluphenazine. *A) Example traces showing inhibition of TREK-2 by 30μM carvedilol at 22oC (left) and 42oC (right), voltage protocol as shown in inset. B) Example traces showing inhibition of TREK-2 by 30μM fluphenazine at 22oC (left) and 42oC (right). C) Percentage inhibition of currents at 0mV provoked by carvedilol and fluphenazine at 22, 37 and 42oC. D) Dose response summary for carvedilol inhibition of whole-cell TASK-1 currents at 22 and 37oC (percentage inhibition of basal currents at 0mV; IC50 at 22oC 4.7 ± 0.8μM, Hill coefficient 1.4 ± 0.1, n = 8; IC50 at 37oC 5.6 ± 0.7μM, Hill coefficient 1.3 ± 0.1, n = 5).*

8.3 Carvedilol and fluphenazine potency is affected by the L320W fenestration binding site mutation

These results indicate that both carvedilol and fluphenazine act as state-dependent inhibitors of TREK-2, a mechanism they share with norfluoxetine. It follows therefore that their binding site is likely in a region which undergoes structural rearrangement in stretch- and temperature activation, again like we have observed for norfluoxetine. The L320W binding site mutation, which affects norfluoxetine potency, without any discernible effect on channel gating, was tested for sensitivity to inhibition by carvedilol and fluphenazine. Interestingly this mutation induced a left-shift in potency for both carvedilol and fluphenazine. Carvedilol inhibited inside-out patch TREK-2 currents with

an IC_{50} of 6.6 ± 0.5 µM (Hill coefficient 1.7 ± 0.1, n = 8) whilst L320W was inhibited with an IC50 of 1.5 ± 0.1 µM (Hill coefficient 1.1 ± 0.1, n =7), see Figure 12. Meanwhile fluphenazine inhibited wild type currents with an IC50 of 3.8 ± 0.5 µM (Hill coefficient 1.1 ± 0.1, n = 8) which was slightly reduced to 1.5 ± 0.5µM (Hill coefficient 1.1 ± 0.1, n = 5) in the L320W mutant, see Figure 12.

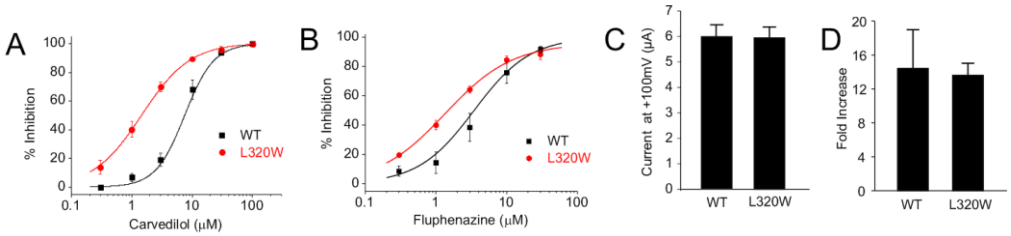

Figure 12: Carvedilol and fluphenazine potency is affected by the fenestration binding site L320W mutation. *A) Summary dose response for carvedilol inhibition of TREK-2 WT (IC50 6.6 ± 0.5 µM, Hill coefficient 1.7 ± 0.1, n = 8) and L320W (IC50 1.5 ± 0.1 µM, Hill coefficient 1.1 ± 0.1, n = 7), percentage inhibition of basal currents at 0mV. B) Summary dose response for fluphenazine inhibition of TREK-2 WT (IC50 3.8 ± 0.5 µM, Hill coefficient 1.1 ± 0.1, n = 8) and L320W (IC50 1.5 ± 0.1 µM, Hill coefficient 0.9 ± 0.1, n = 5), percentage inhibition of basal currents at 0mV. C) Basal whole-cell currents from TEVC recordings at +100mV for TREK-2 WT and L320W. D) Fold activation of currents from inside-out patch clamp recordings upon application of suction (-11 mmHg) for WT and L320W (currents recorded at 0 mV).*

Whilst the shift in potency observed for fluphenazine was relatively small it appears that mutations in the region of the norfluoxetine fenestration binding site impact upon carvedilol and fluphenazine binding. Curiously the direction of the effect in both these cases was opposite to that observed for norfluoxetine.

There are two important inferences from this data, firstly, this allows us to be more confident in the conclusion that the effects of the mutation are not due to a shift in channel gating behaviour. If it was in fact the case that the mutation shifts the gating equilibrium then we would expect to see shifts in potency for all the state dependent inhibitors in the same direction. Secondly, this suggests that the introduction of a bulky tryptophan side chain in the place of L320 may increase either the binding energy of carvedilol and fluphenazine or perhaps affects the on/off rates in the favour of binding.

The former effect could be conferred by increased interactions between the tryptophan sidechain and the drug. Insights into this may arrive from *in silico* docking studies of carvedilol and fluphenazine within the fenestration binding site. Elsewhere effects on on/off rates could be the result of trapping the molecule within the binding site, which could be assessed by measuring the "wash off" rate of the inhibitors, but is yet to be performed.

8.4 State dependence: an emerging property amongst diverse TREK channel inhibitors

Ultimately these results extend the principle of state-dependent inhibition previously described for norfluoxetine to carvedilol and fluphenazine. Further they suggest that the molecules may share a common binding site, implicating the lateral fenestrations in the mechanism of action for structurally diverse TREK channel modulators. As described previously for norfluoxetine the temperature induced decrease in carvedilol and fluphenazine potency may have significant implications for the physiological role of these drugs at TREK-2 channels. Again the potency will be inversely proportional to the time spent in the stretch or temperature activated state, and so drug action is dependent on these properties in native channels.

It will be interesting to expand this study into the range of other TREK channel modulators. Testing for state dependence of inhibition will allow categorisation of known inhibitors into functional classes. If an inhibitor was shown to be non-state-dependent, as seen for barium ions and TPenA, for example, the existence of a novel mechanism of action, and a novel binding site would be predicted. It would be interesting to find this as a non-state-dependent mechanism may in fact be desirable in rational drug design to obviate the complications of open probability dependent changes in potency.

Chapter 6 - Mechanisms of pH regulation in TREK-2

1. Introduction

The results from Chapter 5 indicate that mechano-, temperature- and arachidonic acid activation all decrease norfluoxetine potency. A reasonable conclusion from this data would be that activation via these mechanisms involves conformational changes from a norfluoxetine accessible state to a norfluoxetine inaccessible state. I sought to test whether these conformational changes were shared in regulation by pH.

2. Physiological pH

The control of pH within strict limits is critical for normal physiological function. When one considers the basic structure of proteins it is clear why such precise homeostasis is necessary; secondary, tertiary and quaternary peptide structure is maintained by multiple intra- and intermolecular interactions which are pH sensitive, such as hydrogen bonds and salt bridges. Changes in pH can disrupt such interactions and extreme pH changes (to values < 4 or > 9) can result in complete protein denaturation by interrupting hydrogen bonding (Holzer 2009a).

Thus two clear implications arise: firstly as homeostasis is critical for normal protein function the necessity for exquisite sensing and buffering mechanisms exists. Secondly proteins are inherently pH-sensitive, and therefore it is perhaps

unsurprising when pH changes alter protein function. Therefore in discussing the pH-sensitivity of a protein perhaps the most pertinent considerations are whether pH-dependent changes in protein function occur within a relevant physiological pH range and if the change in protein function is important for a cellular/system function (i.e. has a physiological role).

The "normal" physiological external (interstitial, pH_o) and internal pH (pH_i) can vary between cells and tissues. For example, whilst in the brain external pH is around 7.3 – 7.4, osteoclasts are capable of acidifying their surrounding environment to ~ pH 3 for bone resorption (Roos & Boron 1981; Silver et al. 1988). Normal pH is dependent on the buffering of proton concentration by CO_2 and HCO_3^-, and on metabolic activity, and is maintained by the relative activities of acid-extruding and acid-loading proteins (including proton and HCO_3^- exchangers, co-transporters, and pumps), but can vary significantly in numerous metabolic and respiratory states (Holzer 2009b; Boron 2004; Ruffin et al. 2014; Xiong et al. 2000; Somjen 1984a; Chesler 2003).

Whether TREK channels serve any physiological role as pH sensors remains unknown. Whilst perturbations in mechanical and thermal sensation have been reported in TREK knock-out mice models no alteration in pH sensing at a cellular level, or pH-related systemic functions (e.g. ventilatory response to altered CO_2) have been demonstrated to date, and may not have been assessed. TREK-1 and TREK-2 have been implicated in sour (acid) taste sensation in murine taste buds, though this association is currently lacking strong evidence (Richter et al. 2004). Despite this, clearly the mechanisms by which pH modulates TREK channels is of significant interest. By probing these mechanisms we can learn how the channel is able to gate in activation, and also how different gating modalities interact.

3. Intracellular pH sensing in TREK channels

Early characterisation of TREK-1 showed that the channel was extremely sensitive to changes in the pH of the intracellular recording solution in excised patch clamp recordings. Effects are complex with acidification inducing increases in open probability but decreases in single channel conductance (Honoré et al. 2002; Maingret et al. 1999). Chimeric and truncated channels were used to localise the critical pH sensor region to a charged region of the proximal C-terminus (Honoré et al. 2002; Maingret et al. 1999). This region contains numerous basic charges surrounding an acidic glutamate residue (E306), which was proposed as the proton sensor on the basis of mutagenesis experiments.

Mutation of this glutamate to alanine resulted in channels with large basal currents which could not be significantly activated further by intracellular acidification, membrane stretch or other activatory stimuli. Furthermore the mutation mimicked pH_i in sensitising a truncated TREK-1 channel to mechanical activation. Subsequent investigations have confirmed the critical contribution of this region in pH_i sensing in TREK-2.

It has been suggested that protonation of E306 (E337 in TREK-2) increases the net positive charge of the proximal C-terminus, which increases its propensity for coupling with the membrane via negatively charged phospholipid headgroups (Honoré et al. 2002). Curiously TREK-1 and TREK-2 appear most sensitive to pH over a range (pH 6 – pH 8) some distance from the predicted pKa of a glutamate side chain (pKA approximately pH 4.3). However it is well known that local environment can affect the pKa of amino acid side chains and so it is possible this explains this discrepancy.

3.1 TREK channel gating model

A series of papers demonstrated that intracellular acidification shifts the pressure response curve leftwards resulting in channels which activate at lower pressures (Honoré et al. 2002; Maingret et al. 1999). This led to a model of polymodal gating as represented below in Figure 1, where intracellular pH determined the transition between one closed state (C_1) and a second closed state (C_2), and that acidification decreased occupancy of C_1, whilst pressure activation controlled transition from C_2 to the open state (O) (Honoré et al. 2002; Kennard et al. 2005).

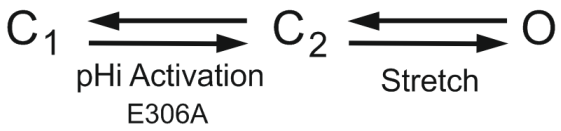

Figure 1: Adaptation of gating model proposed by Honore et al (2002) and Kennard et al (2005).

Therefore changes in intracellular pH would be expected to increase open probability by decreasing time cumulatively spent in any of the potentially numerous closed states. In Chapter 5 I proposed that the closed and open states of TREK-2 exhibit markedly different sensitivities to the state-dependent inhibitor, norfluoxetine. For both this notion and the above gating model to be in agreement, any increase in open probability (and corresponding decrease in closed probability) would necessarily be accompanied by a decrease in norfluoxetine potency due to decreased accessibility of the inhibitor to its binding site. To test this I investigated the effect of pH_i-activation on norfluoxetine potency, which is discussed in section 5 below.

4. Molecular origins of extracellular pH sensitivity

Insightful analysis has previously demonstrated that a conserved histidine located in an extracellular loop linking the cap domain to the first pore helix (PH1) is the critical proton sensor for all three TREK channels (Cohen et al. 2008; Sandoz et al. 2009). The difference in directionality of the response to histidine protonation has been attributed to differences in another extracellular region, the loop linking second p-loop (P2) to M4 (Sandoz et al. 2009), however preliminary studies in our hands have failed to reproduce the finding of these chimera studies, possibly due to species specific differences (Michael Clausen and Conor McClenaghan, unpublished). Regardless it is clear that extracellular loops remain critical for pH_o sensing.

4.1 Extracellular pH modulates open probability

The functional basis for pH_o modulation is believed to be alterations of open probability, as opposed to changes in conductance. This has been demonstrated clearly for TREK-1 where single channel recordings at varying extracellular pH showed comparable single channel conductances (Cohen et al. 2008). It was proposed that pH_o gating in TREK-1 involves collapse of the selectivity gate filter, perhaps in a structural rearrangement similar to C-type inactivation of voltage gated potassium channels (Cohen et al. 2008; Cuello et al. 2010). Accordingly, in the same study by Cohen and colleagues it was reported that elevated extracellular potassium concentration blunts pH_o regulation, a mechanism attributed to stabilisation of the selectivity filter gate in an open, conductive conformation.

Furthermore extracellular acidification impairs barium access in TREK-1, indicating that access for the permeant ion to its binding site within the selectivity filter is impaired by pH_o inhibition (Ma et al. 2011).

Whilst the effect of pH_o on single channel conductance in TREK-2 has not been clearly demonstrated, again pH_o regulation is blunted by high $[K^+]_o$. This suggests that pH_o likely provokes macroscopic current changes in both TREK-1 and TREK-2 via increases in open probability.

5. Results: The effect of pH_i-activation on norfluoxetine potency

Acidification of the intracellular recording solution in inside-out patch clamp experiments provoked marked activation of TREK-2 currents (see Figure 2; currents at pH 6.0 14.3 ± 8.3 times those at pH 8.0, n = 9). As expected in light of previous reports demonstrating the critical effect of truncating the C-terminus of TREK channels, no activation was seen in the TREK-2 crystal construct. In fact acidification induced a marked inhibition of these channels, comparable to the effect reported on TRAAK channels (crystal construct currents at pH 6.0 0.25 ± 0.02 times those at pH 8.0, n = 3), see Figure 2 (Kim, Bang, et al. 2001).

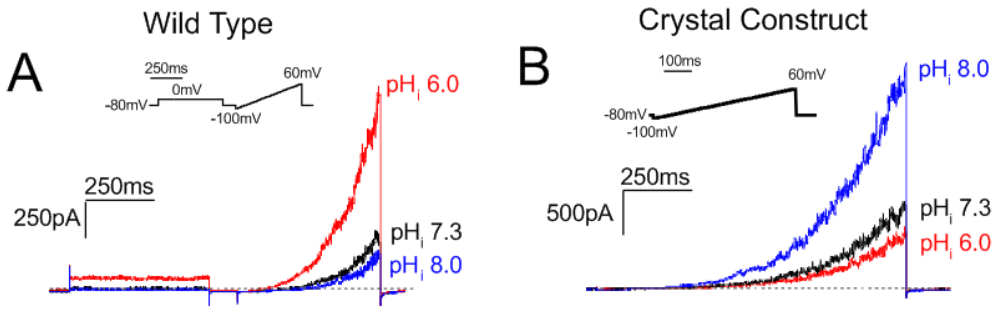

Figure 2: Intracellular pH sensing is reversed in the TREK-2 crystal construct. *Example traces showing pHi-activation of wild type TREK-2 (A) and crystal construct TREK-2 (B), voltage protocols in inset.*

Surprisingly very little effect on norfluoxetine potency was observed in patches in which TREK-2 channels had been activated by acidification. As can be seen in Figure 3, whilst at pH_i 7.3 norfluoxetine IC_{50} was 4.9 ± 0.5 µM (Hill coefficient 1.2 ± 0.1, n = 15) at pH_i IC50 was 5.0 ± 1.1 µM (Hill coefficient 1.9 ± 0.5, n =7). Therefore increases in open probability induced by intracellular acidification from pH 7.3 to pH 6.0 do not appear to affect norfluoxetine affinity. This would be unexpected for a channel which has only one open state, as in the aforementioned gating scheme (Figure 1), as any increase in channel activation would be expected to decrease inhibitor potency. Intracellular acidification must therefore induce activation via a mechanism which opens the channel but does not involve a shift in the equilibrium between the norfluoxetine-sensitive and the norfluoxetine-insensitive conformations.

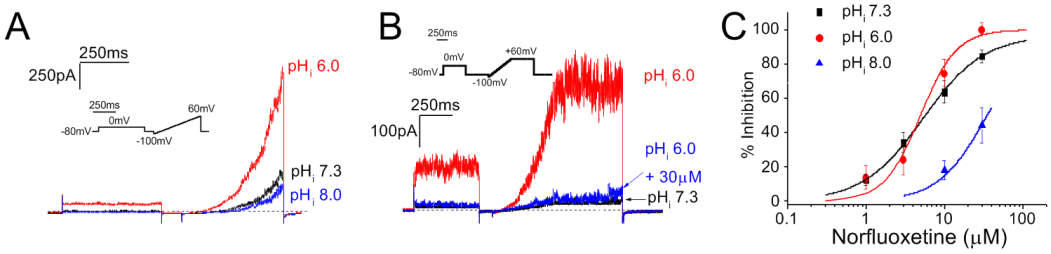

Figure 3: Intracellular pH activation does not decrease norfluoxetine potency in inside-out patch recordings of TREK-2. *A) Example traces showing the effect of varying pH on TREK-2 currents (voltage protocol in inset). B) Example traces showing activation of TREK-2 currents by acidification from pHi 7.3 to pHi 6.0, and subsequent administration of 30µM norfluoxetine at pHi 6.0. C) Summary dose response curves for norfluoxetine at varying pHi (IC_{50} at 7.3 4.9 ± 0.5µM, Hill coefficient 1.2 ± 0.1, n = 15; at 6.0 5.0 ± 1.1µM, Hill coefficient 1.9 ± 0.5, n =7; at 8.0 >30µM, n = 6).*

5.1 The emergence of multiple open states in TREK-2

Hence this finding raises the possibility that there are in fact multiple open states for TREK-2. This conclusion is necessary in order to explain the different effects on

potency observed for activation by stretch and temperature versus intracellular pH. Interestingly, as shown in Chapter 4, transmembrane voltage had little effect on norfluoxetine block. This is curious as TREK channels are known to be activated at depolarised voltages.

Therefore it appears that certain modulatory stimuli may activate TREK-2 via a mechanism involving structural rearrangements which affect norfluoxetine affinity whilst other stimuli may employ structurally distinct conformational changes which have no such impact. Consequently I propose a revised gating scheme as below, Figure 4, whereby channel activation via different stimuli involves different conformational changes to distinct open states.

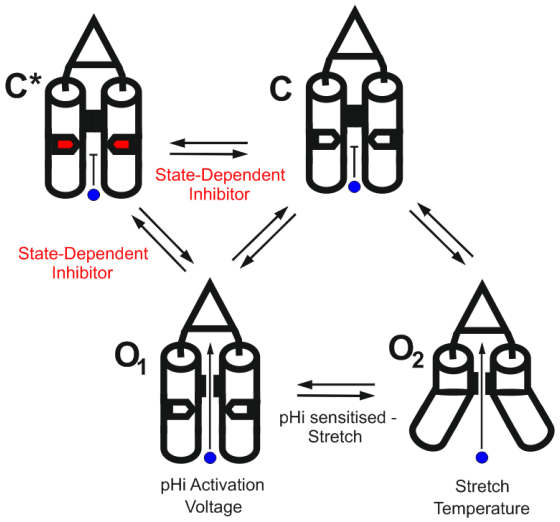

Figure 4: Proposed gating scheme for polymodal activation of TREK-2. *Channels in their closed state (C) are impermeable to potassium ions (blue circle) and contain transmembrane fenestrations (empty boxes). State-dependent inhibitors can bind within the fenestration (red boxes) to lock channel in drug-bound closed state (C*). Alternatively the channel can be activated by conversion to either an open state with fenestrations existent (O_1), as in pH_i and voltage activation, or by conversion to an open state where the fenestration binding site is abolished (O_2), as in stretch-activation.*

Interestingly, in patches where basal currents at pH_i 7.3 were reduced by alkalinisation (pH_i 8.0) norfluoxetine inhibition was markedly decreased, Figure 3. Again, this finding is difficult to reconcile with the gating scheme from Figure 1, as

decreased channel activation would be expected to *increase* potency. However this result can possibly be explained by the new gating scheme as decreasing the proportion of channels in the pH_i-activated, norfluoxetine-sensitive open conformation may be expected to increase the proportion of channels in the stretch-activated conformation. As we know that the stretch-activated conformation displays decreased norfluoxetine potency we would expect the right shift observed. In other words, removing the pH-activated population leaves us only with stretch-activated channels, which display decreased sensitivity to inhibition.

However this proposal is complicated somewhat by the finding that intracellular acidification acts to sensitise channels to stretch (in TREK-1, at least), in which case alkalinisation to pH 8.0 may be expected to decrease stretch activation. With this in mind it is also possible that the decreased potency at pH 8.0 is a reflection of pH effects on the norfluoxetine molecule itself, as opposed to the channel.

Further work is required to determine the basis of the alkalinisation-dependent shift on norfluoxetine potency. However, ultimately, using the state-dependent inhibitor norfluoxetine allows for dissection of distinct gating mechanisms and reveals that TREK-2 is capable of adopting multiple open conformations depending on the stimulus.

The mechanism by which the channel is modulated by extracellular pH remained to be established however.

6. Results: The extracellular pH sensor region in TREK-2

Resolution of the TREK-2 crystal structure provided information for the first time about the precise location of the extracellular pH sensor and its surrounding

environment. As can be seen in Figure 5, the proton sensing H156 exists within a complex hydrogen bonding network within an aqueous extracellular cavity making the sidechain accessible for protonation. Upon acidification it would be expected that the histidine sidechain would experience a higher probability of protonation, which would confer a net positive charge to the sidechain.

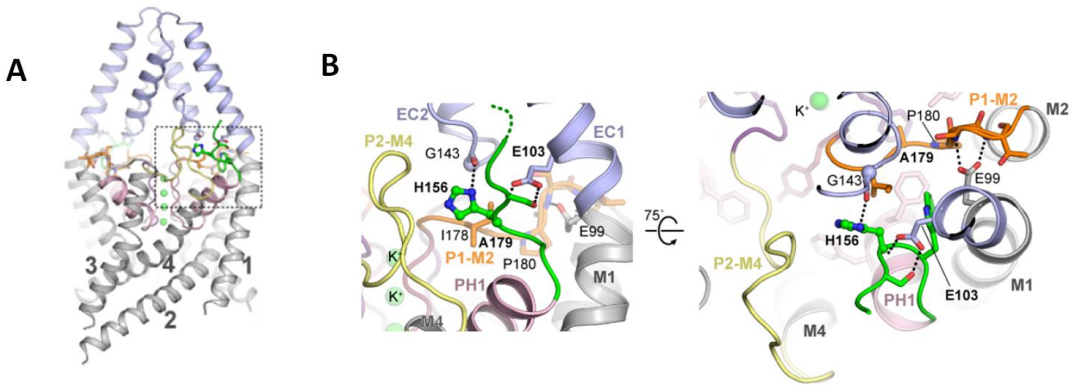

Figure 5: The extracellular pH sensor region as determined by X-ray crystallography. *A) The location of the critical pH sensing histidine (H156, shown in green), which lies in the loop linking the extracellular cap to the pore domain. B) Zoomed in view of the pH sensor region showing E103, H156 and A179, observing through the side of the channel (left panel) and from above (right panel). Extensive hydrogen bonding between H156 and surrounding residues are noted by dashed black lines. Figures adapted from those created by Elizabeth Carpenter and Ashley Pike and published in* (Y. Y. Dong et al. 2015).

Considering this it was interesting to observe two negatively charged glutamate residues in close proximity to the histidine in the crystal structure. We postulated that electrostatic interaction between these acidic residues and the protonated histidine may be important for the structural reorganisation required in pH_o gating. Notably mutation of one of these glutamates (E84 in TREK-1/E99 in TREK-2) has been shown to abrogate pH_o modulation in TREK-1 (Cohen et al. 2008; Mathie et al. 2010). Similarly, as can be seen in Figure 6, mutation of the neighbouring E103 residue to the polar but uncharged glutamine also markedly blunts pHo modulation and increases basal currents. For wild type TREK-2 channels whole cell currents at pH 8.2 were 0.41 ± 0.04 times that at pH6.5 (n = 12), whilst in the E103Q mutation

currents at pH8.2 were 0.90 ± 0.03 times that at pH6.5 (n = 6). Peak whole cell currents in the E103Q mutant were increased to 11.5 ± 0.4 μA (n = 23) compared to 6.0 ± 0.5 μA (n = 30) for wild type TREK-2. This result implies that the negative charge of the glutamate sidechain is critical for pH function and may be involved in stabilising a closed state.

Elsewhere mutagenesis also confirmed the importance of another extracellular loop, the P1-M2 loop, for pH_o gating. A yeast screen assay designed to detect gain of function mutations in TREK-1 uncovered the activatory effect of a S146P mutation in this region (Chetan Sharma, unpublished data). Sequence alignment of TREK-1 with TREK-2 identified the homologous residue as A179 in TREK-2, and so the A179P mutation was tested for pH_o sensitivity. As observed for the E103Q mutation the A179P mutation resulted in a channel with blunted pHo sensitivity (currents at pH 8.2 were 0.97 ± 0.1 times that at pH 6.5, n = 6) and elevated basal currents (peak whole cell currents were 7.6 ± 0.3 μA). Introduction of a proline (with its cyclical secondary amine moiety) is expected to increase rigidity at this site, thus it appears that increased rigidity of the P1-M2 loop in both TREK-1 and TREK-2 stabilises the channel in an open, conductive state.

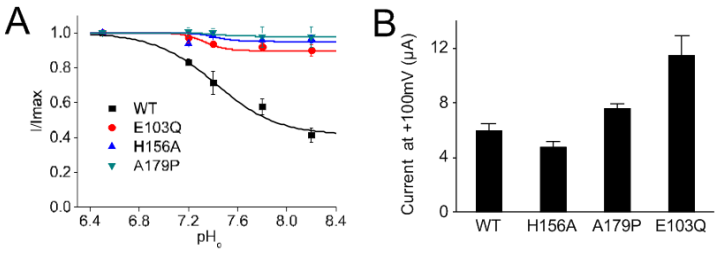

Figure 6: Mutations around the proton sensing histidine abrogate external pH-sensitivity. *A) pH response profile for TREK-2 WT, E103Q, H156A and A179P. B) Basal whole-cell currents from TEVC recordings at +100mV for TREK-2 WT, H156A, A179P and E103Q.*

This data therefore illustrates the critical role of the extracellular loops in coupling proton sensing to modulation of the selectivity filter gate. Clearly these regions are

spatially discrete from the transmembrane regions identified as being involved in mechano- and thermo-activation. Previously it has been suggested that distinct stimuli may converge upon a common gate (namely the selectivity filter) but it is yet to be established whether the stimuli employ the same global conformational changes to do so (Bagriantsev et al. 2011). It was hypothesised that pH_o gating did not necessarily require the large conformational movements seen for stretch and temperature in order to modulate the filter gate. This again can be tested by assessing the effect of extracellular pH activation on norfluoxetine potency.

6.1 Extracellular pH change does not significantly shift norfluoxetine potency

If activation of TREK-2 by extracellular acidification involved the global structural changes proposed for stretch activation, including the abolition of the norfluoxetine fenestration binding site in the active state then one would expect norfluoxetine potency to decrease proportionally with pH_o activation. This was tested using TEVC recordings of whole oocytes perfused with recording solution of varying pH. At pH 7.4, a value chosen to approximately represent physiological extracellular pH, norfluoxetine IC_{50} was 29.4 ± 0.1 μM (Hill coefficient 1.0 ± 0.1, n = 16). Interestingly varying the pH to 6.5 or 8.5 provoked only a negligible shift in potency (norfluoxetine IC_{50} at pH 6.5 was 21.9 ± 10.1 μM, Hill coefficient 0.8 ± 0.1, n = 6; IC_{50} at pH 8.5 was 27.3 ± 2.6 μM, Hill coefficient 0.8 ± 0.1, n = 6), Figure 7. Importantly the rank order of IC_{50} at these differing pH values (pH 7.4 > 8.5 > 6.5) did not correlate with the extent of channel activation (where channel activation at 6.5 > 7.4 > 8.5).

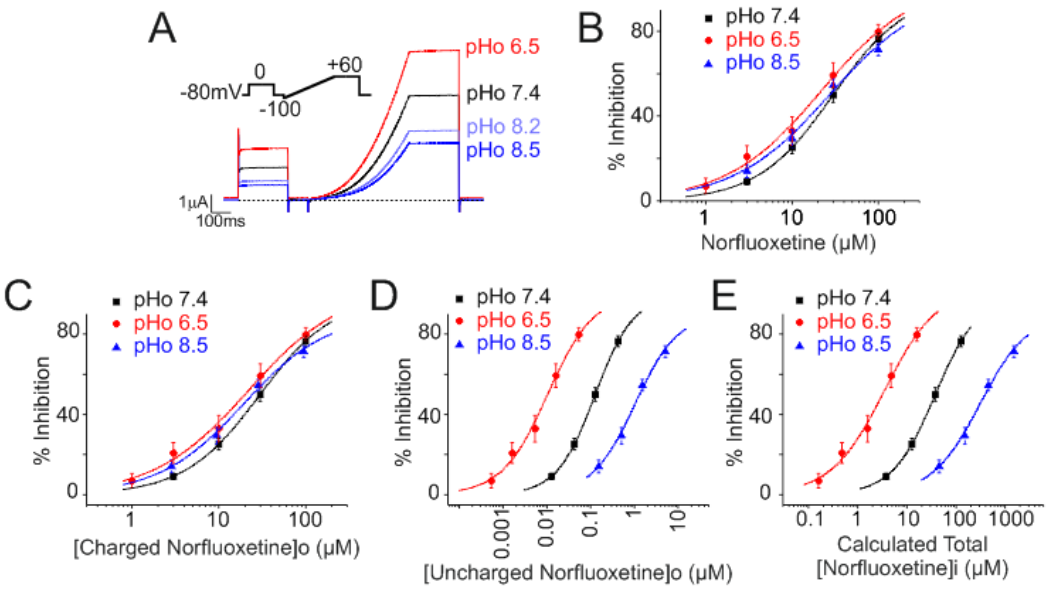

Figure 7: Norfluoxetine inhibition of whole cell TREK-2 currents at varying pHo. *A) Example traces showing extracellular pH modulation of whole cell TREK-2 WT currents. B) Summary dose response for norfluoxetine inhibition at varying pHo (percentage inhibition for current at 0mV; IC_{50} at pHo 7.4 29.4 ± 0.1 μM, Hill coefficient 1.0 ± 0.0, n = 16; IC_{50} at pHo 6.5 21.9 ± 10.1 μM, Hill coefficient 0.8 ± 0.1, n = 6; IC_{50} at pHo 6.5 27.3 ± 2.6 μM, Hill coefficient 0.8 ± 0.1, n = 6). C) Summary dose response curve for inhibition plotted against the calculated concentration of charged norfluoxetine in the extracellular solution at varying pH_o (same data used as that shown in Figure 7B; IC_{50} at pH_o 7.4 29.8 ± 5.0 μM, Hill coefficient 1.2 ± 0.01; IC_{50} at 6.5 20.5 ± 5.2 μM, Hill coefficient 1.2 ± 0.02; IC_{50} at 8.5 18.5 ± 2.8 μM, Hill coefficient 1.2 ± 0.02). D) Summary dose response curve for inhibition plotted against the calculated concentration of uncharged norfluoxetine in the extracellular solution at varying pH_o (same data used that as shown in Figure 7B). E) Summary dose response curve for inhibition plotted against the calculated total intracellular concentration of norfluoxetine (charged and uncharged) at varying pH_o (same data used as that shown in Figure 7B; IC_{50} at pH_o 7.4 35.2 ± 5.7 μM, Hill coefficient 1.2 ± 0.1; IC_{50} at 6.5 3.3 ± 0.8 μM, Hill coefficient 1.2 ± 0.2; IC_{50} at 8.5 268.9 ± 45.1 μM, Hill coefficient 1.2 ± 0.02).*

This result suggests that extracellular pH modulation does not impact upon norfluoxetine potency. However, norfluoxetine is predicted to be a weak base with a calculated pKa of 9.77 (value derived from ChemAxon predictive software as documented by DrugBank (http://www.drugbank.ca/drugs/DB06731), and consequently altering the bulk pH of the extracellular buffer in which norfluoxetine is dissolved is expected to affect the charge state of the drug. By using the Henderson-Hasselbalch equation one can calculate the concentrations of charged

(BH+) and uncharged (B) norfluoxetine molecules at the different extracellular pH tested, as:

$$pH - pKa = \log([B]/[BH^+])$$

And thus $[B]/[BH^+]$ at pH 8.5 can be found, as below, and that ratio can be used to calculate the concentration of charged and uncharged drug at each bulk concentration applied.

$$10^{(8.5-9.77)} = ([B]/[BH^+])$$
$$= 0.053$$

So for 100 μM,

$$100\ \mu M = [BH^+] + (0.053 \times [BH^+])$$
$$100\ \mu M = 1.053\ [BH+]$$
$$95.0\ \mu M = [BH+]$$

The concentration response curve for the charged species, plotted against percentage inhibition, is not drastically altered, see Figure 7C. However, increased protonation of norfluoxetine at acidic pH_o decreases the proportion of uncharged drug which is available to equilibrate across the membrane, and when the pH on either side of the membrane differs "ion-trapping" of charged drugs can result in significant concentration gradients across the membrane. By calculating the concentration of uncharged norfluoxetine at the varying pH_o, in order to determine the available concentration for equilibration across the membrane (plotted in Figure 7D), one can then use the reported oocyte intracellular pH of 7.3 to calculate the total concentration of uncharged and charged drug inside the cell (Webb & Nuccitelli 1981; Kang et al. 1998). This reveals that extracellular alkalinisation results in a marked accumulation of norfluoxetine inside the cell; a bulk 100 μM concentration in the bath results in 125.8 μM inside the cell at pH 7.4, but 15.9 μM at pH 6.5 and 1509.2 at pH 8.5.

The intracellular concentration of drug may be critical as we predict the drug could access its binding site both from the cytoplasmic face of the channel and through

the membrane. When percentage inhibition is plotted against the calculated total concentration within the cell, as in Figure 7E, it is clear that norfluoxetine sensitivity is not decreased with extracellular pH activation, but rather increased (IC_{50} at pH_o 7.4 35.2 ± 5.7 μM, Hill coefficient 1.2 ± 0.1; IC_{50} at 6.5 3.3 ± 0.8 μM, Hill coefficient 1.2 ± 0.2; IC_{50} at 8.5 268.9 ± 45.1 μM, Hill coefficient 1.2 ± 0.02).

These experiments were intended to test whether pH_o-activation results in decreased norfluoxetine sensitivity and the results demonstrate this is not the case. On the contrary it appears that pH_o-activation may in fact increase norfluoxetine sensitivity. Considering the complications of ion-trap accumulation it will be important to reproduce these experiments in inside-out patches using pipette solutions of varying pH. This will allow for modulation of pH_o regulation without significantly changing the concentration of drug available for binding. Further, the effect of pH_o on norfluoxetine inhibition of TREK-1 needs to also be tested.

Meanwhile, to further test whether pH_o-gating effected norfluoxetine inhibition the drug was tested on the H156A, A179P and E103Q TREK-2 mutants, which as previously stated, appear to decouple pH_o-gating.

6.2 Mutations in the extracellular pH-sensing domain do not markedly shift norfluoxetine potency

As previously described these mutations significantly impair pH_o regulation; the H156A mutation causes a decrease in basal whole cell currents whilst A179P and E103Q cause an increase (as assayed by TEVC).

We speculated that these differences in basal whole cell currents are due to decoupling of the proton sensor from the channel gate, with the H156A mutation locking the channel in a pH_o-deactivated state whilst the A179P and E103Q mutation may lock the channel in a pH_o-activated state, to differing extents (mean

whole cell current at +100mV for WT 6.0 ± 0.5 µA, n = 30; H156A 4.8 ± 0.4 µA, n = 23, p = 0.055; A179P 7.6 ± 0.3 µA, n = 24, p < 0.01; E103Q 11.5 ± 1.4 µA, n = 24, p < 0.01 unpaired t-Test). In TEVC experiments the IC_{50} for norfluoxetine at pH 7.4 for inhibition of H156A was 18.6 ± 1.4 µM (Hill coefficient 1.1 ± 0.1, n = 11) whilst for A179P and E103Q IC_{50} was 28.1 ± 2.1 µM (Hill coefficient 1.0 ± 0.1, n = 7 and 19.2 ± 2.1 µM (Hill coefficient 0.9 ± 0.1, n = 8), respectively, see Figure 8. These values again represent minor deviations from the value obtained for wild type TREK-2 and there is no clear effect on norfluoxetine potency which correlates to channel activation.

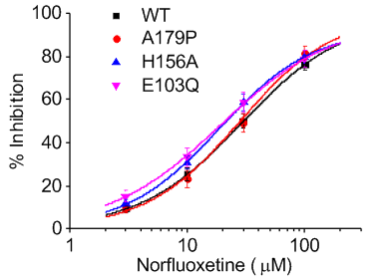

Figure 8: Norfluoxetine inhibition of whole cell TREK-2 currents at pH_o-disrupting mutants. *Summary dose response for norfluoxetine inhibition at varying TREK-2 WT, H156A and E103Q (percentage inhibition for current at 0mV; IC50 at TREK-2 H156A 18.6 ± 1.4µM, Hill coefficient 1.1 ± 0.1, n = 11; IC50 at A179P 28.1 ± 2.1µM, Hill coefficient 1.0 ± 0.1, n = 7; IC50 at E103Q 19.2 ± 3.0µM, Hill coefficient 0.9 ± 0.1, n = 8).*

6.3 Adding extracellular pH modulation to the emerging gating scheme

The magnitude of the effect of extracellular pH on macroscopic currents is clearly smaller than that observed for either stretch or temperature activation. It follows therefore that if pH_o regulation indeed does induce a change in conformation which decreases norfluoxetine potency, this effect would be smaller than that observed for stretch and temperature and so results pertaining to extracellular pH changes should be interpreted with caution, but this data suggests that the structural

mechanism for pH_o gating is fundamentally distinct from the mechanisms of stretch and temperature gating. Perhaps in this regard extracellular pH gating is similar to voltage-dependent gating in TREK channels in that both these mechanisms are believed to exert their effects directly on the SF-gate and occur without the need for global conformational changes, see Figure 9.

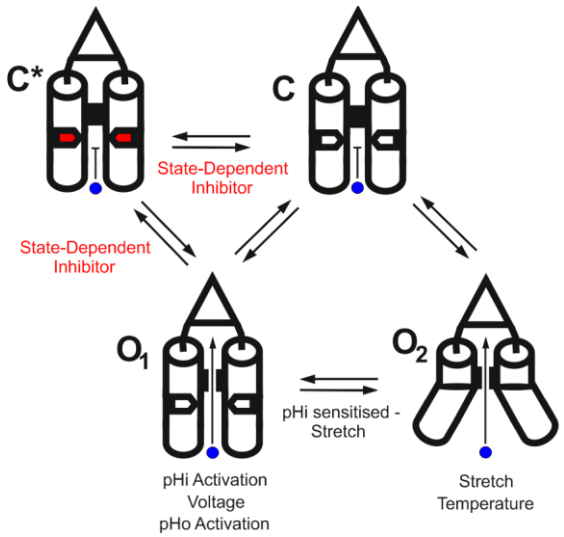

Figure 9: Expanded gating scheme. *Scheme expanded to* **i***nclude pHo activation of TREK-2, which involves activation of the selectivity filter gate independent of conformational changes to the fenestration binding site.*

7. Results: Temperature- and pH_o-gating are structurally distinct but interactive regulatory mechanisms

The use of the state-dependent inhibitor norfluoxetine therefore allows for the dissection of distinct structural mechanisms of TREK-2 regulation. However, it is as yet unclear whether these distinct gating mechanisms are entirely distinct and independent, or interactive. To probe this question I sought to ascertain the effect of temperature activation on pH_o regulation.

7.1 Distinct gating mechanisms are interactive

If the mechanisms by which pH_o and temperature exert their effects on channel gating were completely independent then no effect on pH_o regulation would be expected at varying temperatures. In TEVC experiments the response to varying extracellular pH was tested at 22, 32, 37 and 42°C. As can be seen from Figure 10, at elevated bath temperatures pH_o regulation was significantly diminished. Whilst at room temperature currents at pH 6.5 were 1.41 ± 0.03 times that at pH 7.4 (n = 12), for channels activated by temperature elevation to 37°C pH 6.5 activation was blunted to 1.18 ± 0.03 fold (n = 10, $p < 0.01$), see Figure 10. This could be explained by a 'bumping into the ceiling effect', where temperature activation has raised open probability to a point that cannot be further increased by pH_o, however inhibition by alkalinisation is also significantly decreased: At 22°C currents at 8.2 were 0.60 ± 0.04 times that at pH 7.4 (n = 12) whilst at 37°C currents at pH 8.2 were 0.77 ± 0.03 times that at pH 7.4 (n = 7, $p < 0.01$). Further increasing temperature to 42°C further reduced pH regulation, with currents at pH 8.2 0.80 ± 0.03 times that at pH 7.4 (n = 5, $p < 0.01$), see Figure 10.

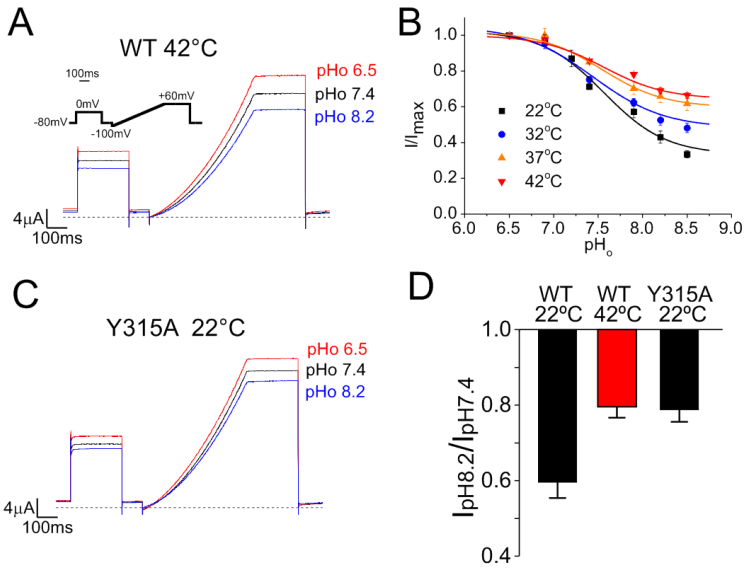

Figure 10: Temperature activation and the Y315A mutation blunt pHo regulation in TEVC experiments. *A) Example traces showing the effect of varying pH (red trace - pH 6.5, black trace - pH 7.4, blue trace - pH 8.2) on TREK-2 WT currents at 42°C (voltage protocol in inset). B) Summary pH response curves for TREK-2 WT currents at 22 (black squares), 32 (blue circles), 37 (orange upward triangles) and 42°C (red downward triangles). Currents were recorded from a 0mV step at each pH tested and normalised to the maximal currents recorded at pH 6.5. C) Example traces showing the effect of varying pH (red trace - pH 6.5, black trace - pH 7.4, blue trace - pH 8.2) on Y315A currents at 22°C. D) Whole cell current upon switching to pH 8.2 (normalised to currents at pH 7.4) for TREK-2 WT at 22 and 42°C, and for Y315A at 22°C. Currents recorded from a 0mV step.*

This suggests that whilst temperature gating and pH_o gating are structurally distinct these mechanisms are interactive. This presents the hypothesis that the up conformation (which we propose represents the temperature activated state) displays reduced sensitivity to pH_o gating compared to the down conformation (non-temperature activated) state. To further test this idea the pH_o sensitivity of the Y315A mutant was tested. As shown in Chapter 4 this mutation increases channel activity due to a destabilisation of the down state and increased occupancy of the up state (the latter property is determined by assessment of norfluoxetine sensitivity, see Chapter 7). As was observed for temperature activation, the Y315A mutation also significantly attenuates pH_o regulation (Figure 10), for the Y315A mutation currents at 8.2 were 0.78 ± 0.03 times currents at pH 7.4 ($n = 11$, $p < 0.01$).

8. Polymodal activation includes activation to distinct open conformations

In summary, these results indicate, firstly, that pH gating occurs via a structurally distinct mechanism to stretch and temperature gating. Importantly this finding (alongside the evidence for voltage-gating) requires the existence of multiple, structurally distinct open states, a novel concept for TREK channels but perhaps an unsurprising one considering their polymodal nature. Furthermore the effects of temperature activation (and the Y315A mutation) on pH_o regulation demonstrate that these discrete mechanisms interact. As has been suggested previously, it is likely that distinct regulatory mechanisms converge upon a common gate, likely to be the selectivity filter gate. One can conclude that the ability for extracellular proton sensing via H156 to induce changes in the conformation of the selectivity filter gate is decreased in channels in which the up conformation is promoted via temperature activation or mutation.

This idea of different regulatory stimuli employing distinct structural mechanisms for activating TREK-2 is particularly significant considering the recent proposal of a mechanism for TRAAK channel activation quite different from that we propose here for membrane stretch (Lolicato et al. 2014), this is discussed in more detail in the following chapter.

Chapter 7: Multiple distinct open states in TREK-2

1. Introduction

The results from Chapters 5 and 6 lead to a working model of TREK-2 channel gating which includes more than one distinct open state, with differences in access to the norfluoxetine binding site distinguishing the underlying conformations. The existence of an open, conductive channel with the fenestration binding site present (O_1), which is predicted by the aforementioned gating model, has not been shown crystallographically for TREK-2. However a recent development in the form of novel TRAAK structures from the Minor Jr. lab may foreshadow this (Lolicato et al. 2014).

2. Results: Different mutations exert different effects on norfluoxetine sensitivity

During the course of my investigations novel crystals structures of gain-of-function TRAAK mutants were published which showed 4 potassium ions in the selectivity filter with the fenestrations open, see Figure 1 (Lolicato et al. 2014). If, as discussed earlier, the selectivity filter is the primary gate for TREK/TRAAK channels and 4-ion occupancy is an indicator of conductivity then these TRAAK structures should be open. In turn, if they are open then this implies that the selectivity filter is able to gate independently of the large conformational changes proposed for stretch and crystallised for TREK-2, confirming the inferences made in Chapter 6.

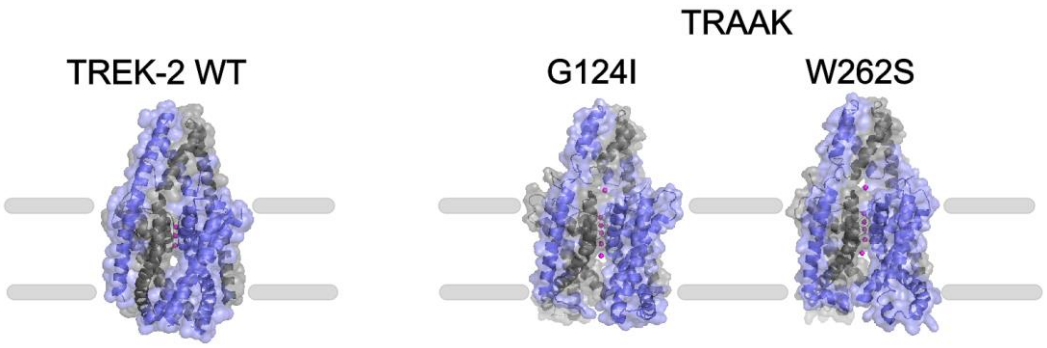

Figure 1: TREK-2 and TRAAK down conformations. *The TREK-2 down structure (left), with 3 ions in the selectivity filter is compared to the G124I (middle) and W262S (right) TRAAK structures published by Lolicato et al which both show four ions in the selectivity filter and open intramembrane fenestrations.*

The G124I and W262S GoF mutations crystallised for TRAAK were previously identified in TREK-1 and were predicted to act by stabilising the open filter gate (Bagriantsev et al. 2011; Bagriantsev, et al. 2012; Lolicato et al. 2014). As seen for both TREK-1 and TRAAK, the analogous mutations in TREK-2 (G167I and W306S) provoke large increases in channel currents, as determined by whole cell TEVC recordings of oocytes, see Figure 2. Furthermore these mutations displayed pronouncedly blunted stretch activation, indicating that the mutations act by decoupling the gate from the mechano-sensitive elements of the channel, see Figure 2. Notably the extent of both whole cell current increases, and the decrease in stretch activation was comparable with another profound GoF mutation, Y315A (Figure 2). This suggests that G167I, W306S and Y315A mutations all activate TREK-2 to similar extents.

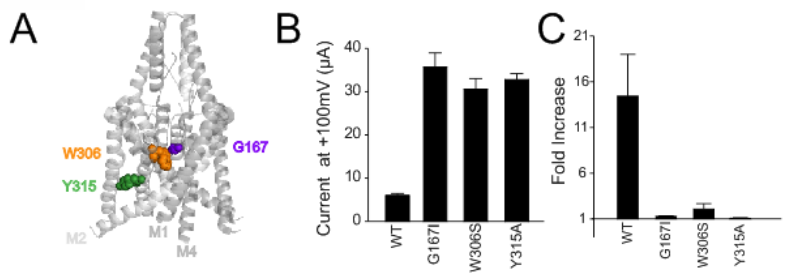

Figure 2: The G167I, W306S and Y315A mutations increase channel activity in TREK-2. *A) The positions of G167I, W306S and Y315A in TREK-2. B) Whole cell currents were recorded in TEVC experiments from cells expressing wild type TREK-2, G167I, W306S and Y315A. The mean peak currents recorded from a voltage step to 100mV were as follows, WT 6.0 ± 0.5µA (n = 30), G167I 35.7 ± 3.3µA (n = 23), W306S 30.5 ± 2.5µA (23) and Y315A 32.8 ± 1.4µA (n = 28). C) Stretch activation in inside-out patches expressing wild type, G167I, W306S and Y315A channels. Mean fold activation induced by administration of -11mmHg of pressure were as follows, WT 14.4 ± 4.6 (n = 8), G167I 1.3 ± 0.1 (n = 6), W306S 2.1 ± 0.6 (n = 5) and Y315A 1.1 ± 0.1 (n = 5).*

2.1 The G167I and W306S mutations do not shift norfluoxetine potency

Interestingly however, the GoF mutations had clearly different effects on norfluoxetine potency: whilst Y315A appears to drastically shift norfluoxetine potency compared to WT (IC_{50} for WT 4.9 ± 0.5 µM; Y315A >30 µM, n = 8) potency for W306S and G167I were not drastically decreased (IC50 at G167I 7.0 ± 0.6 µM, Hill coefficient 1.1 ± 0.1, n = 10; W306S 5.0 ± 0.4 µM, Hill coefficient 1.1 ± 0.1, n = 10), see Figure 3.

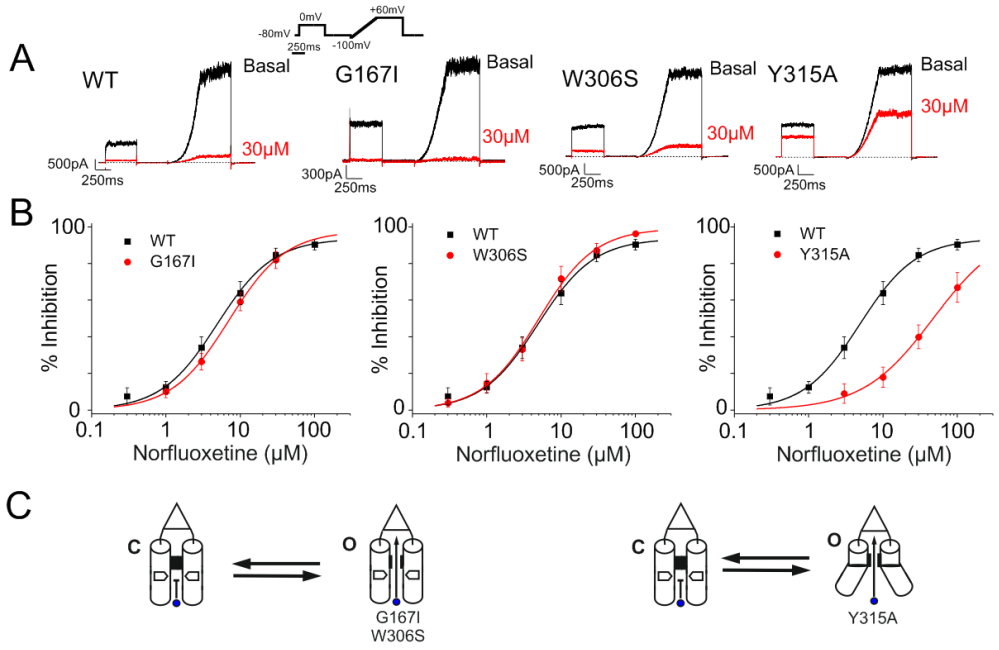

Figure 3: The G167I and W306S mutations show different effects on norfluoxetine potency to the Y315A mutation. *A) Example traces of recordings from inside-out patch clamp recordings showing the effect of 30μM norfluoxetine (red traces) on basal currents (black traces) for wild type TREK-2 (left), G167I (middle left), W306S (middle right) and Y315A (right) (voltage protocol as shown in inset). B) Summary dose response curves for norfluoxetine inhibition of wild type TREK-2 (IC_{50} 4.9 ± 0.5 μM, Hill coefficient 1.2 ± 0.1, n = 15) compared to G167I (left; IC_{50} 7.0 ± 0.6 μM, Hill coefficient 1.1 ± 0.1, n = 10), W306S (middle; IC_{50} 5.0 ± 0.4 μM, Hill coefficient 1.1 ± 0.1, n = 10) and Y315A (right; IC50 >30 μM, n = 8), mean inhibition recorded at current steps to 0mV. C) Schematic representation of the effect of G167I and W306S mutations which open TREK-2 (O) without obscuring the fenestration binding site (left) compared to the effect of the Y315A mutation which opens TREK-2 (O) whilst obscuring the fenestration binding site (right).*

Again, if only one open state for TREK-2 exists, and norfluoxetine cannot access its binding site in the open conformation then any increase in channel activation should inescapably decrease norfluoxetine potency. This occurs as expected for Y315A, where one can conclude that the mutation activates the channel by shifting the equilibrium between the closed, norfluoxetine sensitive state and the open, norfluoxetine-insensitive state. However clearly G167I and W306S increase channel activity via a different mechanism, which does not significantly affect inhibitor binding.

A potential alternative explanation for the effects on potency of the Y315A and G167I/W306S mutations would be that the Y315A mutation itself decreases binding affinity, by modifying the binding site. This appears unlikely however considering the crystallographic data which places the Y315 sidechain pointing away from the binding site, with phenylalanine 316 between the sites, see Figure 4.

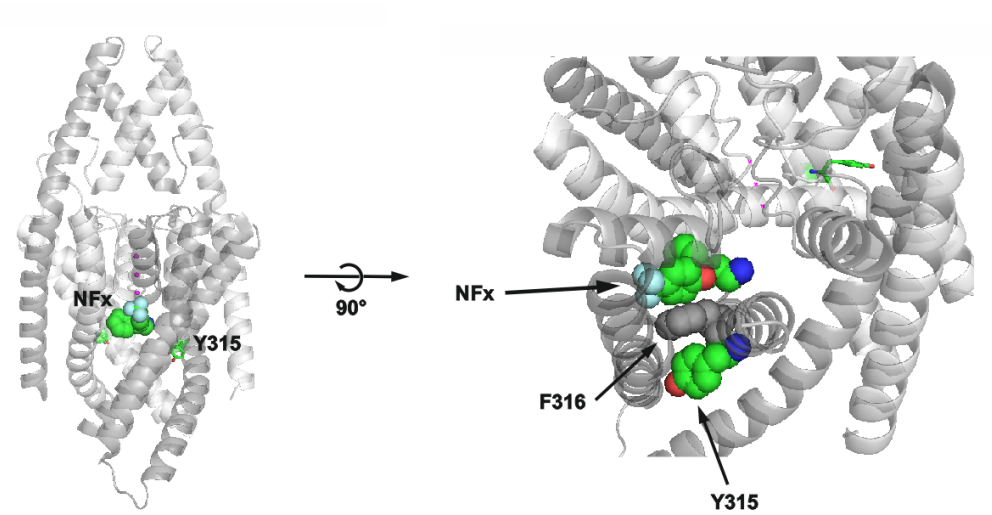

Figure 4: The relative positions of the norfluoxetine binding site and Y315A, which are separated by F316.

This evidence therefore indicates that mutating the TREK-2 channels can promote an open conformation distinct from the stretch activation observed in the wild type channel. However, at this point it remained to be established whether these discrete open conformations can occur within the same channel. To address this question I assessed the effect of stretch on norfluoxetine inhibition in the G167I mutant.

2.2 Distinct open conformations exist within the same channel

Repeated 10 μM norfluoxetine administrations were tested to demonstrate that inhibition was reproducible, see Figure 5A (1st admin provoked 67.7 ± 6.8% inhibition, 2nd admin provoked 68.7 ± 7.6% inhibition, n = 7), then inhibition was tested in G167I before and during the application of -11 mmHg of suction. Prior to the admin of pressure 10μM norfluoxetine evoked a 64.7 ± 8.1% inhibition of G167I currents (n = 11), this inhibition was fully reversible, see Figure 5. Subsequent administration of suction failed to provoke a marked increase in current (current after -11mmHg was 1.2 ± 0.1 times that pre-pressure admin, n = 11) suggesting that channels were already close to maximal activation, see Figure 5. However secondary co-administration of 10μM norfluoxetine in the continued presence of pressure administration now evoked significantly reduced inhibition, 13.9 ± 2.1% (n = 11), Figure 5B. This decrease in inhibition in the presence of membrane stretch is of course also observed for the wild type channel (see Figure 5C and D) however in this case stretch administration provokes a large increase in currents (see Figure 5C and 2C).

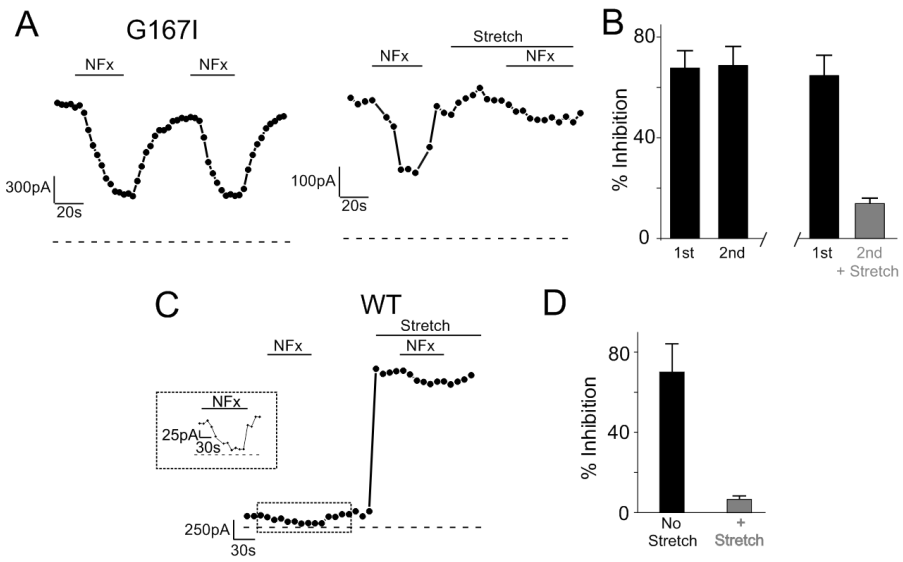

Figure 5: Two distinct activated conformations observed in the same G167I channel. *A) I/t plots of example experiments showing G167I currents recorded at voltage steps to 0mV every 5s. Left panel, repeated administration of 10 μM norfluoxetine produces reversible and reproducible inhibition. Right panel, I/t plot showing the effect of 10μM norfluoxetine in the absence and presence of stretch activation (-11 mmHg pressure). B) Mean percentage inhibition of G167I provoked by repeated 10 μM norfluoxetine first administration provoked 67.7 ± 6.8% inhibition, second admin provoked 68.7 ± 7.6% inhibition, n = 7. This is compared to the mean percentage inhibition provoked in experiments where norfluoxetine applied in the presence and absence of stretch activation (first administration in the absence of stretch provokes 64.7 ± 8.1% inhibition, second administration in the presence of stretch provokes 13.9 ± 2.1% inhibition (n = 11). C) Example I/t plot showing the effect of 10μM norfluoxetine in the presence and absence of stretch in wild type TREK-2, note the large increase in current evoked by application of stretch (-11mmHg). D) Mean percentage inhibition of wild type TREK-2 by 10 μM norfluoxetine in the absence (70.1 ± 14.0%) and presence (6.6 ± 1.8%) of stretch (n = 6).*

This shows in a single experiment that a TREK-2 channel is capable of adopting distinct open conformations, which differ in their sensitivity to norfluoxetine. In the absence of stretch the channel is gated open by the G167I mutation, but this is de-coupled from transmembrane helix movements and therefore the fenestration binding site is open. However once stretch is applied a conformational change is induced which has little effect on current amplitude as the channels are already open but decreases accessibility for the binding site.

3. Multiple open states in TREK-2 channels

Taken together, these results show that activation of the selectivity filter gate by mutations can occur in the absence of the global conformational changes postulated for stretch and temperature activation. In turn this provides some validation of the proposals from Chapter 6 where intracellular- and extracellular pH, and voltage activation were predicted to mediate their effects via a direct modulation of the filter gate, independent of significant transmembrane helix rearrangement.

We can include these findings in the emerging TREK-2 gating scheme to align the direct selectivity filter gate activation induced by G167I and W306S with the modulation via intracellular- and extracellular pH, and with voltage, see Figure 6. Meanwhile the Y315A mutation appears to activate channels in a similar mechanism to that observed for stretch and temperature.

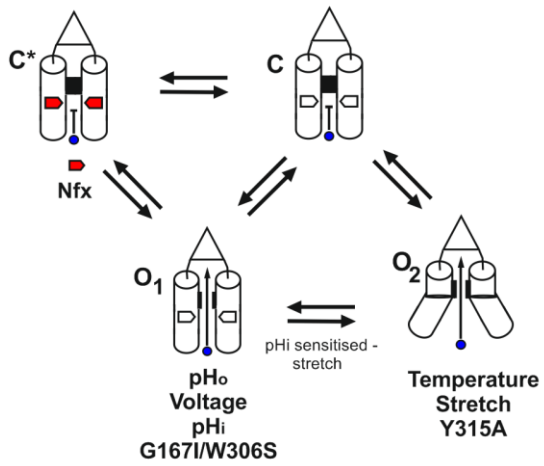

Figure 6: Gating scheme for polymodal regulation of TREK-2. *Channels exist in their closed conformation (C) with a non-conductive selectivity filter gate (blue potassium ion cannot permeate) and intramembrane fenestrations (white pentagonal boxes). Activation to one open state (O1) is provoked by extracellular acidification (pHo), voltage, intracellular acidification (pHi) and the G167I and W306S mutations. This open state retains the fenestration binding site. Norfluoxetine (NFx, red pentagon) can bind to either the closed state of the O1 open state thereby inhibiting the channel (C*). Conversely, closed channels can also be activated to a structurally distinct open state (O2) by temperature, stretch and the Y315A mutation. In this open state the fenestration binding site is abolished and thus norfluoxetine cannot bind.*

Chapter 8: Discussion

In the previous chapters I have reported a series of functional investigations into the gating mechanisms of TREK channels. These findings provide insights into the binding site and mechanism of action of state-dependent inhibitors, and the conformational changes involved in channel activation for a range of regulatory stimuli. Together these findings provide an emerging structural model of polymodal gating in TREK channels.

1. State-dependent inhibition of TREK-2

I have shown that norfluoxetine, carvedilol and fluphenazine (see Figure 1) all act to inhibit TREK-2 in a state-dependent manner, and that their potency is impaired when channels are activated by mechanical force, temperature and arachidonic acid.

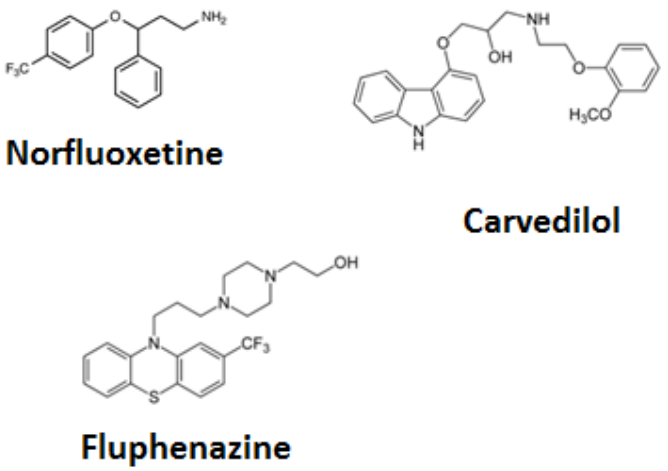

Figure 1: Chemical structures of the TREK channel inhibitors norfluoxetine, carvedilol and fluphenazine.

These drugs are amphiphilic molecules and likely partition at the lipid/water interface of the membrane. A number of potential mechanisms of perturbing channel function then present: the effect of the molecules could be due to direct lock-and-key interactions with the channel, by disruption of protein/lipid interactions at the interface (Lopes et al. 2005; Chemin et al. 2007; Ferrer et al. 2011), by changing membrane curvature (Sheetz & Singer 1974; Martinac et al. 1990; Patel et al. 1998; Patel et al. 2001; Honoré 2007), or perhaps due to non-specific perturbations of the membrane biophysics altering in the energetics of protein conformational changes (Yang & Sachs 1990; Ermakov et al. 2010; Suchyna et al. 2000; Suchyna et al. 2004; Bae et al. 2011; Lundbaek et al. 2010).

Direct modulation of TREK channels by small molecules

To my knowledge little is known about the effects of norfluoxetine, carvedilol and fluphenazine on membrane dynamics. The norfluoxetine precursor fluoxetine (which differs from norfluoxetine only by a single additional methyl group) has been studied however, and high concentrations (2.5 - 10mM) have been reported to increase membrane fluidity in liposomes, due to drug partitioning in the membrane and postulated interactions with phosphate head groups (Momo et al. 2005). Notably, a number of other TREK channel modulators have also been reported to affect membrane properties including Triton, chloroform, curcumin, capsezapine, halothane and arachidonic acid (Lundbaek et al. 2010 for review).

Therefore, it may be hypothesised that these amphiphilic compounds exert effects on mechano-sensitive K2P channels by partitioning into the membrane and changing bilayer dynamics: is this true, or do these drugs directly interact with the channel?

The evidence presented in this thesis demonstrates a direct interaction of norfluoxetine, carvedilol and fluphenazine with TREK channels. Firstly, the crystal structures of TREK-2 bound by norfluoxetine and bromo-fluoxetine demonstrate that the drug occupies a binding site within the intramembrane fenestrations of the channel.

The crystallographic binding site is confirmed via mutagenesis of a fenestration lining leucine residue. As I show, the L320W mutation shifts the potency of norfluoxetine, carvedilol and fluphenazine without noticeably affecting normal channel activity. This finding would be unexpected if the drugs were exerting their effects indirectly via perturbation of membrane dynamics. To date L320W represents the only binding site mutation which has been found to shifts norfluoxetine potency without any apparent confounding effects on normal channel gating. It is my hope that the MD simulations may provide us with additional candidates for mutagenesis to allow for further functional confirmation of the site.

1.1 The fenestration binding site

This fenestration binding site is a convenient home for an amphiphilic molecule. The abutting lipids would accommodate hydrophobic moieties whilst the apposed aqueous inner pore would favour polar or charged regions of the drug. Interestingly, there have been other recent examples of ion channel modulators binding within fenestration-like sites, as discussed below.

Notably, the lateral fenestration binding site may also provide an explanation for inhibition of other K2P channels by such amphiphilic drugs (Staudacher et al. 2011; Eckert et al. 2011; Kiper et al. 2014; Streit et al. 2011; Chokshi et al. 2015; and Chapter 5).

Fenestration binding sites in ion channels

Crystal structures for two bacterial sodium channels have recently been solved which show lateral fenestrations in the membrane lining transmembrane regions (Payandeh et al. 2011; Bagnéris et al. 2014). Interestingly, Bagnéris and colleagues have shown binding of a number of sodium channel blockers in close proximity to the fenestrations. Comparison with structurally related mammalian channels suggest that the fenestrations may also represent the binding site of norfluoxetine and fluoxetine in voltage-gated sodium channels (Poulin et al. 2014).

Additionally, a "side-pocket" binding site within the voltage-gated $K_V1.5$ channel has been proposed for the selective inhibition of K_V1 channels by Psora-4 (Marzian et al. 2013). These side pockets do not represent a true fenestration into the lipid bilayer, as the central pore is shielded by the surrounding S1-S4 domains in the 6 TM K_V channels. However the location of the binding pocket between the pore forming helices, and underneath the selectivity filter is reminiscent of the TREK-2 binding site we propose (Marzian et al. 2013).

The mechanism of inhibition of fenestration-bound drugs

Recent single channel recordings of reconstituted TREK-2 in proteoliposomes indicate that norfluoxetine decreases open probability by increasing occupancy of a long closed state without affecting single channel conductance or the short closures observed in burst openings (Michael Clausen, unpublished). This is in agreement with previous findings that the drug binds to closed channels (Kennard et al. 2005). However, how the drug prevents conduction once bound remains to be definitively established.

A mechanism for sodium channel blockade by fenestration-binding drugs has been proposed which involves steric occlusion of the ion permeation pathway with the drugs protruding into the selectivity filter (Bagnéris et al. 2014). This is possibly a mechanism by which TREK channel inhibitors may exert their effects. Alternatively blockade may be conferred via the introduction of a positive charge (from the cationic drugs) resulting in large energies for permeation. Better knowledge of the orientation of the molecules within the binding site may help to elucidate this.

Other plausible mechanisms include norfluoxetine inducing collapse of the selectivity filter gate, which can be probed by future experiments of Ba^{2+} accessibility, or perhaps alteration in the hydration/dehydration energy for the permeant potassium ion.

Further knowledge of how these and other drugs inhibit the TREK is highly desirable. It appears that the fenestration binding site is a common property for all K2Ps, and consequently norfluoxetine and carvedilol appear relatively non-selective (both inhibit TREK and TASK channels for example) (Eckert et al. 2011; Staudacher et al. 2011). However in each channel the residues which surround the fenestration do vary. Now the binding site is known rational drug design may aid in the development of more selective and potent inhibitors. This has significant potential therapeutic impact and is an exciting possibility (Mathie & Veale 2007).

2. TREK channel mechano-sensitivity

Here I report the use of state-dependent TREK inhibitors not as drugs with clinical potential but as tools for probing channel function. The results discussed in this thesis provide novel insights into the structural basis for mechanical activation of the TREK-2 channel. This model for mechano-activation is based primarily on the

finding that the stretch activated state of TREK-2 displays markedly reduced sensitivity to norfluoxetine. By coupling this functional data with the recently resolved crystal structures for the channel in two distinct conformations we propose that activation involves a concerted helical movement involving the upwards translocation of M2, M3 and M4, see Figure 2. This movement results in the closure of the lateral fenestrations observed in the down conformation and the abolition of the norfluoxetine binding site.

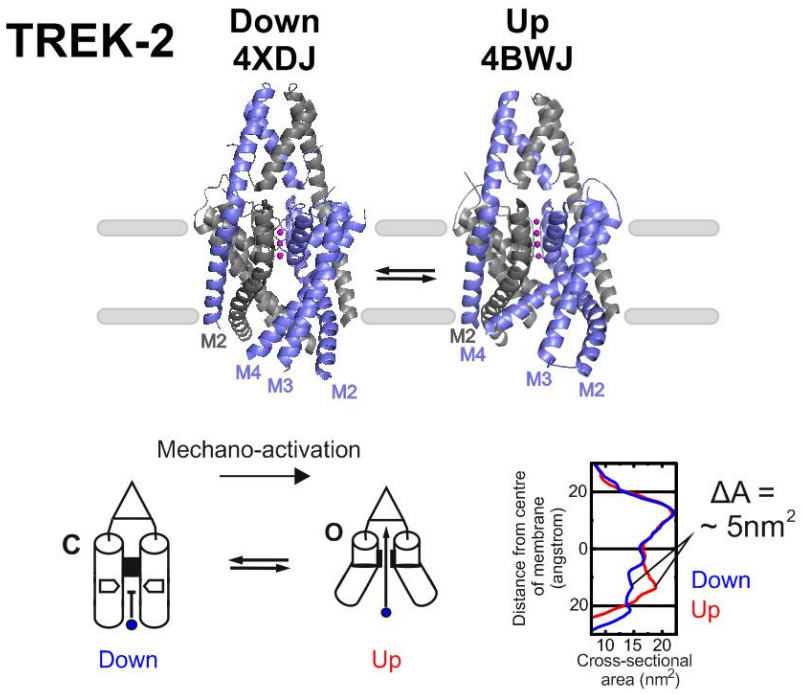

Figure 2: The proposed model for mechano-activation of TREK-2. *Mechano-activation provokes a conformational change from the down conformation to the up conformation (with the associated increase in cross-sectional area) which stabilises the open selectivity filter gate.*

2.1 Conformational changes in adaptation to stretched membranes

The down-to-up transition also results in an increase in the cross sectional area of TREK-2 of ~5nm^2, which provides a potential explanation for the mechano-sensitivity of the protein, see Figure 2. The application of pressure to a membrane

results in a decrease in membrane height which would expose hydrophobic residues of the transmembrane regions of TREK-2 to solvent. The significant energetic cost of this exposure would be expected to drastically destabilise the protein if no accommodating conformational change occurred. By changing conformation from down to up, and by increasing cross sectional area, the channel decreases its height within the membrane. This adaptation minimises hydrophobic mismatch and therefore represents a stable conformation within the thinned, stretched membrane.

Ongoing molecular dynamics simulations show that in an unstretched membrane the channel remains stable, resembling the crystallographic down conformation. However upon the application of stretch in atomistic simulations the channel rearranges via an upward movement of the transmembrane helices to resemble the crystallographic up conformation (Prafulla Aryal - unpublished). Similar results have also been observed for coarse-grain MD simulations of TREK-2 in bilayers of varying heights (Viwan Jarerattanachat - unpublished).

Pleasingly, the observed change in cross sectional area (ΔA) between the simulated conformation in the presence and absence of stretch is in clear agreement with the predicted value from kinetic analysis. Maksaev and colleagues estimated in plane increases in cross sectional area of ~4nm^2 for stretch activation of TREK-1 based upon the slope of open probability *versus* tension curves. In molecular dynamics simulations ΔA between the stable stretched and unstretched conformations is ~5nm^2 (Prafulla Aryal - unpublished). This value is also comparable to another estimate, again derived from functional data for ΔA of 1.8nm^2 for TREK-1 (Honoré et al. 2006). In their description of TRAAK channel gating Brohawn and colleagues report a ΔA of 2.7nm^2 which again is in general agreement to that which we report for TREK-2.

This change in cross sectional area between the open and closed conformations is considerably smaller than that predicted for the bacterial mechano-sensitive MscS and MscL channels, and this likely provides the explanation for the relatively increased tension sensitivity for TREK channels (Chiang et al. 2004).

2.2 Similarities in the TREK-2 and TRAAK mechano-gating models

Despite differences in the identity of the proposed gating element for the TREK-2 and TRAAK stretch activation models, where Brohawn and colleagues suggest an occlusive lipid gates the channel, there are marked similarities in the global protein conformational change. As discussed, it is asserted that activation of both channels involves an upward movement of M4, closure of the fenestrations and increases in conformational area.

In support of this notion in TRAAK Brohawn and colleagues performed cross-linking experiments to demonstrate that the channel can be locked into an open state via the formation of disulphide bridges which were predicted to promote the up conformation (Brohawn et al. 2014). Unfortunately despite significant effort, including using mutations analogous to those used in TRAAK, I was unable to conclusively show disulphide bridge locking of the TREK-2 channel. Regardless, the underlying conclusions from the TRAAK studies are in agreement with the conclusions of my norfluoxetine state-dependence studies, namely that the up conformation represents a stretch-activated channel.

2.3 Stretch gating is not conserved throughout the K2P family

Considering the force-from-lipid principle and the assertion that, to some extent, all membrane proteins are likely subject to significant varying forces upon the application of stretch to a membrane perhaps it is perhaps surprising that other K2P channels fail to show marked mechano-sensitivity (Bang et al. 2000; Kim, Gnatenco, et al. 2001; Kim, Bang, et al. 2001; Brohawn et al. 2014). Notably MD simulations show that, unlike TREK-2, TWIK-1 does not respond to membrane thinning with an increase in cross sectional area (Viwan Jarerattanachat - unpublished).

The transmembrane helices of TREK-2, TREK-1 and TRAAK contain a number of glycine residues within transmembrane helices which are not conserved amongst the wider family of channels. The flexibility conferred by these glycine residues may be crucial in allowing the channel to adapt to the stretch-altered membrane by increasing cross-sectional area through a conformational change which is coupled to channel gating.

Interestingly, studies of distantly related K2P channels in plants add complexity to this situation as AtK2P channels in plants appear to be mechanosensitive yet these channels do not contain the conserved hinge-glycine in TM4 (Maathuis 2011; González et al. 2015).

The model of mechano-sensitivity we propose states that the tension-sensitive transition is the upward movement of the helices. Taken further this means that the final closed to open (C→O) transition at the selectivity filter gate is not necessarily tension-sensitive. If we assume all K2P channels gate in similar ways at the selectivity filter (which may be an oversimplification), then if the C→O transition is not tension-sensitive we would not expect mechano-sensitivity to be conserved.

Rather, conservation of mechano-sensitivity requires the facilitation of the helical movements, which in turn makes the C→O transition energetically favourable.

2.4 How does TREK-2 gate in mechano-activation?

If the occlusive lipid proposed by Brohawn and colleagues is not the primary gating element, what is?

The first structural clue for this comes from the difference in ion occupancy in the selectivity filter between the TREK-2 down and up states. As described in Chapter 1, gating at the selectivity filter has been proposed in numerous previous reports (Piechotta et al. 2011; Rapedius et al. 2012; Bagriantsev et al. 2011). Further, a conductive potassium channel selectivity filter is expected to crystallise with electron density for 4 ions within it, as observed in the TREK-2 up structure (4BW5). In contrast structural deviations resulting in the perturbation of the 4-ion binding site structure is expected to result in a non-conductive channel (Bernèche & Roux 2005; Köpfer et al. 2014). In turn, this was observed in the TREK-2 down structure, with the absence of density for a potassium ion in the S1 position.

Exactly how the filter changes conformation to accommodate 4 ions remains to be established, and should be the focus of future efforts in order to fully understand mechano-activation in the TREK channels.

Ultimately we propose that mechano-activation of TREK-2 involves the direct adaptation to changes in force vectors and membrane geometry in a stretched membrane. The channel increases in cross sectional area to minimise hydrophobic mismatch in the thinned bilayer, see Figure 3. This increase in conformational area is mediated by a concerted movement of the M2, M3 and M4 helices which is in turn facilitated by flexibility conferred through numerous glycine residues in these helices. The coupling of mechanically-induced conformational changes to channel

opening means TREK channels can act as functional mechano-sensors. This property likely underlies the fine tuning and regulation of touch sensation in primary afferent neurones.

3. The conformational changes involved in temperature activation of TREK-2

In Chapter 5 I demonstrate that temperature activation decreases the potency of norfluoxetine inhibition of TREK-2. This result is similar to that observed for mechano-activation and is also seen for different state-dependent inhibitors carvedilol and fluphenazine. The logical interpretation of this finding is that accessibility or binding energy for these inhibitors is reduced in temperature-activated channels. This would be consistent with the channel converting in activation from a down-like conformation, in which the fenestration binding site is present, to an up-like conformation, where the upward movement of M4 has closed the fenestration, see Figure 3.

In this model, as with mechano-activation, this upward movement would ultimately have to couple to opening the selectivity filter gate, which is consistent with previous reports of temperature activation being blunted by elevated extracellular K^+ (Bagriantsev et al. 2012). How the open filter gate may be stabilised in temperature activation remains to be established.

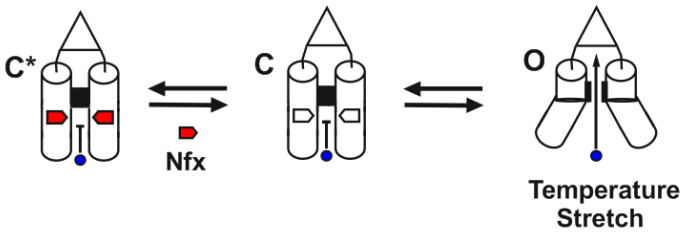

Figure 3: Temperature- and mechano-activation of TREK-2. *Both stimuli activate TREK-2 via conformational changes which abolish the norfluoxetine binding site (empty pentagon in closed channel, C). Norfluoxetine (red pentagon) can only bind within the fenestration binding site in the closed channel.*

4. pH regulation of TREK

pH_o regulation

My results which show that pH_o regulation in TREK-2 does not impact upon norfluoxetine potency and must therefore not include the large conformational changes observed in mechano-activation (see Chapter 6). Together, these results indicate that the TREK-2 channel is able to gate in multiple structurally different mechanisms.

In addition I show that pH_o regulation is blunted at elevated temperatures (see Chapter 6). Considering that temperature-activation shifts norfluoxetine potency this result indicates that these two regulatory stimuli act by distinct but interactive mechanisms. Previously positive allosteric coupling between distinct gates in *KCNK0* has been proposed (Ben-Abu et al. 2009). In TREK channels the existence of multiple gates appears unlikely (Piechotta et al. 2011; Rapedius et al. 2012), but consistent with the results from Ben-Abu and colleagues is my demonstration that an activated channel becomes less sensitive to inhibition by external gating modalities.

pH_i regulation

Such allosteric interactions between regulatory stimuli have been hinted at before in the demonstration that intracellular pH regulation sensitises mechano-activation in TREK-1, TREK-2 and TRAAK (Maingret et al. 1999; Kim 2001; Kim, et al. 2001). I show that pH_i activation, unlike mechano- or temperature activation fails to significantly shift norfluoxetine potency. This, again, suggests the existence of multiple transduction pathways for activation of TREK-2.

How pH_i-activation of TREK-2 occurs at a structural level remains to be established, but these experiments further illustrate that polymodal behaviour in TREK-2 is the result of multiple distinct and interactive structural mechanisms, see Figure 5.

5. Polymodal gating in TREK-2

As described previously (see Chapters 1 and 7) a number of recent structural mechanisms have been proposed for activation of TREK channels (Brohawn et al. 2014; Lolicato et al. 2014; Dong et al. 2015). Based on the results detailed here we propose a model where the polymodal behaviour of TREK channels may be the result of distinct conformational changes in response to different stimuli.

5.1 TREK-2 gating model

The existence of distinct open conformations

Numerous examples of ion channels demonstrating multiple open states have been reported (Nagy 1987; McManus & Magleby 1988; Hui et al. 2003), but interestingly,

only one open state has been suggested for TREK channels based on single channel analysis (Kang et al. 2005). Here, however, the authors also state that whilst temperature activation induced a significant decrease in open dwell time in 85% of patches, a further 15% exhibited different behaviour (Kang et al. 2005). Perhaps this provides a glimpse of polymodal gating behaviour at the single channel level.
The notion that the channel can gate in distinct conformations is supported by studies of the gain of function G167I and W306S mutations in TREK-2 which profoundly activate TREK-2 yet do not shift norfluoxetine potency.

Selectivity filter gating

Clearly the selectivity filter appears to be a key element in TREK channel gating, yet little is known about the structural changes here. Thus far crystallographic resolution has not been sufficient to observe any clear changes in protein conformation of the filter, yet in the TREK-2 down structure an absence of density at the S1 potassium ion binding site was observed (Dong et al. 2015). Apart from the aforementioned lipid-like density in the pore this is perhaps the best correlate for impaired conduction we can derive from the TREK-2 crystal structures, but how the S1 binding site is disrupted is as yet unclear.

TREK channels as integrated modular sensors

That the selectivity filter can gate independently of the helical movements involved in mechano-activation implies a structural decoupling from regulatory domains within the protein, in turn suggesting that TREK channels assemble from interactive yet distinct modules, in agreement with previous reports (Bagriantsev et al. 2011; Bagriantsev et al. 2012; Sandoz et al. 2009; Kim, Gnatenco, et al. 2001).

If a protein is regulated by numerous stimuli acting at distinct sensors, the interaction of each sensor with the pore, and with each other, will determine the overall activity of the channel, which can be described in terms of allosteric coupling.

Allosteric coupling and multiple open states in TREK channels

Allosteric coupling was originally defined for ligand binding to oligomeric proteins, but is now generalised to refer to local events which induce conformational changes in a distinct modules of a protein, including ion channels (Monod et al. 1965; Craig et al. 2008; Jara-Oseguera & Islas 2013).

For multimodal ion channels the overall free energy change in gating is driven by the multiple individual free energies for the component modular parts, including the equilibrium constants for sensor activation, coupling constants between the sensor and the gate, and coupling constants between the distinct regulatory pathways (Chowdhury & Chanda 2013; Yifrach 2013; Qin 2010).

This theory therefore includes descriptions of how different regulatory pathways can interact, which could help to provide an explanation for synergistic interaction between different stimuli seen in the TREK channels (Maingret et al. 1999; Kim 2001; Kim, Gnatenco, et al. 2001). However so far this model for allosteric coupling has only been postulated for pathways driving channels towards a common open state, a situation which does not appear to be the case in our model for TREK-2, where pH_i- and mechano-activation apparently act to induce conformationally different open states.

So how else may pH_i sensitise mechano-activation? Perhaps the effect is the manifestation of a decreased energy barrier in transition from the pH_i-activated state to the mechano-activated state compared to transitions from a closed state to

the mechano-activated state. In this situation increasing the occupancy of the pH_i-activated state would increase the relative probability of channels transitioning to the mechano-activated state at any pressure step. Alternatively pH_i could alter the coupling constant for mechano-activation and thereby accentuate the positive effects of mechano-sensor activation on open probability. Further work is required to establish the precise mechanisms of interaction in the complex gating of these polymodal channels.

Towards a structural gating scheme for TREK-2

Ultimately these results lead to the gating scheme represented in Figure 5.

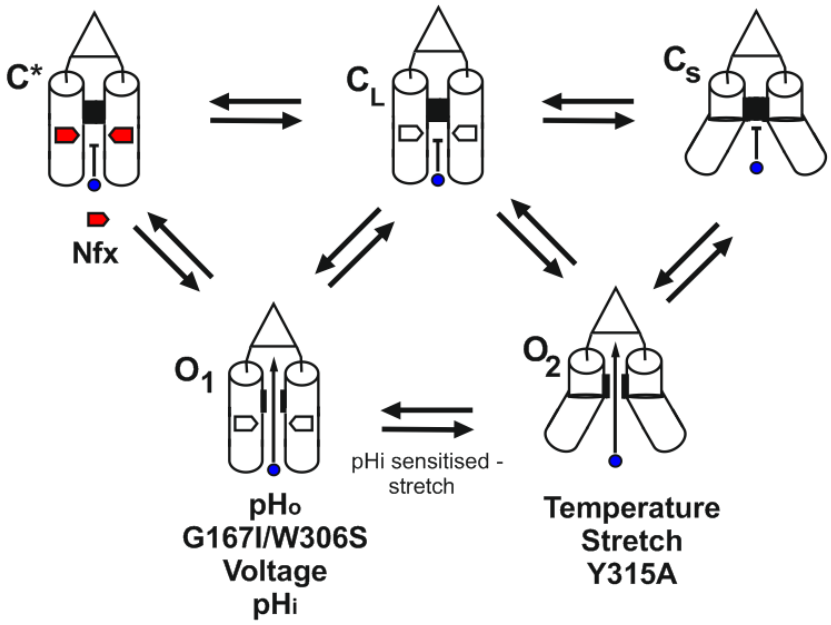

Figure 5: Proposed gating scheme for polymodal regulation of TREK-2. *C_L represents the long closed state, C* the norfluoxetine bound closed state, C_S is a predicted conformation for the brief closed state observed in single channel recordings, O_1 represents the pH- and voltage-activated state and O_2 represents the mechano- and temperature-activated state.*

Here a closed channel with intramembrane fenestrations (empty pentagons) and a non-conductive selective filter is represented as C_L (for long closed), this channel

can be activated in a mechanism in which the lateral fenestrations remain open, by intracellular- or extracellular pH, by voltage or by certain gating mutations such as G167I and W306S (O_1). Alternatively the channel can be opened by temperature, stretch or particular gating mutations (such as Y315A) in a conformational change which involves significant helical translocation and a closure of the fenestrations (O_2). Energetically favourable conversion from the O_1 to O_2 state may underlie pH_i-sensitisation of mechano-gating.

In contrast the closed state can be stabilised by binding of norfluoxetine (red pentagon) within the fenestration as shown in the C* state. An additional speculative short closed state (C_S) may involve selectivity filter collapse from activated conformations, which may represent the structural correlate to the brief closures observed in single channel burst openings.

References

Acosta, C. et al., 2014. TREK2 expressed selectively in IB4-binding C-fiber nociceptors hyperpolarizes their membrane potentials and limits spontaneous pain. *The Journal of neuroscience : the official journal of the Society for Neuroscience*, 34(4), pp.1494–509. Available at: http://www.pubmedcentral.nih.gov/articlerender.fcgi?artid=3898302&tool=pmcentrez&rendertype=abstract.

Alloui, A. et al., 2006. TREK-1, a K+ channel involved in polymodal pain perception. *The EMBO journal*, 25(11), pp.2368–2376.

Anderson, P. a V & Greenberg, R.M., 2001. Phylogeny of ion channels: Clues to structure and function. *Comparative Biochemistry and Physiology - B Biochemistry and Molecular Biology*, 129(1), pp.17–28.

Anishkin, A. et al., 2014. Feeling the hidden mechanical forces in lipid bilayer is an original sense. *Proceedings of the National Academy of Sciences of the United States of America*, 111(22), pp.7898–905. Available at: http://www.ncbi.nlm.nih.gov/pubmed/24850861.

Aryal, P. et al., 2014. A hydrophobic barrier deep within the inner pore of the TWIK-1 K2P potassium channel. *Nature Communications*, 5(February), pp.1–9. Available at: http://www.nature.com/doifinder/10.1038/ncomms5377.

Ashcroft, F.M., 2000. *Ion Channels and Disease*, Elsevier. Available at: http://www.sciencedirect.com/science/article/pii/B9780120653102500023 [Accessed August 29, 2015].

Ashmole, I., Goodwin, P.A. & Stanfield, P.R., 2001. TASK-5, a novel member of the tandem pore K+ channel family. *Pflugers Archiv European Journal of Physiology*, 442(6), pp.828–833.

Bagnéris, C. et al., 2014. Prokaryotic NavMs channel as a structural and functional model for eukaryotic sodium channel antagonism. *Proceedings of the National Academy of Sciences of the United States of America*, 111(23), pp.8428–33. Available at: http://www.ncbi.nlm.nih.gov/pubmed/24850863.

Bagriantsev, S.N. et al., 2013. A high-throughput functional screen identifies small molecule regulators of temperature- and mechano-sensitive K2P channels. *ACS Chemical Biology*, 8(8), pp.1841–1851.

Bagriantsev, S.N. et al., 2011. Multiple modalities converge on a common gate to control K(2P) channel function. *The EMBO journal*, 30(17), pp.3594–3606.

Bagriantsev, S.N., Clark, K. a & Minor, D.L., 2012. Metabolic and thermal stimuli control K2P2.1 (TREK-1) through modular sensory and gating domains. *The EMBO Journal*, 31(15), pp.3297–3308. Available at: http://dx.doi.org/10.1038/emboj.2012.171.

Bagriantsev, S.N., Clark, K.A. & Minor, D.L., 2012. Metabolic and thermal stimuli control K2P2.1 (TREK-1) through modular sensory and gating domains. *The EMBO Journal*, 31(15), pp.3297–3308.

Baker, S. a et al., 2008. Methionine and its derivatives increase bladder excitability by inhibiting stretch-dependent K(+) channels. *British journal of pharmacology*, 153(6), pp.1259–1271.

Baker, S.A. et al., 2010. Role of TREK-1 Potassium Channel in Bladder Overactivity After Partial Bladder Outlet Obstruction in Mouse. *Journal of Urology*, 183(2), pp.793–800.

Bang, H., Kim, Y. & Kim, D., 2000. TREK-2, a new member of the mechanosensitive tandem-pore K+ channel family. *Journal of Biological Chemistry*, 275(23), pp.17412–17419.

Bautista, D.M. et al., 2008. Pungent agents from Szechuan peppers excite sensory neurons by inhibiting two-pore potassium channels. *Nature neuroscience*, 11(7), pp.772–779.

Bavro, V.N. et al., 2012. Structure of a KirBac potassium channel with an open bundle crossing indicates a mechanism of channel gating. *Nature Structural & Molecular Biology*, 19(2), pp.158–163.

Bearzatto, B. et al., 2000. Axonal transport of TREK and TRAAK potassium channels in rat sciatic nerves. *Neuroreport*, 11(5), pp.927–930.

Beltrán, L. et al., 2013. 2-aminoethoxydiphenyl borate activates the mechanically gated human KCNK channels KCNK 2 (TREK-1), KCNK 4 (TRAAK), and KCNK 10 (TREK-2). *Frontiers in Pharmacology*, 4 MAY.

Ben-Abu, Y. et al., 2009. Inverse coupling in leak and voltage-activated K+ channel gates underlies distinct roles in electrical signaling. *Nature structural & molecular biology*, 16(1), pp.71–79.

Bernèche, S. & Roux, B., 2005. A gate in the selectivity filter of potassium channels. *Structure (London, England : 1993)*, 13(4), pp.591–600. Available at: http://www.sciencedirect.com/science/article/pii/S0969212605000742 [Accessed June 16, 2015].

Berrier, C. et al., 1992. Gadolinium ion inhibits loss of metabolites induced by osmotic shock and large stretch-activated channels in bacteria. *European Journal of Biochemistry*, 206(2), pp.559–565.

Bittner, S. et al., 2013. Endothelial TWIK-related potassium channel-1 (TREK1) regulates immune-cell trafficking into the CNS. *Nature medicine*, 19(9), pp.1161–5. Available at: http://dx.doi.org/10.1038/nm.3303\npapers3://publication/doi/10.1038/nm.3303.

Blondeau, N. et al., 2007. Polyunsaturated fatty acids are cerebral vasodilators via the TREK-1 potassium channel. *Circulation Research*, 101(2), pp.176–184.

Bockenhauer, D., Zilberberg, N. & Goldstein, S. a, 2001. KCNK2: reversible conversion of a hippocampal potassium leak into a voltage-dependent channel. *Nature neuroscience*, 4(5), pp.486–491.

Boron, W.F., 2004. Regulation of intracellular pH. *Advances in physiology education*, 28(1-4), pp.160–79. Available at: http://advan.physiology.org/content/28/4/160 [Accessed June 5, 2015].

Braun, G. et al., 2015. Differential sensitivity of TREK-1, TREK-2 and TRAAK background potassium channels to the polycationic dye ruthenium red. *British Journal of Pharmacology*, p.n/a–n/a. Available at: http://doi.wiley.com/10.1111/bph.13019.

Brohawn, S.G., Campbell, E.B. & MacKinnon, R., 2013. Domain-swapped chain connectivity and gated membrane access in a Fab-mediated crystal of the human TRAAK K+ channel. *Proceedings of the National Academy of Sciences of the United States of America*, 110(6), pp.2129–34. Available at: http://www.pubmedcentral.nih.gov/articlerender.fcgi?artid=3568379&tool=pmcentrez&rendertype=abstract.

Brohawn, S.G., Campbell, E.B. & MacKinnon, R., 2014. Physical mechanism for gating and mechanosensitivity of the human TRAAK K+ channel. *Nature*, 516(7529), pp.126–130. Available at: http://dx.doi.org/10.1038/nature14013.

Brohawn, S.G., del Marmol, J. & MacKinnon, R., 2012. Crystal Structure of the Human K2P TRAAK, a Lipid- and Mechano-Sensitive K+ Ion Channel. *Science*, 335(6067), pp.436–441.

Brohawn, S.G., Su, Z. & MacKinnon, R., 2014. Mechanosensitivity is mediated directly by the lipid membrane in TRAAK and TREK1 K+ channels. *Proceedings of the National Academy of Sciences of the United States of America*, 111(9), pp.3614–9. Available at: http://www.pnas.org/content/111/9/3614.long.

Buckler, K.J. & Honoré, E., 2005. The lipid-activated two-pore domain K+ channel TREK-1 is resistant to hypoxia: implication for ischaemic neuroprotection. *The Journal of physiology*, 562(Pt 1), pp.213–222.

Buxton, I.L.O., Singer, C.A. & Tichenor, J.N., 2010. Expression of stretch-activated two-pore potassium channels in human myometrium in pregnancy and labor. *PLoS ONE*, 5(8).

Cadaveira-Mosquera, A. et al., 2011. Activation of TREK currents by the neuroprotective agent riluzole in mouse sympathetic neurons. *The Journal of neuroscience : the official journal of the Society for Neuroscience*, 31(4), pp.1375–1385.

Cadaveira-Mosquera, A. et al., 2012. Expression of K2P channels in sensory and motor neurons of the autonomic nervous system. *Journal of Molecular Neuroscience*, 48(1), pp.86–96.

Cantor, R.S., 1997. Lateral pressures in cell membranes: A mechanism for modulation of protein function. *Journal Of Physical Chemistry B*, 101(96), pp.1723–1725. Available at:

http://apps.isiknowledge.com/InboundService.do?Func=Frame&product=WOS&action=retrieve&SrcApp=Papers&UT=A1997WL76700002&SID=Q1lNCI49hDP4D1N9PEC&Init=Yes&SrcAuth=mekentosj&mode=FullRecord&customersID=mekentosj&DestFail=http://access.isiproducts.com/custom_i.

Chavez, R.A. et al., 1999. TWIK-2, a new weak inward rectifying member of the tandem pore domain potassium channel family. *Journal of Biological Chemistry*, 274(12), pp.7887–7892.

Chemin, J. et al., 2005. A phospholipid sensor controls mechanogating of the K+ channel TREK-1. *The EMBO journal*, 24(1), pp.44–53.

Chemin, J. et al., 2003. Mechanisms underlying excitatory effects of group I metabotropic glutamate receptors via inhibition of 2P domain K: +: channels : Figure 6 : The EMBO Journal. , 22(20), pp.5403–5411. Available at: http://www.nature.com/emboj/journal/v22/n20/fig_tab/7595438a_F6.html.

Chemin, J. et al., 2007. Up- and down-regulation of the mechano-gated K2P channel TREK-1 by PIP2 and other membrane phospholipids. *Pflugers Archiv European Journal of Physiology*, 455(1), pp.97–103.

Chen, H., Chatelain, F.C. & Lesage, F., 2014a. Altered and dynamic ion selectivity of K+ channels in cell development and excitability. *Trends in Pharmacological Sciences*, 35(9), pp.461–469. Available at: http://linkinghub.elsevier.com/retrieve/pii/S0165614714000947.

Chen, H., Chatelain, F.C. & Lesage, F., 2014b. Altered and dynamic ion selectivity of K+ channels in cell development and excitability. *Trends in Pharmacological Sciences*, 35(9), pp.461–469.

Chiang, C.-S., Anishkin, A. & Sukharev, S., 2004. Gating of the large mechanosensitive channel in situ: estimation of the spatial scale of the transition from channel population responses. *Biophysical journal*, 86(5), pp.2846–2861.

Chowdhury, S. & Chanda, B., 2013. Free-energy relationships in ion channels activated by voltage and ligand. *The Journal of general physiology*, 141(1), pp.11–28. Available at: http://www.pubmedcentral.nih.gov/articlerender.fcgi?artid=3536522&tool=pmcentrez&rendertype=abstract.

Chowdhury, S., Jarecki, B.W. & Chanda, B., 2014. A Molecular Framework for Temperature-Dependent Gating of Ion Channels. *Cell*, 158(5), pp.1148–1158. Available at: http://dx.doi.org/10.1016/j.cell.2014.07.026.

Clapham, D.E. & Miller, C., 2011. Inaugural Article: A thermodynamic framework for understanding temperature sensing by transient receptor potential (TRP) channels. *Proceedings of the National Academy of Sciences*, 108(49), pp.19492–19497.

Clarke, C.E. et al., 2008. The M1P1 loop of TASK3 K2P channels apposes the selectivity filter and influences channel function. *Journal of Biological Chemistry*, 283(25), pp.16985–16992.

Cohen, A. et al., 2008. A novel mechanism for human K2P2.1 channel gating: Facilitation of C-type gating by protonation of extracellular histidine residues. *Journal of Biological Chemistry*, 283(28), pp.19448–19455.

Comoglio, Y. et al., 2014. Phospholipase D2 specifically regulates TREK potassium channels via direct interaction and local production of phosphatidic acid. *Proceedings of the National Academy of Sciences*, 111(37), pp.13547–13552. Available at: http://www.pnas.org/lookup/doi/10.1073/pnas.1407160111.

Congiu, C. et al., 2015. The role of the potassium channel gene KCNK2 in major depressive disorder. *Psychiatry Research*, 225(3), pp.489–492. Available at: http://linkinghub.elsevier.com/retrieve/pii/S0165178114009548.

Cossins, a R. & Prosser, C.L., 1978. Evolutionary adaptation of membranes to temperature. *Proceedings of the National Academy of Sciences of the United States of America*, 75(4), pp.2040–2043.

Craig, T.J., Ashcroft, F.M. & Proks, P., 2008. How ATP inhibits the open K(ATP) channel. *The Journal of general physiology*, 132(1), pp.131–144.

Cuello, L.G. et al., 2010. Structural mechanism of C-type inactivation in K(+) channels. *Nature*, 466(7303), pp.203–208. Available at: http://dx.doi.org/10.1038/nature09153.

Cybulski, L.E. et al., 2015. Activation of the bacterial thermosensor DesK involves a serine zipper dimerization motif that is modulated by bilayer thickness. *Proceedings of the National Academy of Sciences*, 112(20), p.201422446. Available at: http://www.pnas.org/lookup/doi/10.1073/pnas.1422446112.

Czirják, G. & Enyedi, P., 2002. Formation of functional heterodimers between the TASK-1 and TASK-3 two-pore domain potassium channel subunits. *Journal of Biological Chemistry*, 277(7), pp.5426–5432.

Dallas, M.L., Scragg, J.L. & Peers, C., 2008. Modulation of hTREK-1 by carbon monoxide. *Neuroreport*, 19(3), pp.345–348.

Delmas, P., Coste, B. & Honoré, E., 2014. A special issue on physiological aspects of mechanosensing. *Pflügers Archiv - European Journal of Physiology*, 467(1), pp.1–2. Available at: http://link.springer.com/10.1007/s00424-014-1653-5.

Delmas, P., Hao, J. & Rodat-Despoix, L., 2011. Molecular mechanisms of mechanotransduction in mammalian sensory neurons. *Nature reviews. Neuroscience*, 12(3), pp.139–153. Available at: http://dx.doi.org/10.1038/nrn2993.

Deng, P.Y. et al., 2009. GABAB Receptor Activation Inhibits Neuronal Excitability and Spatial Learning in the Entorhinal Cortex by Activating TREK-2 K+ Channels. *Neuron*, 63(2), pp.230–243.

Descoeur, J. et al., 2011. Oxaliplatin-induced cold hypersensitivity is due to remodelling of ion channel expression in nociceptors. *EMBO Molecular Medicine*, 3(5), pp.266–278.

Devilliers, M. et al., 2013. Activation of TREK-1 by morphine results in analgesia without adverse side effects. *Nature communications*, 4, p.2941. Available at: http://www.ncbi.nlm.nih.gov/pubmed/24346231.

Dong, Y.Y. et al., 2015. K2P channel gating mechanisms revealed by structures of TREK-2 and a complex with Prozac. *Science*, 347(6227), pp.1256–1259. Available at: http://www.sciencemag.org/cgi/doi/10.1126/science.1261512.

Dong, Y.Y. et al., 2015. K2P channel gating mechanisms revealed by structures of TREK-2 and a complex with Prozac. , 347(6227).

Doyle, D. a et al., 1998. The structure of the potassium channel: molecular basis of K+ conduction and selectivity. *Science (New York, N.Y.)*, 280(5360), pp.69–77.

Dubey, S. et al., 2013. Phytochemistry , Pharmacology and Toxicology of Spilanthes acmella : A Review. , 2013.

Duprat, F. et al., 1997. TASK, a human background K+ channel to sense external pH variations near physiological pH. *EMBO Journal*, 16(17), pp.5464–5471.

Duprat, F. et al., 2000. The neuroprotective agent riluzole activates the two P domain K(+) channels TREK-1 and TRAAK. *Molecular pharmacology*, 57(5), pp.906–912.

Eckert, M. et al., 2011. TREK-1 isoforms generated by alternative translation initiation display different susceptibility to the antidepressant fluoxetine. *Neuropharmacology*, 61(5-6), pp.918–923. Available at: http://dx.doi.org/10.1016/j.neuropharm.2011.06.020.

Enyeart, J. a., Liu, H. & Enyeart, J.J., 2008. Curcumin inhibits bTREK-1 K+ channels and stimulates cortisol secretion from adrenocortical cells. *Biochemical and Biophysical Research Communications*, 370(4), pp.623–628.

Enyeart, J.A., Liu, H. & Enyeart, J.J., 2008. Curcumin inhibits bTREK-1 K+ channels and stimulates cortisol secretion from adrenocortical cells. *Biochemical and Biophysical Research Communications*, 370(4), pp.623–628.

Enyeart, J.J. et al., 2002. An ACTH- and ATP-regulated background K+ channel in adrenocortical cells is TREK-1. *Journal of Biological Chemistry*, 277(51), pp.49186–49199.

Ermakov, Y. a. et al., 2010. Gadolinium ions block mechanosensitive channels by altering the packing and lateral pressure of anionic lipids. *Biophysical Journal*, 98(6), pp.1018–1027. Available at: http://dx.doi.org/10.1016/j.bpj.2009.11.044.

Feng, Q., 2014. Temperature sensing by thermal TRP channels: thermodynamic basis and molecular insights. *Current topics in membranes*, 74, pp.19–50. Available at: http://www.sciencedirect.com/science/article/pii/B9780128001813000026 [Accessed May 25, 2015].

Ferrer, T. et al., 2011. Carvedilol inhibits Kir2.3 channels by interference with PIP 2-channel interaction. *European Journal of Pharmacology*, 668(1-2), pp.72–77. Available at: http://dx.doi.org/10.1016/j.ejphar.2011.05.067.

Fink, M. et al., 1998. A neuronal two P domain K+ channel activated by arachidonic acid and polyunsaturated fatty acid. *Embo J.*, 17(12), pp.3297–3308.

Fink, M. et al., 1998. A neuronal two P domain K+ channel stimulated by arachidonic acid and polyunsaturated fatty acids. *EMBO Journal*, 17(12), pp.3297–3308.

Fink, M. et al., 1996. Cloning, functional expression and brain localization of a novel unconventional outward rectifier K+ channel. *The EMBO journal*, 15(24), pp.6854–6862.

Gardener, M.J. et al., 2004. Functional evidence of a role for two-pore domain potassium channels in rat mesenteric and pulmonary arteries. *British journal of pharmacology*, 142(1), pp.192–202.

Garry, A. et al., 2007. Altered acetylcholine, bradykinin and cutaneous pressure-induced vasodilation in mice lacking the TREK1 potassium channel: the endothelial link. *EMBO reports*, 8(4), pp.354–359.

Girard, C. et al., 2001. Genomic and functional characteristics of novel human pancreatic 2P domain K(+) channels. *Biochemical and biophysical research communications*, 282(1), pp.249–256.

Gnatenco, C. et al., 2002. Functional expression of TREK-2 K+ channel in cultured rat brain astrocytes. *Brain Research*, 931(1), pp.56–67.

Goldin, A.L., 2006. Expression of Ion Channels in Xenopus Oocytes. *Expression and Analysis of Recombinant Ion Channels: From Structural Studies to Pharmacological Screening*, pp.1–25.

Goldstein, S. a et al., 1996. ORK1, a potassium-selective leak channel with two pore domains cloned from Drosophila melanogaster by expression in Saccharomyces cerevisiae. *Proceedings of the National Academy of Sciences of the United States of America*, 93(23), pp.13256–13261.

Gomora, J.C., Enyeart, J.A. & Enyeart, J.J., 1999. Mibefradil Potently Blocks ATP-Activated K ς Channels in Adrenal Cells. , 1197, pp.1192–1197.

Gomora, J.C. & Enyeart, J.J., 1999. Dual pharmacological properties of a cyclic AMP-sensitive potassium channel. *The Journal of pharmacology and experimental therapeutics*, 290(1), pp.266–275.

González, W. et al., 2015. K2P channels in plants and animals. *Pflügers Archiv - European Journal of Physiology*, 467(5), pp.1091–1104. Available at: http://link.springer.com/10.1007/s00424-014-1638-4.

Gruss, M. et al., 2004. Two-pore-domain K+ channels are a novel target for the anesthetic gases xenon, nitrous oxide, and cyclopropane. *Molecular pharmacology*, 65(2), pp.443–452.

Gullingsrud, J. & Schulten, K., 2004. Lipid bilayer pressure profiles and mechanosensitive channel gating. *Biophysical journal*, 86(6), pp.3496–3509.

Hamill, O.P. et al., 1981. Improved patch-clamp techniques for high-resolution current recording from cells and cell-free membrane patches. *Pflügers Archiv European Journal of Physiology*, 391(2), pp.85–100.

Harinath, S. & Sikdar, S.K., 2005. Inhibition of human TREK-1 channels by caffeine and theophylline. *Epilepsy Research*, 64(3), pp.127–135.

Heurteaux, C. et al., 2006. Deletion of the background potassium channel TREK-1 results in a depression-resistant phenotype. *Nature neuroscience*, 9(9), pp.1134–1141.

Heurteaux, C. et al., 2004. TREK-1, a K+ channel involved in neuroprotection and general anesthesia. *The EMBO journal*, 23(13), pp.2684–2695.

Hibino, H. et al., 2010. Inwardly Rectifying Potassium Channels : Their Structure, Function, and Physiological Roles. *Physiology Reviews*, 90, pp.291–366.

Hodgkin, A.L. & Huxley, A.F., 1952. A quantitative description of membrane current and its application to conduction and excitation in nerve. *J Physiol*, 117(4), pp.500–44.

Holmgren, M., Shin, K.S. & Yellen, G., 1998. The activation gate of a voltage-gated K+ channel can be trapped in the open state by an intersubunit metal bridge. *Neuron*, 21(3), pp.617–621.

Holzer, P., 2009a. Acid-sensitive ion channels and receptors. *Handbook of Experimental Pharmacology*, 194, pp.283–332. Available at: http://nashaucheba.ru/docs/9/8900/conv_1/file1.pdf#page=18.

Holzer, P., 2009b. Acid-sensitive ion channels and receptors. *Handbook of Experimental Pharmacology*, 194, pp.283–332.

Honoré, E. et al., 2002. An intracellular proton sensor commands lipid- and mechano-gating of the K+ channel TREK-1. *EMBO Journal*, 21(12), pp.2968–2976.

Honoré, E. et al., 2006. Desensitization of mechano-gated K 2P channels. , 103(18), pp.6859–64.

Honoré, E., 2007. The neuronal background K2P channels: focus on TREK1. *Nature reviews. Neuroscience*, 8(4), pp.251–261.

Hossain, H. et al., 2012. Evaluation of Antinociceptive and Antioxidant Potential from the Leaves of Spilanthes paniculata Growing in Bangladesh. *International Journal of Pharmaceutical and Phytopharmacological Research*, 1(178), pp.178–186.

Hu, J. et al., 2010. Evidence for a protein tether involved in somatic touch. *The EMBO journal*, 29(4), pp.855–867. Available at: http://dx.doi.org/10.1038/emboj.2009.398.

Hudspeth, a J., 2014. Integrating the active process of hair cells with cochlear function. *Nature reviews. Neuroscience*, 15(9), pp.600–614. Available at: http://www.ncbi.nlm.nih.gov/pubmed/25096182.

Hughes, S. et al., 2006. Expression of the mechanosensitive 2PK+ channel TREK-1 in human osteoblasts. *Journal of Cellular Physiology*, 206(3), pp.738–748.

Hui, K., Liu, B. & Qin, F., 2003. Capsaicin activation of the pain receptor, VR1: multiple open states from both partial and full binding. *Biophysical journal*, 84(5), pp.2957–2968.

Hund, T.J. et al., 2014. βiV-Spectrin regulates TREK-1 membrane targeting in the heart. *Cardiovascular Research*, 102(1), pp.166–175.

Imai, K., Tatsumi, H. & Katayama, Y., 2000. Mechanosensitive chloride channels on the growth cones of cultured rat dorsal root ganglion neurons. *Neuroscience*, 97(2), pp.347–355.

Islas, L.D., 2014. Thermal effects and sensitivity of biological membranes. *Current topics in membranes*, 74, pp.1–17. Available at: http://www.sciencedirect.com/science/article/pii/B9780128001813000014 [Accessed August 27, 2015].

Jara-Oseguera, A. & Islas, L.D., 2013. The role of allosteric coupling on thermal activation of thermo-TRP channels. *Biophysical Journal*, 104(10), pp.2160–2169.

Jiang, Y. et al., 2002. The open pore conformation of potassium channels. *Nature*, 417(6888), pp.523–526.

Kang, D., Kim, S.H., et al., 2007. Expression of thermosensitive two-pore domain K+ channels in human keratinocytes cell line HaCaT cells. *Experimental Dermatology*, 16(12), pp.1016–1022.

Kang, D., Han, J., et al., 2004. Functional expression of TASK-1/TASK-3 heteromers in cerebellar granule cells. *The Journal of physiology*, 554(Pt 1), pp.64–77.

Kang, D. et al., 2008. Lamotrigine inhibits TRESK regulated by G-protein coupled receptor agonists. *Biochemical and biophysical research communications*, 367(3), pp.609–15. Available at: http://www.sciencedirect.com/science/article/pii/S0006291X0800034X [Accessed June 16, 2015].

Kang, D., Choe, C., et al., 2007. Properties of single two-pore domain TREK-2 channels expressed in mammalian cells. *The Journal of physiology*, 583(Pt 1), pp.57–69.

Kang, D., Choe, C. & Kim, D., 2004. Functional expression of TREK-2 in insulin-secreting MIN6 cells. *Biochemical and Biophysical Research Communications*, 323(1), pp.323–331.

Kang, D., Choe, C. & Kim, D., 2005. Thermosensitivity of the two-pore domain K+ channels TREK-2 and TRAAK. *The Journal of physiology*, 564(Pt 1), pp.103–116.

Kang, D., Han, J. & Kim, D., 2006. Mechanism of inhibition of TREK-2 (K2P10.1) by the Gq-coupled M3 muscarinic receptor. *American journal of physiology. Cell physiology*, 291(4), pp.C649–C656.

Kang, D. & Kim, D., 2006. TREK-2 (K2P10.1) and TRESK (K2P18.1) are major background K+ channels in dorsal root ganglion neurons. *American journal of physiology. Cell physiology*, 291(1), pp.C138–C146.

Kang, M.G., Kulisz, A. & Wasserman, W.J., 1998. Raf-1 kinase, a potential regulator of intracellular pH in Xenopus oocytes. *Biology of the Cell*, 90(6-7), pp.477–485.

Kelly, D. et al., 2006. Proceedings of the Australian Physiological Society (AHMRC) Symposium : Stretch Activated Ion Channels GENE EXPRESSION OF STRETCH-ACTIVATED CHANNELS AND MECHANOELECTRIC FEEDBACK IN THE HEART. , (December 2005), pp.642–648.

Kennard, L.E. et al., 2005. Inhibition of the human two-pore domain potassium channel, TREK-1, by fluoxetine and its metabolite norfluoxetine. *British journal of pharmacology*, 144(6), pp.821–829.

Ketchum, K. a et al., 1995. A new family of outwardly rectifying potassium channel proteins with two pore domains in tandem. *Nature*, 376(6542), pp.690–695.

Kiehn, J. et al., 1996. Molecular physiology and pharmacology of HERG. Single-channel currents and block by dofetilide. *Circulation*, 94(10), pp.2572–2579.

Kim, D. & Clapham, D.E., 1989. Potassium channels in cardiac cells activated by arachidonic acid and phospholipids. *Science*, 244(4909), pp.1174–1176.

Kim, D. & Gnatenco, C., 2001. TASK-5, a new member of the tandem-pore K(+) channel family. *Biochemical and biophysical research communications*, 284(4), pp.923–930.

Kim, E. et al., 2010. Enhancement of TREK1 channel surface expression by protein-protein interaction with ??-COP. *Biochemical and Biophysical Research Communications*, 395(2), pp.244–250. Available at: http://dx.doi.org/10.1016/j.bbrc.2010.03.171.

Kim, E.J. et al., 2010. Chemoselective regulation of TREK2 channel: Activation by sulfonate chalcones and inhibition by sulfonamide chalcones. *Bioorganic and Medicinal Chemistry Letters*, 20(14), pp.4237–4239.

Kim, E.J., Kang, D. & Han, J., 2011. Baicalein and wogonin are activators of rat TREK-2 two-pore domain K+ channel. *Acta Physiologica*, 202(2), pp.185–192.

Kim, J.-S. et al., 2005. Zinc activates TREK-2 potassium channel activity. *The Journal of pharmacology and experimental therapeutics*, 314(2), pp.618–625.

Kim, Y., Gnatenco, C., et al., 2001. Localization of trek-2 k+channel domains that regulate channel kinetics and sensitivity to pressure, fatty acids and phi. *Pflugers Archiv European Journal of Physiology*, 442(6), pp.952–960.

Kim, Y., Bang, H., et al., 2001. Synergistic interaction and the role of C-terminus in the activation of TRAAK K+ channels by pressure, free fatty acids and alkali. *Pflugers Archiv European Journal of Physiology*, 442(1), pp.64–72.

Kim, Y., Bang, H. & Kim, D., 2000. TASK-3, a new member of the tandem pore K+ channel family. *Journal of Biological Chemistry*, 275(13), pp.9340–9347.

Kim, Y., Lee, S.-H. & Ho, W.-K., 2007. Hydrogen peroxide selectively increases TREK-2 currents via myosin light chain kinases. *Frontiers in bioscience : a journal and virtual library*, 12, pp.1642–1650.

Kisselbach, J. et al., 2014. Modulation of K_{2P} 2.1 and K_{2P} 10.1 K^+ channel sensitivity to carvedilol by alternative mRNA translation initiation. *British Journal of Pharmacology*, 171(23), pp.5182–5194. Available at: http://doi.wiley.com/10.1111/bph.12596.

Klausner, R.D. et al., 1980. Lipid domains in membranes. Evidence derived from structural perturbations induced by free fatty acids and lifetime heterogeneity analysis. *Journal of Biological Chemistry*, 255(4), pp.1286–1295.

Koh, S.D. et al., 2001. TREK-1 regulation by nitric oxide and cGMP-dependent protein kinase: An essential role in smooth muscle inhibitory neurotransmission. *Journal of Biological Chemistry*, 276(47), pp.44338–44346.

Koo, J.Y. et al., 2007. Hydroxy-alpha-sanshool activates TRPV1 and TRPA1 in sensory neurons. *European Journal of Neuroscience*, 26(5), pp.1139–1147.

Köpfer, D.A. et al., 2014. Ion permeation in K+ channels occurs by direct Coulomb knock-on. *Science*, 346(6207), pp.352–355.

Krieg, P. a. & Melton, D. a., 1984. Functional messenger RNAs are produced by SP6 in vitro transcription of cloned cDNAs. *Nucleic Acids Research*, 12(18), pp.7057–7070.

Kuo, A. et al., 2003. Crystal structure of the potassium channel KirBac1.1 in the closed state. *Science (New York, N.Y.)*, 300(5627), pp.1922–1926.

Laigle, C. et al., 2012. Deletion of TRAAK Potassium Channel Affects Brain Metabolism and Protects against Ischemia. *PLoS ONE*, 7(12), pp.1–12.

Laitko, U., Juranka, P.F. & Morris, C.E., 2006. Membrane stretch slows the concerted step prior to opening in a Kv channel. *The Journal of general physiology*, 127(6), pp.687–701.

Lauritzen, I. et al., 2005. Cross-talk between the mechano-gated K2P channel TREK-1 and the actin cytoskeleton. *EMBO reports*, 6(7), pp.642–648.

Lauritzen, I. et al., 2000. Polyunsaturated fatty acids are potent neuroprotectors. *The EMBO journal*, 19(8), pp.1784–1793.

Lei, Q. et al., 2014. Response of the human detrusor to stretch is regulated by TREK-1, a two-pore-domain (K2P) mechano-gated potassium channel. *The Journal of physiology*, 592(Pt 14), pp.3013–30. Available at: http://www.ncbi.nlm.nih.gov/pubmed/24801307.

Leng, T.C. et al., 2011. Detection of bioactive compounds from Spilanthes acmella (L.) plants and its various in vitro culture products. *J.Med.Aromat.Plants Sci.*, 5(3), pp.371–378. Available at: \\Robsrv-05\reference manager\Articles\13852.pdf.

Lennertz, R.C. et al., 2010. Physiological basis of tingling paresthesia evoked by hydroxy-alpha-sanshool. *The Journal of neuroscience : the official journal of the Society for Neuroscience*, 30(12), pp.4353–4361. Available at: http://www.ncbi.nlm.nih.gov/pubmed?term=Lennertz AND stucky\nhttp://www.ncbi.nlm.nih.gov/pubmed?term=Lennertz AND Bautista.

Lesage, F. et al., 1996. Dimerization of TWIK-1 K+ channel subunits via a disulfide bridge. *The EMBO journal*, 15(23), pp.6400–6407.

Lesage, F., Terrenoire, C., et al., 2000. Human TREK2, a 2P Domain Mechano-sensitive K+ Channel with Multiple Regulations by Polyunsaturated Fatty Acids, Lysophospholipids, and Gs, Gi, and Gq Protein-coupled Receptors. *Journal of Biological Chemistry*, 275(37), pp.28398–28405.

Lesage, F. et al., 1996. TWIK-1, a ubiquitous human weakly inward rectifying K+ channel with a novel structure. *The EMBO journal*, 15(5), pp.1004–1011.

Lesage, F., Maingret, F. & Lazdunski, M., 2000. Cloning and expression of human TRAAK, a polyunsaturated fatty acids-activated and mechano-sensitive K+ channel. *FEBS Letters*, 471(2-3), pp.137–140.

Levina, N. et al., 1999. Protection of Escherichia coli cells against extreme turgor by activation of MscS and MscL mechanosensitive channels: identification of genes required for MscS activity. *The EMBO journal*, 18(7), pp.1730–1737.

Lin, D.-H. et al., 2015. The Role of the Two-Pore Domain Potassium Channel TREK-1 in the Therapeutic Effects of Escitalopram in a Rat Model of Poststroke Depression. *CNS Neuroscience & Therapeutics*, 21, p.n/a–n/a. Available at: http://doi.wiley.com/10.1111/cns.12384.

Liou, Y.-J. et al., 2009. Support for the involvement of the KCNK2 gene in major depressive disorder and response to antidepressant treatment. *Pharmacogenetics and genomics*, 19(10), pp.735–741.

Liu, H., Enyeart, J. a & Enyeart, J.J., 2007. Potent inhibition of native TREK-1 K+ channels by selected dihydropyridine Ca2+ channel antagonists. *The Journal of pharmacology and experimental therapeutics*, 323(1), pp.39–48.

Liu, W. & Saint, D. a., 2004. Heterogeneous expression of tandem-pore K+ channel genes in adult and embryonic rat heart quantified by real-time polymerase chain reaction. *Clinical and Experimental Pharmacology and Physiology*, 31(3), pp.174–178.

Liu, X. et al., 2008. Stretch-activated potassium channels in hypotonically induced blebs of atrial myocytes. *Journal of Membrane Biology*, 226(1-3), pp.17–25.

Lloyd, E.E., Marrelli, S.P. & Bryan, R.M., 2009. cGMP does not activate two-pore domain K+ channels in cerebrovascular smooth muscle. *American journal of physiology. Heart and circulatory physiology*, 296(6), pp.H1774–H1780.

Lolicato, M. et al., 2014. Article Transmembrane Helix Straightening and Buckling Underlies Activation of Mechanosensitive and Thermosensitive K 2P Channels. *Neuron*, 84(6), pp.1198–1212. Available at: http://dx.doi.org/10.1016/j.neuron.2014.11.017.

Long, S.B. et al., 2007. Atomic structure of a voltage-dependent K+ channel in a lipid membrane-like environment. *Nature*, 450(7168), pp.376–382.

Lopes, C.M.B. et al., 2005. PIP2 hydrolysis underlies agonist-induced inhibition and regulates voltage gating of two-pore domain K+ channels. *The Journal of physiology*, 564(Pt 1), pp.117–129.

Lundbaek, J. a et al., 2010. Lipid bilayer regulation of membrane protein function: gramicidin channels as molecular force probes. *Journal of the Royal Society, Interface / the Royal Society*, 7(44), pp.373–395.

Ma, X.-Y. et al., 2011. External BA2+ block of two-pore-domain potassium channel trek-1 defines conformational transition in its selectivity filter. *The Journal of biological chemistry*, pp.1–20. Available at: http://www.ncbi.nlm.nih.gov/pubmed/21965685.

Maathuis, F.J.M., 2011. Vacuolar two-pore K+ channels act as vacuolar osmosensors. *New Phytologist*, 191(1), pp.84–91.

MacKenzie, G., Franks, N.P. & Brickley, S.G., 2014. Two-pore domain potassium channels enable action potential generation in the absence of voltage-gated potassium channels. *Pflügers Archiv - European Journal of Physiology*, pp.989–999. Available at: http://link.springer.com/10.1007/s00424-014-1660-6.

Maingret, F. et al., 2000. Lysophospholipids open the two-pore domain mechano-gated K+ channels TREK-1 and TRAAK. *Journal of Biological Chemistry*, 275(14), pp.10128–10133.

Maingret, F. et al., 1999. MEMBRANES AND BIOENERGETICS : Mechano- or Acid Stimulation , Two Interactive Modes of Activation of the TREK-1 Potassium Channel Mechano- or Acid Stimulation , Two Interactive Modes of Activation of the TREK-1 Potassium Channel *. , 274(38), pp.26691–26696.

Maingret, F. et al., 2002. Molecular basis of the voltage-dependent gating of TREK-1, a mechano-sensitive K(+) channel. *Biochemical and biophysical research communications*, 292(2), pp.339–346.

Maingret, F. et al., 2000. TREK-1 is a heat-activated background K(+) channel. *The EMBO journal*, 19(11), pp.2483–2491.

Maksaev, G. et al., 2011. Analyses of gating thermodynamics and effects of deletions in the mechanosensitive channel TREK-1: Comparisons with structural models. *Channels*, 5(1), pp.34–42.

Martinac, B. et al., 1987. Pressure-sensitive ion channel in Escherichia coli. *Proceedings of the National Academy of Sciences of the United States of America*, 84(8), pp.2297–2301.

Martinac, B., 2014. The ion channels to cytoskeleton connection as potential mechanism of mechanosensitivity. *Biochimica et Biophysica Acta - Biomembranes*, 1838(2), pp.682–691. Available at: http://dx.doi.org/10.1016/j.bbamem.2013.07.015.

Martinac, B., Adler, J. & Kung, C., 1990. Mechanosensitive ion channels of E. coli activated by amphipaths. *Nature*, 348(6298), pp.261–263.

Marzian, S. et al., 2013. Side pockets provide the basis for a new mechanism of Kv channel-specific inhibition. *Nature chemical biology*, 9(8), pp.507–13. Available at: http://www.ncbi.nlm.nih.gov/pubmed/23728494.

Mathie, A., Al-Moubarak, E. & Veale, E.L., 2010. Gating of two pore domain potassium channels. *The Journal of physiology*, 588(Pt 17), pp.3149–3156.

Mathie, A. & Veale, E.L., 2007. Therapeutic potential of neuronal two-pore domain potassium-channel modulators. *Current opinion in investigational drugs (London, England : 2000)*, 8(7), pp.555–562.

Mazella, J. et al., 2010. Spadin, a sortilin-derived peptide, targeting rodent TREK-1 channels: A new concept in the antidepressant drug design. *PLoS Biology*, 8(4).

McManus, O.B. & Magleby, K.L., 1988. Kinetic states and modes of single large-conductance calcium-activated potassium channels in cultured rat skeletal muscle. *The Journal of physiology*, 402, pp.79–120.

Meadows, H.J. et al., 2001. The neuroprotective agent sipatrigine (BW619C89) potently inhibits the human tandem pore-domain K+ channels TREK-1 and TRAAK. *Brain Research*, 892(1), pp.94–101.

Medhurst, A.D. et al., 2001. Distribution analysis of human two pore domain potassium channels in tissues of the central nervous system and periphery. *Molecular Brain Research*, 86(1-2), pp.101–114. Available at: http://dx.doi.org/10.1016/S0169-328X(00)00263-1.

Menozzi, C. et al., 2009. Synthesis and evaluation of new alkylamides derived from ??-hydroxysanshool, the pungent molecule in szechuan pepper. *Journal of Agricultural and Food Chemistry*, 57(5), pp.1982–1989.

Meves, H., 2008. Arachidonic acid and ion channels: an update. *British journal of pharmacology*, 155(1), pp.4–16.

Meves, H., 1994. Modulation of ion channels by arachidonic acid. *Progress in Neurobiology*, 43(2), pp.175–186.

Mi Hwang, E. et al., 2014. A disulphide-linked heterodimer of TWIK-1 and TREK-1 mediates passive conductance in astrocytes. *Nature communications*, 5, p.3227. Available at: http://www.ncbi.nlm.nih.gov/pubmed/24496152.

Miller, A. & Long, S., 2012. Crystal Structure of the Human Two – Pore Domain Potassium Channel K2P1. *Science*, 335, p.432.

Miller, A.N. & Long, S.B., 2012. Crystal Structure of the Human Two-Pore Domain Potassium Channel K2P1. *Science*, 335(6067), pp.432–436.

Miller, C., 2000. An overview of the potassium channel family. *Genome biology*, 1(4), p.REVIEWS0004.

Minieri, L. et al., 2013. The inhibitor of volume-regulated anion channels DCPIB activates TREK potassium channels in cultured astrocytes. *British Journal of Pharmacology*, 168(5), pp.1240–1254.

Mirkovic, K. et al., 2012. Behavioral characterization of mice lacking Trek channels. *Frontiers in Behavioral Neuroscience*, 6(September), pp.1–9.

Moe, P. & Blount, P., 2005. Assessment of potential stimuli for mechano-dependent gating of MscL: Effects of pressure, tension, and lipid headgroups. *Biochemistry*, 44(36), pp.12239–12244.

Moha Ou Maati, H. et al., 2012. Spadin as a new antidepressant: Absence of TREK-1-related side effects. *Neuropharmacology*, 62(1), pp.278–288. Available at: http://dx.doi.org/10.1016/j.neuropharm.2011.07.019.

Momo, F., Fabris, S. & Stevanato, R., 2005. Interaction of fluoxetine with phosphatidylcholine liposomes. *Biophysical Chemistry*, 118(1), pp.15–21.

Monod, J., Wyman, J. & Changeux, J.P., 1965. on the Nature of Allosteric Transitions: a Plausible Model. *Journal of molecular biology*, 12(December), pp.88–118.

Monshausen, G.B. & Haswell, E.S., 2013. A force of nature: Molecular mechanisms of mechanoperception in plants. *Journal of Experimental Botany*, 64(15), pp.4663–4680.

Morth, J.P. et al., 2007. Crystal structure of the sodium-potassium pump. *Nature*, 450(7172), pp.1043–1049.

Murbartián, J. et al., 2005. Sequential phosphorylation mediates receptor- and kinase-induced inhibition of TREK-1 background potassium channels. *Journal of Biological Chemistry*, 280(34), pp.30175–30184.

Nagy, K., 1987. Evidence for multiple open states of sodium channels in neuroblastoma cells. *The Journal of membrane biology*, 96(3), pp.251–262.

Naitoh, Y. & Eckert, R., 1969. Ionic mechanisms controlling behavioral responses of paramecium to mechanical stimulation. *Science (New York, N.Y.)*, 164(882), pp.963–965.

Namiranian, K. et al., 2010. Cerebrovascular responses in mice deficient in the potassium channel, TREK-1. *American journal of physiology. Regulatory, integrative and comparative physiology*, 299(2), pp.R461–R469.

Nayak, T.K. et al., 2009. Inhibition of human two-pore domain K+ channel TREK1 by local anesthetic lidocaine: negative cooperativity and half-of-sites saturation kinetics. *Molecular pharmacology*, 76(4), pp.903–917.

Nishida, M. et al., 2007. Crystal structure of a Kir3 . 1-prokaryotic Kir channel chimera. , 26(17), pp.4005–4015.

Noël, J. et al., 2009. The mechano-activated K+ channels TRAAK and TREK-1 control both warm and cold perception. *The EMBO journal*, 28(9), pp.1308–1318.

Noël, J., Sandoz, G. & Lesage, F., 2011. Molecular regulations governing TREK and TRAAK channel functions. *Channels (Austin, Tex.)*, 5(5), pp.402–409.

Ohara, a et al., 2006. Single-channel recordings of TREK-1 K+ channels in periodontal ligament fibroblasts. *Journal of dental research*, 85(7), pp.664–669.

Opsahl, L.R. & Webb, W.W., 1994. Lipid-glass adhesion in giga-sealed patch-clamped membranes. *Biophysical journal*, 66(1), pp.75–79.

Ostmeyer, J. et al., 2013. Recovery from slow inactivation in K+ channels is controlled by water molecules. *Nature*, 501(7465), pp.121–4. Available at: http://www.pubmedcentral.nih.gov/articlerender.fcgi?artid=3799803&tool=pmcentrez&rendertype=abstract.

Papke, R.L. & Smith-Maxwell, C., 2009. High throughput electrophysiology with Xenopus oocytes. *Combinatorial chemistry & high throughput screening*, 12(1), pp.38–50.

Park, K.S. et al., 2008. The inhibition of TREK2 channel by an oxidizing agent, 5,5-dithio-bis (2-nitrobenzoic acid), via interaction with the C-terminus distal to the 353rd amino acid. *Korean Journal of Physiology and Pharmacology*, 12(4), pp.211–216.

Patel, a J. et al., 1999. Inhalational anesthetics activate two-pore-domain background K+ channels. *Nature neuroscience*, 2(5), pp.422–426.

Patel, a. J., Lazdunski, M. & Honoré, E., 2001. Lipid and mechano-gated 2P domain K+ channels. *Current Opinion in Cell Biology*, 13(4), pp.422–427.

Patel, A.J. et al., 1998. A mammalian two pore domain mechano-gated S-like K+ channel. *EMBO Journal*, 17(15), pp.4283–4290.

Patel, A.J. et al., 2000. TWIK-2, an inactivating 2P domain K+ channel. *Journal of Biological Chemistry*, 275(37), pp.28722–28730.

Pathak, M.M. et al., 2014. Stretch-activated ion channel Piezo1 directs lineage choice in human neural stem cells. *Proceedings of the National Academy of Sciences*, 111(45), pp.16148–16153. Available at: http://www.pnas.org/lookup/doi/10.1073/pnas.1409802111.

Payandeh, J. et al., 2011. The crystal structure of a voltage-gated sodium channel. *Nature*, 475(7356), pp.353–358. Available at: http://dx.doi.org/10.1038/nature10238.

Peiris, K.P.R.A., Silva, G.K.J. & Ratnasooriya, W.D., 2001. Analgesic Activity of Water Extract of Spilanthes acmella Flowers on Rats. , 2(2), p.2001.

Pereira, V. et al., 2014. Role of the TREK2 potassium channel in cold and warm thermosensation and in pain perception. *Pain*, 155(12), pp.2534–2544. Available at: http://content.wkhealth.com/linkback/openurl?sid=WKPTLP:landingpage&an=00006396-201412000-00015.

Perlis, R.H. et al., 2008. Pharmacogenetic analysis of genes implicated in rodent models of antidepressant response: association of TREK1 and treatment resistance in the STAR(*)D study. *Neuropsychopharmacology : official publication of the American College of Neuropsychopharmacology*, 33(12), pp.2810–2819.

Peyronnet, R. et al., 2012. Mechanoprotection by Polycystins against Apoptosis Is Mediated through the Opening of Stretch-Activated K2P Channels. *Cell Reports*, 1(3), pp.241–250.

Piechotta, P.L. et al., 2011. The pore structure and gating mechanism of K2P channels. *The EMBO journal*, 30(17), pp.3607–3619. Available at: http://dx.doi.org/10.1038/emboj.2011.268.

Poole, K. et al., 2014. Tuning Piezo ion channels to detect molecular-scale movements relevant for fine touch. *Nature communications*, 5, p.3520. Available at: http://www.pubmedcentral.nih.gov/articlerender.fcgi?artid=3973071&tool=pmcentrez&rendertype=abstract.

Poulin, H. et al., 2014. Fluoxetine Blocks Nav1.5 Channels Via a Mechanism Similar to That of Class 1 Antiarrhythmics. *Molecular pharmacology*, (D), pp.378–389. Available at: http://www.ncbi.nlm.nih.gov/pubmed/25028482.

Prole, D.L. & Taylor, C.W., 2013. Identification and Analysis of Putative Homologues of Mechanosensitive Channels in Pathogenic Protozoa. *PLoS ONE*, 8(6).

Punke, M. a et al., 2003. Inhibition of human TREK-1 channels by bupivacaine. *Anesthesia and analgesia*, 96(6), pp.1665–1673, table of contents.

Qin, F., 2013. Demystifying thermal channels: Driving a channel both forwards and backwards with a single gear? *Biophysical Journal*, 104(10), pp.2118–2120. Available at: http://dx.doi.org/10.1016/j.bpj.2013.04.017.

Qin, F., 2010. Hill coefficients of a polymodal Monod-Wyman-Changeux model for ion channel gating. *Biophysical Journal*, 99(3), pp.L29–L31. Available at: http://dx.doi.org/10.1016/j.bpj.2010.05.018.

Rajan, S. et al., 2000. TASK-3, a novel tandem pore domain acid-sensitive K+ channel. An extracellular histidine as pH sensor. *Journal of Biological Chemistry*, 275(22), pp.16650–16657.

Rajan, S. et al., 2001. THIK-1 and THIK-2, a Novel Subfamily of Tandem Pore Domain K+ Channels. *Journal of Biological Chemistry*, 276(10), pp.7302–7311.

Ranade, S.S. et al., 2014. Piezo2 is the major transducer of mechanical forces for touch sensation in mice. *Nature*.

Rapedius, M. et al., 2012. State-independent intracellular access of quaternary ammonium blockers to the pore of TREK-1. *Channels*, 6(6), pp.473–478.

Renigunta, V., Schlichthörl, G. & Daut, J., 2015. Much more than a leak: structure and function of K2P-channels. *Pflügers Archiv - European Journal of Physiology*, 467(5), pp.867–894. Available at: http://link.springer.com/10.1007/s00424-015-1703-7.

Reyes, R. et al., 1998. Cloning and expression of a novel pH-sensitive two pore domain K+ channel from human kidney. *Journal of Biological Chemistry*, 273(47), pp.30863–30869.

Richieri, G. V, Mescher, M.F. & Kleinfeld, a M., 1990. Short term exposure to cis unsaturated free fatty acids inhibits degranulation of cytotoxic T lymphocytes. *Journal of immunology (Baltimore, Md. : 1950)*, 144(2), pp.671–677.

Richter, T. a et al., 2004. Acid-sensitive two-pore domain potassium (K2P) channels in mouse taste buds. *Journal of neurophysiology*, 92(3), pp.1928–1936.

Riera, C.E. et al., 2009. Compounds from Sichuan and Melegueta peppers activate, covalently and non-covalently, TRPA1 and TRPV1 channels. *British Journal of Pharmacology*, 157(8), pp.1398–1409.

Rinné, S. et al., 2014. A splice variant of the two-pore domain potassium channel TREK-1 with only one pore domain reduces the surface expression of full-length TREK-1 channels. *Pflugers Archiv European Journal of Physiology*, 466(8), pp.1559–1570.

Roos, A. & Boron, W.F., 1981. Intracellular pH. *Physiological reviews*, 61(2), pp.296–434.

Ruffin, V. a. et al., 2014. Intracellular pH regulation by acid-base transporters in mammalian neurons. *Frontiers in Physiology*, 5 FEB(February), pp.1–11.

Salinas, M. et al., 1999. Cloning of a new mouse two-P domain channel subunit and a human homologue with a unique pore structure. *Journal of Biological Chemistry*, 274(17), pp.11751–11760.

Salmi, M.L. et al., 2011. Changes in gravity rapidly alter the magnitude and direction of a cellular calcium current. *Planta*, 233(5), pp.911–920.

Sanders, K.M. & Koh, S.D., 2006. Two-pore-domain potassium channels in smooth muscles: new components of myogenic regulation. *The Journal of physiology*, 570(Pt 1), pp.37–43.

Sandoz, G. et al., 2006. AKAP150, a switch to convert mechano-, pH- and arachidonic acid-sensitive TREK K(+) channels into open leak channels. *The EMBO journal*, 25(24), pp.5864–5872.

Sandoz, G. et al., 2009. Extracellular acidification exerts opposite actions on TREK1 and TREK2 potassium channels via a single conserved histidine residue. *Proceedings of the National Academy of Sciences of the United States of America*, 106(34), pp.14628–14633.

Sandoz, G. et al., 2008. Mtap2 is a constituent of the protein network that regulates twik-related K+ channel expression and trafficking. *The Journal of neuroscience : the official journal of the Society for Neuroscience*, 28(34), pp.8545–8552.

Sandoz, G., Bell, S.C. & Isacoff, E.Y., 2011. Optical probing of a dynamic membrane interaction that regulates the TREK1 channel. *Proceedings of the National Academy of Sciences of the United States of America*, 108(6), pp.2605–2610.

Sano, Y. et al., 2003. A novel two-pore domain K+ channel, TRESK, is localized in the spinal cord. *Journal of Biological Chemistry*, 278(30), pp.27406–27412.

Schmidt, C. et al., 2014. Cardiac expression and atrial fibrillation-associated remodeling of K 2P2.1 (TREK-1) K+ channels in a porcine model. *Life Sciences*, 97(2), pp.107–115. Available at: http://dx.doi.org/10.1016/j.lfs.2013.12.006.

Schneider, E.R. et al., 2014. Temperature sensitivity of two-pore (K2P) potassium channels. *Current topics in membranes*, 74, pp.113–33. Available at: http://www.sciencedirect.com/science/article/pii/B9780128001813000051 [Accessed May 25, 2015].

Schwingshackl, a. et al., 2012. Regulation of interleukin-6 secretion by the two-pore-domain potassium channel Trek-1 in alveolar epithelial cells. *AJP: Lung Cellular and Molecular Physiology*, 304(4), pp.L276–L286. Available at: http://ajplung.physiology.org/cgi/doi/10.1152/ajplung.00299.2012.

Sheetz, M.P. & Singer, S.J., 1974. Biological membranes as bilayer couples. A molecular mechanism of drug-erythrocyte interactions. *Proceedings of the National Academy of Sciences of the United States of America*, 71(11), pp.4457–4461.

Siegelbaum, S.A., Camardo, J.S. & Kandel, E.R., 1982. Serotonin and cyclic AMP close single K+ channels in Aplysia sensory neurones. *Nature*, 299(5882), pp.413–417.

Siemens, J. et al., 2004. Cadherin 23 is a component of the tip link in hair-cell stereocilia. *Nature*, 428(6986), pp.950–955.

Silver, I.A., Murrills, R.J. & Etherington, D.J., 1988. Microelectrode studies on the acid microenvironment beneath adherent macrophages and osteoclasts. *Experimental cell research*, 175(2), pp.266–276.

Simkin, D., Cavanaugh, E.J. & Kim, D., 2008. Control of the single channel conductance of K2P10.1 (TREK-2) by the amino-terminus: role of alternative translation initiation. *The Journal of physiology*, 586(Pt 23), pp.5651–5663.

Snyder, S.H., 2009. Neurotransmitters, receptors, and second messengers galore in 40 years. *The Journal of neuroscience : the official journal of the Society for Neuroscience*, 29(41), pp.12717–12721.

Sokabe, M., Sachs, F. & Jing, Z.Q., 1991. Quantitative video microscopy of patch clamped membranes stress, strain, capacitance, and stretch channel activation. *Biophysical journal*, 59(3), pp.722–728.

Söllner, C. et al., 2004. Mutations in cadherin 23 affect tip links in zebrafish sensory hair cells. *Nature*, 428(6986), pp.955–959.

Staudacher, K. et al., 2011. Carvedilol targets human K 2P3.1 (TASK1) K + leak channels. *British Journal of Pharmacology*, 163(5), pp.1099–1110.

Suchyna, T.M. et al., 2004. Bilayer-dependent inhibition of mechanosensitive channels by neuroactive peptide enantiomers. *Nature*, 430(6996), pp.235–240.

Suchyna, T.M. et al., 2000. Identification of a peptide toxin from Grammostola spatulata spider venom that blocks cation-selective stretch-activated channels. *The Journal of general physiology*, 115(5), pp.583–598.

Suchyna, T.M., Markin, V.S. & Sachs, F., 2009. Biophysics and structure of the patch and the gigaseal. *Biophysical Journal*, 97(3), pp.738–747. Available at: http://dx.doi.org/10.1016/j.bpj.2009.05.018.

Sukharev, S.I. et al., 1997. Mechanosensitive channels of Escherichia coli: the MscL gene, protein, and activities. *Annual review of physiology*, 59, pp.633–657.

Sun, L.N. et al., 2008. Protective effects of TREK-1 against oxidative injury induced by SNP and H2O2. *Acta Pharmacologica Sinica*, 29(10), pp.1150–1156.

Takahira, M. et al., 2005. Fenamates and diltiazem modulate lipid-sensitive mechano-gated 2P domain K+ channels. *Pflugers Archiv European Journal of Physiology*, 451(3), pp.474–478.

Tan, J.H.C., Liu, W. & Saint, D. a, 2004. Differential expression of the mechanosensitive potassium channel TREK-1 in epicardial and endocardial myocytes in rat ventricle. *Experimental physiology*, 89(3), pp.237–242.

Tan, J.H.C., Liu, W. & Saint, D. a, 2002. Trek-like potassium channels in rat cardiac ventricular myocytes are activated by intracellular ATP. *The Journal of membrane biology*, 185(3), pp.201–207.

Teng, J. et al., 2014. The force-from-lipid (FFL) principle of mechanosensitivity, at large and in elements. *Pfl??gers Archiv - European Journal of Physiology*, pp.27–37.

Terrenoire, C. et al., 2001. A TREK-1-like potassium channel in atrial cells inhibited by beta-adrenergic stimulation and activated by volatile anesthetics. *Circulation research*, 89(4), pp.336–342.

Tertyshnikova, S. et al., 2005. BL-1249 [(5,6,7,8-Tetrahydro-napthalen-1-yl)-[2-(1H-tetrazol-5-yl) -phenyl] -amine]: A Putative Potassium Channel Opener with Bladder-Relaxant Properties. *The Journal of Pharmacology and Experimental Therapeutics*, 313(1), pp.250–259.

Thiel, G. et al., 2013. Potassium Ion Channels: Could They Have Evolved from Viruses? *Plant Physiology*, 162(3), pp.1215–1224. Available at: http://www.plantphysiol.org/cgi/doi/10.1104/pp.113.219360.

Thomas, D. et al., 2008. Alternative Translation Initiation in Rat Brain Yields K2P2.1 Potassium Channels Permeable to Sodium. *Neuron*, 58(6), pp.859–870.

Thümmler, S., Duprat, F. & Lazdunski, M., 2007. Antipsychotics inhibit TREK but not TRAAK channels. *Biochemical and Biophysical Research Communications*, 354(1), pp.284–289.

Toombes, G.E.S. & Swartz, K.J., 2014. Divining the design principles of voltage sensors. *The Journal of general physiology*, 143(2), pp.139–44. Available at: http://jgp.rupress.org/content/143/2/139.short.

Tsunozaki, M. et al., 2013. A “toothache tree” alkylamide inhibits Aδ mechanonociceptors to alleviate mechanical pain. *The Journal of physiology*, 591(Pt 13), pp.3325–40. Available at: http://jp.physoc.org/content/591/13/3325.long.

Tulleuda, A. et al., 2011. TRESK channel contribution to nociceptive sensory neurons excitability: modulation by nerve injury. *Molecular pain*, 7(1), p.30. Available at: http://www.molecularpain.com/content/7/1/30.

Vallee, N. et al., 2012. Neuroprotective role of the TREK-1 channel in decompression sickness. *Journal of Applied Physiology*, 112(7), pp.1191–1196.

Vardanyan, V. & Pongs, O., 2012. Coupling of voltage-sensors to the channel pore: A comparative view. *Frontiers in Pharmacology*, 3 JUL(July), pp.1–10.

Veale, E.L. et al., 2014. Influence of the N terminus on the biophysical properties and pharmacology of TREK1 potassium channels. *Molecular pharmacology*, 85(5), pp.671–81. Available at: http://www.ncbi.nlm.nih.gov/pubmed/24509840.

Veech, R.L. et al., 1979. Cytosolic phosphorylation potential. *Journal of Biological Chemistry*, 254(14), pp.6538–6547.

Voloshyna, I. et al., 2008. TREK-1 is a novel molecular target in prostate cancer. *Cancer Research*, 68(4), pp.1197–1203.

Webb, D.J. & Nuccitelli, R., 1981. Direct measurement of intracellular pH chages in Xenopus eggs at fertilization and cleavage. *J. Cell Biol.*, 91 (November), pp.562–567.

Wechselberger, M. et al., 2006. Ionic channels and conductance-based models for hypothalamic neuronal thermosensitivity. *American journal of physiology. Regulatory, integrative and comparative physiology*, 291(3), pp.R518–R529.

Wells, G.D. et al., 2012. A unique alkaline pH-regulated and fatty acid-activated tandem pore domain potassium channel (K2P) from a marine sponge. *Journal of Experimental Biology*, 215(14), pp.2435–2444.

Woo, D.H. et al., 2012. TREK-1 and Best1 Channels Mediate Fast and Slow Glutamate Release in Astrocytes upon GPCR Activation. *Cell*, 151(1), pp.25–40.

Xian Tao Li et al., 2006. The stretch-activated potassium channel TREK-1 in rat cardiac ventricular muscle. *Cardiovascular Research*, 69(1), pp.86–97.

Xiao, Z. et al., 2014. Activation of neurotensin receptor 1 facilitates neuronal excitability and spatial learning and memory in the entorhinal cortex: beneficial actions in an Alzheimer's disease model. *J Neurosci*, 34(20), pp.7027–7042.

Yamamoto, Y., Hatakeyama, T. & Taniguchi, K., 2009. Immunohistochemical colocalization of TREK-1, TREK-2 and TRAAK with TRP channels in the trigeminal ganglion cells. *Neuroscience Letters*, 454(2), pp.129–133.

Yang, B.X. & Sachs, F., 1990. Charcterization of Stretch-Activated Ion Channels in Xenopus Oocytes. *Journal of Physiology*, 431, pp.103–122.

YASUDA, I., TAKEYA, K. & ITOKAWA, H., 1980. The Geometric Structure of Spilanthol. *Chemical & pharmaceutical bulletin*, 28(7), pp.2251–2253. Available at: http://ci.nii.ac.jp/naid/110003662647/en/ [Accessed July 18, 2015].

Ye, S., Li, Y. & Jiang, Y., 2010. Novel insights into K+ selectivity from high-resolution structures of an open K+ channel pore. *Nature structural & molecular biology*, 17(8), pp.1019–1023.

Zhang, H., Shepherd, N. & Creazzo, T.L., 2008. Temperature-sensitive TREK currents contribute to setting the resting membrane potential in embryonic atrial myocytes. *The Journal of physiology*, 586(Pt 15), pp.3645–3656.

Zheng, H. et al., 2009a. Identification of the large-conductance background K+ channel in mouse B cells as TREK-2. *American journal of physiology. Cell physiology*, 297(1), pp.C188–C197.

Zheng, H. et al., 2009b. Identification of the large-conductance background K+ channel in mouse B cells as TREK-2. *American journal of physiology. Cell physiology*, 297(1), pp.C188–97. Available at: http://ajpcell.physiology.org/content/297/1/C188 [Accessed June 29, 2015].

Zhou, M. et al., 2009. TWIK-1 and TREK-1 are potassium channels contributing significantly to astrocyte passive conductance in rat hippocampal slices. *The*

Journal of neuroscience : the official journal of the Society for Neuroscience, 29(26), pp.8551–8564.

Zhou, X.-L. et al., 2003. The transient receptor potential channel on the yeast vacuole is mechanosensitive. *Proceedings of the National Academy of Sciences of the United States of America*, 100(12), pp.7105–7110.

Zhuo, R.-G. et al., 2015. Insights into the stimulatory mechanism of 2-aminoethoxydiphenyl borate on TREK-2 potassium channel. *Neuroscience*, 300, pp.85–93. Available at: http://linkinghub.elsevier.com/retrieve/pii/S0306452215004443.

Zhuo, R.-G. et al., 2015. The isoforms generated by alternative translation initiation adopt similar conformation in the selectivity filter in TREK-2. *Journal of Physiology and Biochemistry*, 2. Available at: http://link.springer.com/10.1007/s13105-015-0422-z.

Zilberberg, N., Ilan, N. & Goldstein, S. a N., 2001. KCNK??: Opening and closing the 2-P-domain potassium leak channel entails “C-type” gating of the outer pore. *Neuron*, 32(4), pp.635–648.